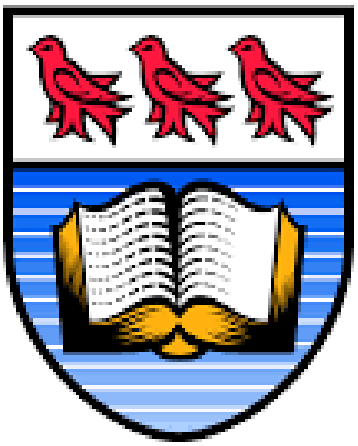

University of Victoria

MECH 360 - Design of Mechanical Elements

Final Design Report

Instructor: Dr. Flavio Firmani
Design Team 18

December 4th, 2023

Dhruv Jethwa – V00964626
Jack Walmsley – V00963479
Cole Manton – V00917415
Jack Martin – V01016907
Marek Ooms – V00970967
Brandon Groot –V00959247

Executive Summary

In this final design report of a small-scale ferris wheel we explore different designs, gearboxes, themes, and locations of a proposed ferris wheel in the Greater Victoria District. Throughout this report, we discuss some of the different styles of ferris wheel designs that exist as well as the history of these machines, which helps us better understand what is and is not important to our design. Each member of the group individually researched and drafted their proposed theme, location, and general design concept, which allowed us to further narrow down what would best suit our proposal.

In terms of theme and location, we discussed as a group which would be best in terms of marketability and potential revenue, and decided that our theme would be local animals and our ferris wheel would operate on the grounds of Butchart Gardens, where it will be seen by over 1 million guests annually. As for the design of the structure and gearbox, we implemented a weighted objectives chart to decide which design was favorable given our needs and the project requirements. Many of the project's constraints were outlined in the project description. Additional constraints and performance specifications were chosen by the group, such as arm length and output speed. Using these constraints, we performed an external load analysis to determine what gear ratios and power input would be required to achieve the desired angular velocity and torque output.

The final proposed design features six evenly spaced cars attached to the center of the drive shaft by 2 2m-long I-beam arms. The drive shaft is driven by a 0.5kW motor connected to a gearbox which will implement compound gear reduction to reduce the output speed and increase output torque. The use of compound gear reduction to reduce output speed to our desired 2 rad/s will create more than enough torque to drive the ferris wheel. The drive shaft will be supported by the base on both sides to negate the cantilever effect which results from a single sided support system. The side which is not connected to the motor will be attached to the base with a bearing to ensure smooth rotation and reduce unwanted friction. The ferris wheel will stand at 6m in height to allow for adequate ground clearance as well as an enjoyable ride. Final designs will be produced in later reports, however this report outlines all the crucial elements that will be used going forward.

For the preliminary design report, much more analysis was required as we began to design the specific gearbox layout. The group decided on factors like pressure angle and preliminary shaft lengths. From there we were able to calculate parameters like contact ratios, pitch, length of action, and the overall efficiency of our gearbox.

Next, with the basic shaft layout chosen, the group performed a load analysis to evaluate forces acting on the shafts by creating shear and moment diagrams. By solving for the critical diameter algebraically we were able to create a Matlab script which takes in parameters of tensile strength and Neuber's constant and returns critical diameters. This allowed us to easily test many different material options and find one that best fit the scope of the project.

With shaft lengths and diameters established, we were able to determine bearing support, and keyhole placements on the shafts. The shafts and gears were then modeled on SolidWorks and

the group was able to create preliminary gearbox layout drawings. In this stage, temporary bearings were chosen for modeling purposes. Specific bearings which meet the requirements of the project will be determined in the final design report.

In the final design report, extensive analysis was done on the gears and shafts of the gearbox. It was crucial that a failure analysis be run on the gears to determine what materials and face widths were required to achieve proper safety factors. To accomplish this, the group wrote an extensive MATLAB program which took material properties and gear contact specs as parameters and returned the minimum acceptable face width and the associated safety factors against bending and surface fatigue. The group had determined that minimum safety factors of 1.5 for both bending and surface fatigue. The implementation of this program assigned a small face width and determined what the associated safety factors would be at that width, and if they were not met it would increment the face width until adequate safety factors were achieved. This allowed the group to easily determine minimum face widths of the critical gear contacts with different materials, eventually proving that 4340 normalized (870°C) steel was the optimal material for the scope of the project. This material provided a minimum face width of 3.2cm at the critical contact with associated safety factors of 1.5 and 1.59 for bending fatigue and surface fatigue respectively.

In the final report, shaft designs were finalized. Alterations were made to the preliminary designs as more space was required for the housing of the bearings. In addition, the group removed final gear reduction of the preliminary gearbox design to increase the output speed. Detailed engineering drawings of all shafts with critical locations where detailed fatigue analysis was performed. Using a Matlab script developed by the group, critical diameters were found for each shaft, which were then sized up to accommodate appropriate bearings. After determining the diameter of all shafts, fatigue failure analysis was performed using the stress-life method. Additionally, the group analyzed the shaft that connects a car with the body of the ferris wheel. Appropriate bearings were selected for each shaft in the gearbox by calculating the expected lives.

The final gearbox housing was decided upon by the group, this includes the materials used, layout, fasteners, seals, and couplings. The overall size of the gearbox was made to be 77.2 cm x 58.6 cm x 56.3 cm. The final speed output of the gearbox was determined to be 4 rpm. To conclude the report, the group reflected on the design and commented on further work that may be done to improve the overall function of the gearbox.

TABLE OF CONTENTS:

List of Figures and Tables

Introduction & Background

The City of Victoria is planning to build a ferris wheel to bring excitement to local families. The objective of this report is to provide six conceptual designs for a children's ferris wheel to be installed in the Greater Victoria District. The report will also highlight the project's design objectives and constraints, the ferris wheel specifications and design, an external load analysis, and a conceptual gearbox design. Each conceptual design in this report will be evaluated using a weighted objectives chart (WOC) developed by the group.

The ferris wheel is an iconic component of amusement parks and fairs worldwide as it is an extraordinary feat of engineering. The first ferris wheel was constructed for the 1893 World's Columbian Exposition in Chicago, designed by George Washington Gale Ferris. Ferris was inspired to create a large-scale attraction to rival the Eiffel Tower at the previous World's Fair in Paris. Ferris' outstanding creation stood at 80 meters tall, with 36 cars capable of holding up to 2,160 people.

Although the City of Victoria is not looking for a ferris wheel as large as Ferris', the same engineering principles and challenges still apply for this project. Ferris wheels are complex machines due to the multitude of moving parts. Ferris wheels must have a strong support structure upon which the wheel rotates. The cars must provide both safety and comfort and must be attached to the frame to ensure they stay upright during operation. Ferris wheels are powered by a sophisticated drive system consisting of a combination of motors and gears. This project will be powered by an electric motor that has 1750 rpm and a power output of 0.5-5 kW. The gearbox for this project is assumed to be 97% efficient. Lastly, the safety of the passengers is of critical importance. The group must ensure that the structure is capable of handling the load of all of the passengers and have an expected lifetime of 20 years. The daily time of operation and ferris wheel operating speed will dictate the lifetime of the project, both of which will be determined by the group to provide a comfortable and safe experience for users.

Literature Review

Commercial Ferris Wheel Designs

Commercial ferris wheel designs vary in size, complexity, and features, but they all share the same basic concept of a rotating vertical wheel with passenger cabins or gondolas attached. The most common ferris wheel designs are known as motorized capsules, centerless wheels, transportable wheels, double/triple wheels, and eccentric wheels.

- Motorized capsule
    - Rotates about a central hub.
    - Wheels with passenger cars mounted externally to the rim and independently rotated by electric motors to stay upright.
    - Holds the record for the current tallest ferris wheel, the 250m tall Ain Dubai.

Figure 1: Ain Dubai [1]

Figure 2: Ain Dubai Capsule [2]

- Centerless wheels
    - There is no central hub and the rim of the ferris wheel stays fixed in place. Each capsule travels around the circumference of the rim..

Figure 3: Bailang River Bridge Ferris Wheel [3]

- Transportable wheels
    - Designed to be operated at multiple locations, either permanently mounted on trailers for smaller ferris feels or designed to be repeatedly dismantled and rebuilt for larger ferris wheels.

Figure 4: Trailer mounted ferris wheel[4]

Figure 5: Partially Dismantled Ferris Wheel [5]

- Double and triple wheels
    - Consists of multiple independent ferris wheels, each rotation at either end of a cantilever arm rotating about its middle pivot point.

Figure 6: Double Ferris Wheel[6]

Figure 7: SKY WHIRL Triple Ferris Wheel [7]

- Eccentric wheels
    - Commonly known as sliding or coaster wheel.
    - Some or all of its passenger cars are not fixed directly to the rim of the wheel, but instead slide on rails between the rim and the hub as the wheel rotates.

Figure 8: Pixar Pal-A-Round [8]

Figure 9: Pixar Pal-A-Round Sliding Capsules [9

Documented safety issues

Ferris Wheels are subject to rigorous regulations and inspections to ensure the safety of passengers. Over the years there have been documented incidents and safety issues. Some of the safety issues include:

- Mechanical Failures
  - Issues with the rides motor, gears, or structural components causing the ride coming to a sudden stop or other unexpected movements.

- Capsule or Gondola Malfunctions
  - Occasionally capsules or gondolas can become detached or experience issues with their safety restraints.

- Structural Problems
  - Corrosion or material fatigue in the wheels frame or support structure can compromise the rides safety.
  - Regular inspections are crucial to identifying and addressing these issues.

- Electrical Issues
  - Can lead to problems with the rides lighting, safety systems, or controls.

- Operator error
  - Either by rides operators or maintenance personnel.

- Extreme weather
    - Such as strong winds, lightning or heavy rain. Most ferris wheels are designed to withstand a certain level of adverse weather, but extreme conditions can still pose a threat.

- Passenger behavior
    - Passengers who disregard safety instructions, lean out of capsules, or engage in risky activities can put themselves and others at risk.

Drive Mechanisms

Ferris Wheels use various drive mechanisms to rotate the wheel and provide a safe and enjoyable ride experience. The choice of drive mechanism depends on factors such as wheel size, design, and location. Some common ferris wheel drive systems are:

- Electric motor drive
    - Many modern ferris wheels are powered by electric motors typically located at the center of the wheels axle or hub. Can be located on the rim of the wheel.
    - Provide consistent and precise control over the wheels rotation speed and direction.

Figure 10: Electric motor drive [10]

- Hydraulic drives
    - Hydraulic cylinders or motors are connected to the wheels axle or frame and use pressurized fluid to generate rotational force.
    - Generally used on larger ferris wheels.

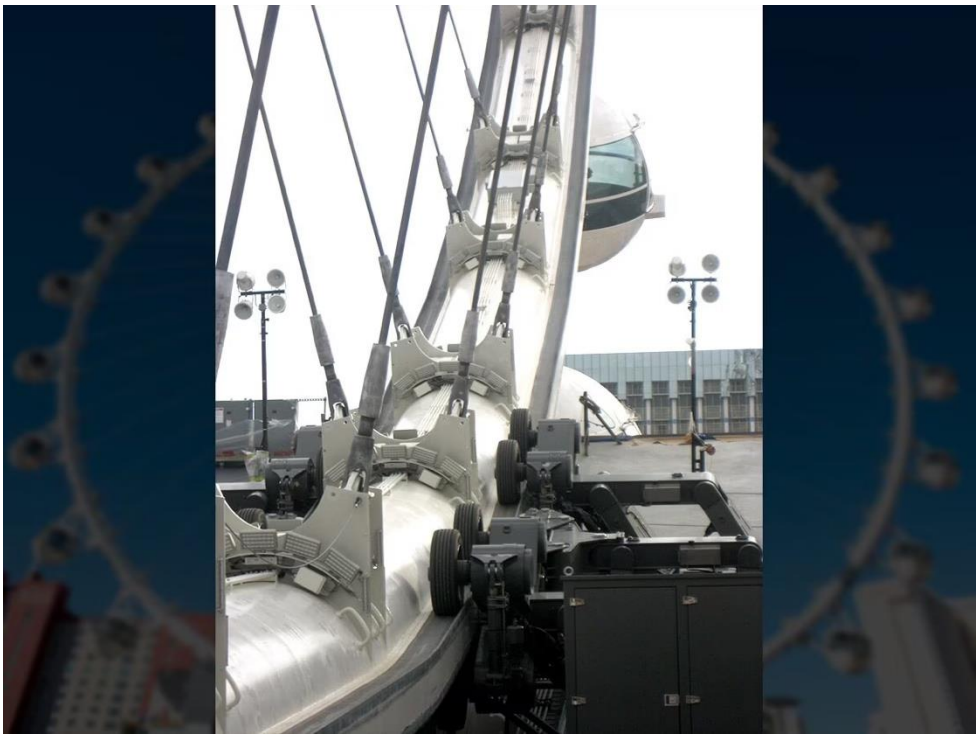

Figure 11: Hydraulic drive system for Las Vegas Observation Wheel [11]

- Friction drives
    - Commonly used in smaller ferris wheels.
    - These systems use friction between a rotating wheel and a stationary surface to generate motion.
    - The operator can adjust the pressure to control the wheels speed.

- Chain drives
    - Commonly used in smaller ferris wheels and resemble bicycle chains.
    - A motor drives a sprocket, which is connected to a chain that is wrapped around the wheels axle or hub. As the motor turns the sprocket, it causes the wheel to rotate.

Figure 12: Chain Driven Double Ferris Wheel [12]

- Geared drives
    - Utilize a system of gears and gearboxes to transfer power from a motor to the ferris wheel.
    - These drives offer precise control over speed and direction.
    - Often used in larger ferris wheels where fine adjustments are crucial.

- Counterweight systems
    - Commonly found in historic ferris wheels such as the original 1893 ferris wheel designed by George Ferris.
    - A system of counterweights, ropes, and pulleys would provide the force to turn the wheel.

- External drives
    - Drive mechanism is located externally such as at the base of the wheels support structure.
    - Can use various drive methods such as gears, chains, or hydraulic systems to transmit power to the wheel.

Alternative Concepts

Concept 1: Jurassic Fun Wheel (Cole Manton)

In this design concept, the main theme will be dinosaurs. Instead of traditional ferris wheel carts, this ride would feature custom-made carts that mimic various kid friendly dinosaur species. Passengers would step into carts designed to look like the body of a stegosaurus, triceratops, or even a T-rex. As the ferris wheel rotates, it would emit sound effects to recreate the ambient sounds of a prehistoric world. Visitors might hear the roars of different dinosaurs, the rustling of vegetation, creating a multisensory experience. The ferris wheel would operate on the grounds of the royal BC museum, where there is currently a dinosaur's of BC exhibit. The royal BC museum welcomes many tourists both from Canada and around the world from the many cruise ships docking not far away. Passengers could tour the exhibits and take a ride on the dinosaur themed ferris wheel to complete their journey to a prehistoric world.

This ferris wheel will consist of a central support structure with six individual arms connected to one passenger cart each. The carts will have a low center of gravity ensuring they stay vertical as the arms rotate about the central support connection. The carts will be connected at the rear to the support arm via a rod and bearing allowing them to freely rotate. The central support arm will be mounted to a large rectangular water ballast, which will also act as the base of the structure. This will allow for relatively easy relocation or transportation. This design will utilize a helical gearbox. This gearbox design offers efficiency, quiet and smooth operation, and a high load carrying capacity. A helical gearbox is ideal for this application because it offers a compact design. This is crucial as this gearbox will be mounted directly to the rear of the central support structure.

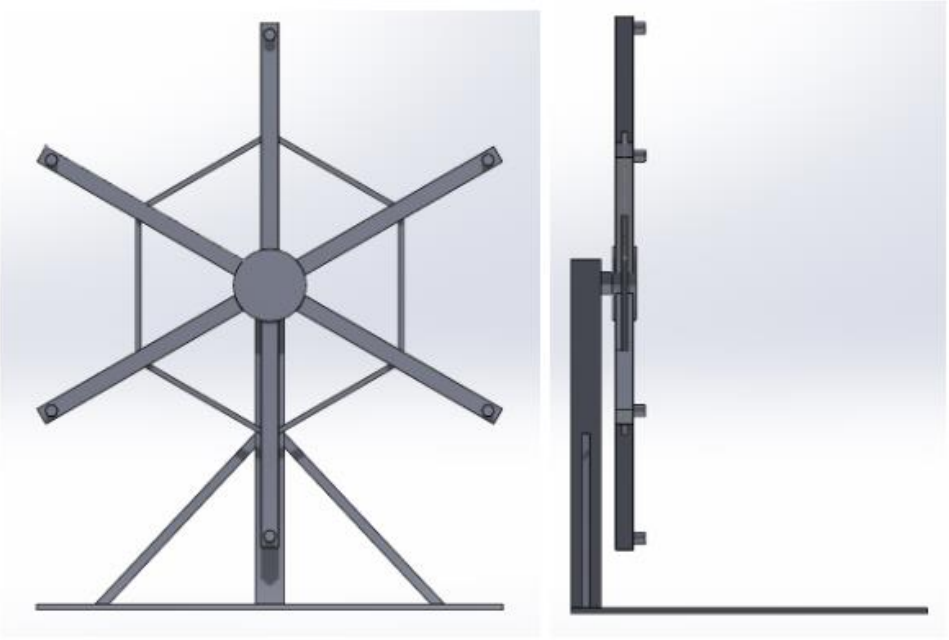

Figure 13: Cole's ferris wheel design

Concept 2: Race Car Championship (Marek Ooms)

For this concept, the theme would be a car race, with each cart being a different coloured and styled race car. Each car could model existing racing car classes, such as Formula 1, NASCAR, World Rally Championship, etc allowing customers to each have a unique car. The ride would have six cars and be an externally driven ferris wheel.

The wheel would be supported on the backside only, and riders would enter and exit each car from the front. This design would be safer for the riders of the ferris wheel, most of which would be children. This design would create a cantilevered mass on the top of the support structure, and would require proper bracing/strength of the support structure.

The ferris wheel would be driven by a motor located in the base of the support structure directly driving a drive chain. The drive chain would then be the input to a planetary gearbox located at the top of the support structure behind the wheel and cars. This design features a lowered center of gravity, as the mass of the motor is located at the base, and thus less of a torque acting on the base of the support structure. Additionally, the motor is easier to access and service being close to the ground. A planetary design allows for a compactly packaged gearbox, and adding additional planetary gears allows for lower net stresses on each individual gearset.

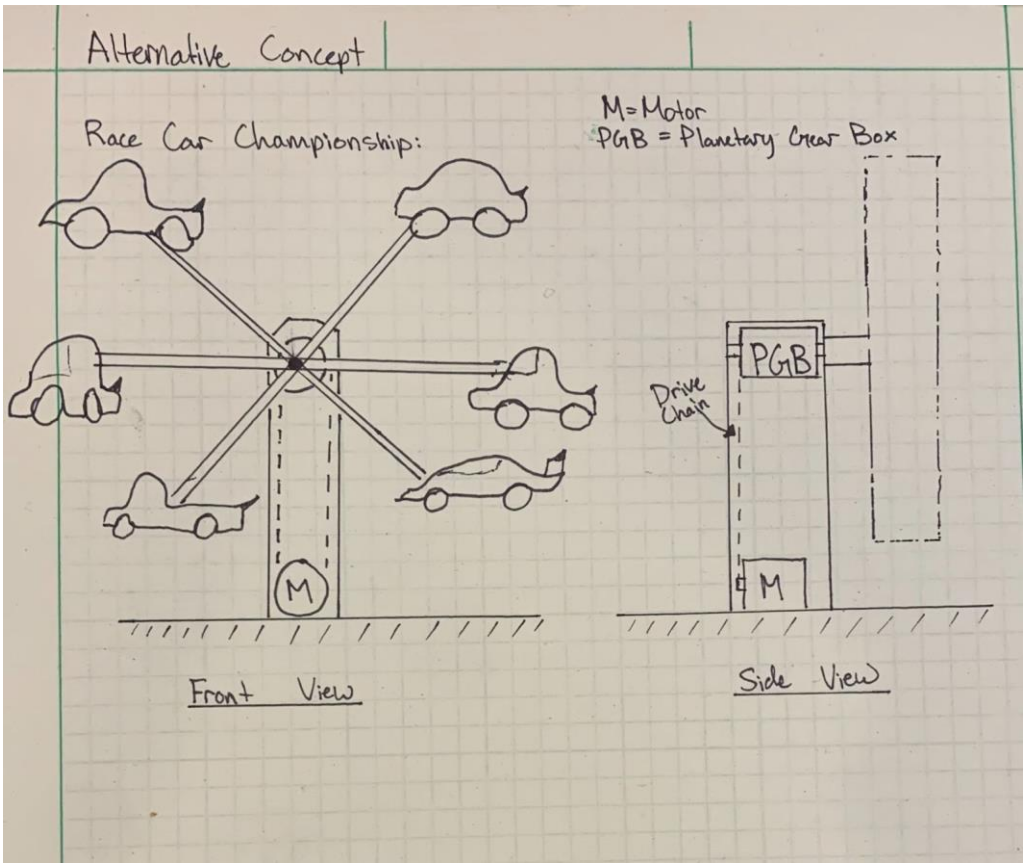

Figure 14: Marek's Ferris Wheel Design

Concept 3: The Space Odyssey (Dhruv Jethwa)

In this design concept, one of the main things that would be evident is the spaceship theme where all the baskets for the customers would be in the form of tiny spaceships along with carrying this theme along to the rest of the Ferris wheel as well. In this case, all the baskets would be different and would try to take the form of some of the greatest rockets designed by mankind.

The location proposed to place The Space Odyssey would be by The Dominion Astrophysical Observatory. It would be best displayed around the summertime when there is a larger crowd of tourists to showcase all that the observatory has to offer regarding the wonders of space exploration and the essential role that observatories play in the development of the future of space exploration.

Along with the visual design mentioned, the Ferris wheel itself would be one with overhanging arms over the baskets and fashioned in the form for enough clearance upon revolution. There would be six arms to support the six baskets (reflecting the number of people in our group). The Ferris wheel in this design would be supported from one side so that the loading and unloading can be done from the front side.

The gearbox proposed to be used in this design is the Planetary Gearbox. This is because this type of gearbox is best used with electric motors that need to provide high torque. The planetary gearbox is best used for its high torque and low speed which meets the requirements of a wheel design of this specification.

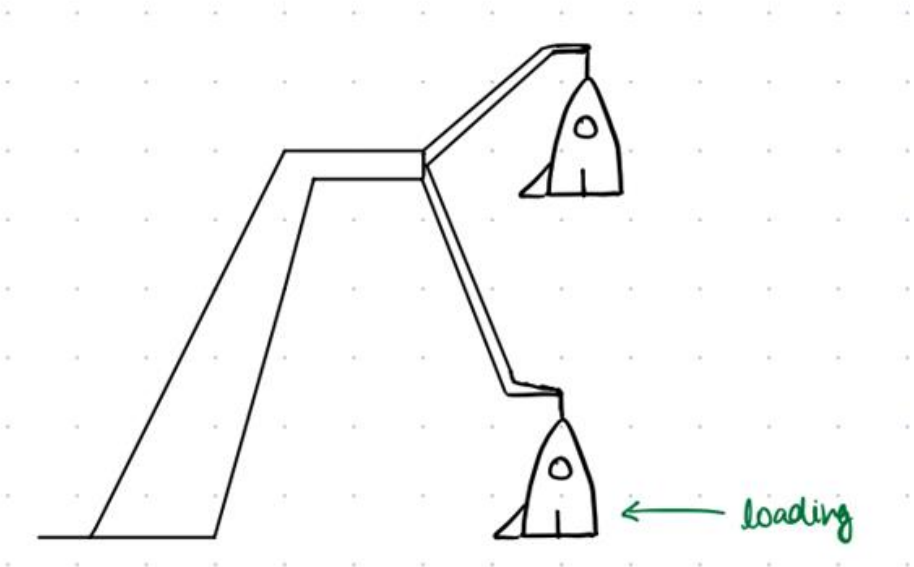

Figure 15: Side Profile of The Space Odyssey front loading design

Concept 4: Garden Excursion (Jack Martin)

The design of this concept will feature some of Victoria's most popular animals. The outdoor themed ferris wheel will have six cars, each painted and designed as a different animal local to the greater Victoria area (rabbit, squirrel, deer, bear, cougar, eagle). The idea is that although they all follow a theme, they are each unique and will therefore draw children in for different reasons.

The ferris wheel will operate on the grounds of Butchart Gardens. Butchart gardens welcomes over 1 million visitors each year, many of which are families. The gardens are a popular attraction in both the summer, when the flowers are in bloom, as well as in the winter, when the gardens feature holiday-themed lights. This location will allow the ferris wheel to operate year-round, or just in peak seasons if that is preferable, and take advantage of the large amounts of traffic it sees each year.

The ride will be attached in the center with six equally-spaced double arms extending from the center wheel, which will be supported on both sides. The users will enter the car through a gate on the left (when viewed from the front) when the car is at the bottom position, this will ensure that the ride has a uniform weight distribution when at rest. This ferris wheel will implement a helical gearbox as it will need to be compact and low power consumption is preferable. The helical gearbox is also known for producing a very smooth operation which will be crucial as the ride is for children. Additionally, a helical gearbox will produce lower noise compared to other gearbox configurations which is ideal considering the ride will be located in a garden setting.

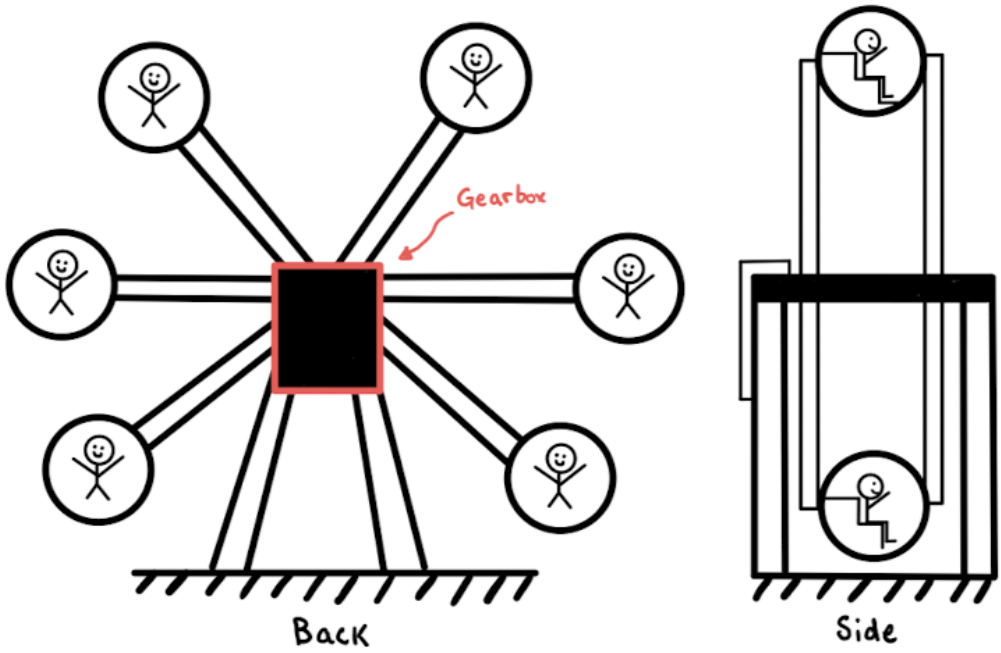

Figure 16: Jack's ferris wheel design

Concept 5: Petting Zoo Carousel (Jack Walmsley)

The Beacon Hill Park Petting Zoo is a common attraction for both tourists and locals in the Greater Victoria area. The addition of a ferris wheel to the community will bring much needed change and create a great atmosphere for young families. The cars of the ferris wheel will be decorated with cartoon goats created by local artists.

The six cars of the ferris wheel will be supported at the center and should be designed to ensure safety, stability, and comfort for the riders. A central support structure should be utilized to ensure that the cars rotate around a stable axis. Additionally, a counterweight system would need to be implemented to maintain stability of the cars as well as the entire system. Because the cars will be supported at the center, high quality bearings will be required to ensure smooth rotation of the cars around the central axis. Regular testing will need to be done on the bearings to ensure that they are properly lubricated.

This design will use a helical gearbox. This type of gearbox has excellent efficiency and can transmit high torque while minimizing noise and vibration. Helical gearboxes provide smooth and continuous meshing of teeth, resulting in less vibration in comparison to other gearbox assemblies. Additionally, helical gears can handle high torque loads, which is critical in ferris wheels for supporting the weight of the passenger cars.

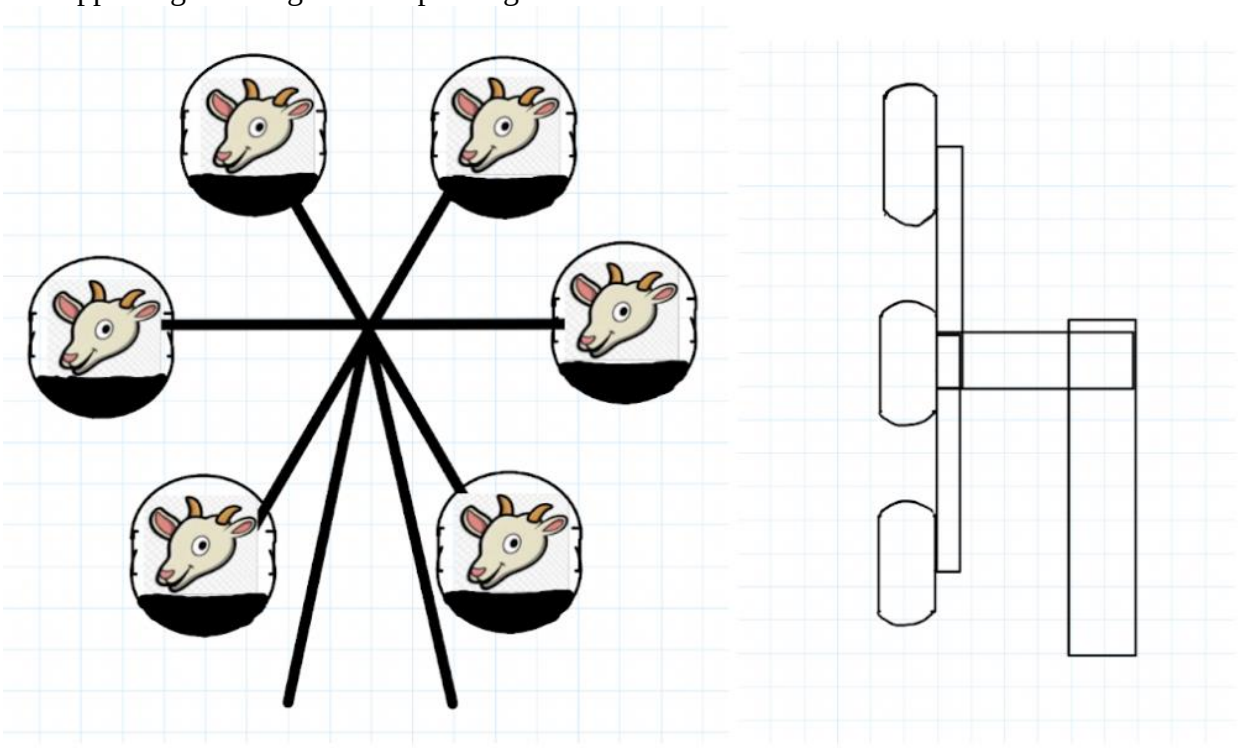

Figure 17: Initial design of Petting Zoo Carousel

Concept 6: Bubbles (Brandon Groot)

The theme of this ferris wheel will be bubbles. It will consist of six single-person carts that will be spherical and clear to simulate that the kids are in bubbles. The carts will be made out of a strong plastic like polycarbonate and will attach to the arms of the ferris wheel via a bar that inserts across the center of the bubble. The bar will also act as a hand hold for the children. There will be a seat at the bottom of the bubble to support the children as well. The seats will be flat and rectangular with cushioning on the top rather than ergonomically shaped because the size and shape of children varies tremendously.

The structure for the ferris wheel will be made up of a metal frame and sheet metal to cover the frame, motor, and gearbox. The motor and gearbox will be mounted to the top of the structure directly behind the spinning part of the ride. Although the placement of the motor and gearbox may give the ferris wheel a higher center of gravity, it will greatly reduce the difficulty of transferring the power from the bottom to the top of the structure. The motor will be connected to the helical-style gearbox which will reduce the speed of the motor to the desired speed for the ride.

The spinning part of the ferris wheel will consist of six arms with the bubble carts attached at the ends of each. There will be bars connecting each arm together to improve strength and prevent there from being too much stress at the point of attachment to the center.

The following sketch provides a visual of the ferris wheel where M is the motor and G is the gearbox:

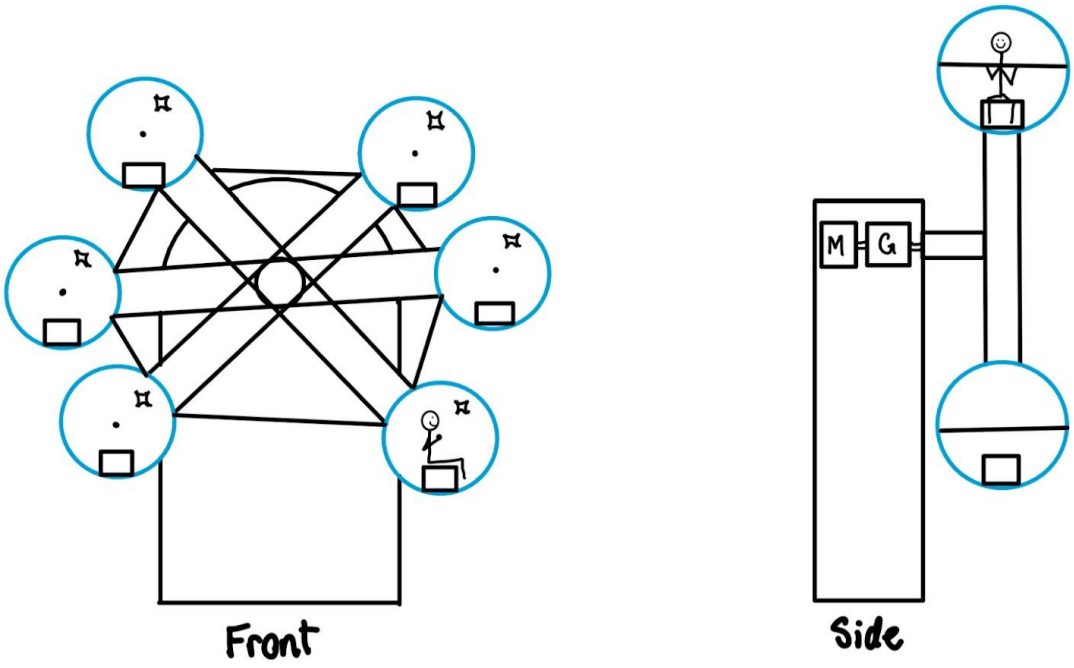

Figure 18: Brandon's ferris wheel design

List of Design Objectives and Constraints

Table 1: Design Objectives and Constraints

Design Objective/Constraint	Quantifiable Value	Justification
Height	≤ 6m	The height of the ferris wheel be less than or equal to 6 feet to meet both cost and safety requirements
Number of passengers	6	The ferris wheel should have 6 carts, capable of carrying one child each
Cart mass	≤ 120 kg	Ferris wheel carts should have a mass less than 100 kg to avoid unnecessarily large moment to be created about shaft
Output Velocity	4 revolutions/min	The ferris wheel must operate at 2 cycles per minute to ensure adequate safety and comfortability for riders while also providing an exciting experience
Factor of Safety	1.5	As well researched and reliable materials will be used to complete this project a factor of safety of 1.5 is adequate to ensure the safety of the riders
Daily time of operation	8 hours	The ferris wheel will run for 8 hours per day as overuse will diminish the project's lifespan
Power	≤ 5 kW	Power output of the motor is limited to 5 kW
Gearbox efficiency	≥ 97%	Gearbox designed to drive the ferris wheel should be at least 87% efficient

Design Selection

In order to decide between the different design concepts proposed by each member, we implemented a decision matrix to determine the relative strength of each design. Each design concept is scored on a variety of criteria, the weight of which is proportional to the overall importance of the criteria in relation to the project. Criteria were weighted 1-5, with 1 being of lesser relative importance and 5 being of utmost importance. Each design concept is then given a score of 1, 3, or 5, in each category (1 being a low score and 5 being a high score), which is multiplied by the weight of the criteria. Finally the scores of each concept are tallied and the winning concept is the one with the highest overall score.

Some factors such as cost of construction, cost of materials, and cost of upkeep were not directly scored. Without more complete designs it is difficult to estimate the exact costs of each design, we will therefore assume they will all be comparable and as such neglect them from this analysis. Upkeep costs are factored into the ease of maintenance and durability criteria.

Table 2: Design concept weighted objectives chart

	Ease of Maintenance	**Durability**	**Gearbox Design**	**Structural Design**	**Total**
Relative Importance (1-5)	**2**	**4**	**3**	**5**	
Dinosaurs (Cole)	**2** x 3 = 6	**4** x 3 = 12	**3** x 5 = 15	**5** x 3 = 15	48
Racecars (Marek)	**2** x 5 = 10	**4** x 2 = 8	**3** x 5 = 15	**5** x 1 = 5	38
Space (Dhruv)	**2** x 5 = 10	**4** x 3 = 12	**3** x 3 = 9	**5** x 3 = 15	46
Animals (Jack M)	**2** x 1 = 2	**4** x 5 = 20	**3** x 5 = 15	**5** x 5 = 25	62
Petting zoo (Jack W)	**2** x 3 = 6	**4** x 3 = 12	**3** x 5 = 15	**5** x 1 = 5	38
Bubbles (Brandon)	**2** x 3 = 6	**4** x 1 = 4	**3** x 5 = 15	**5** x 3 = 15	40

Ferris Wheel Specifications and Design

Table 3: Ferris Wheel Specifications

Height	6 m
Width	5.25 m
Depth	2 m
Total mass	3000 kg
Output speed	4 cycles / minute
Motor power	0.5 kW
Daily time of operation	8 hours

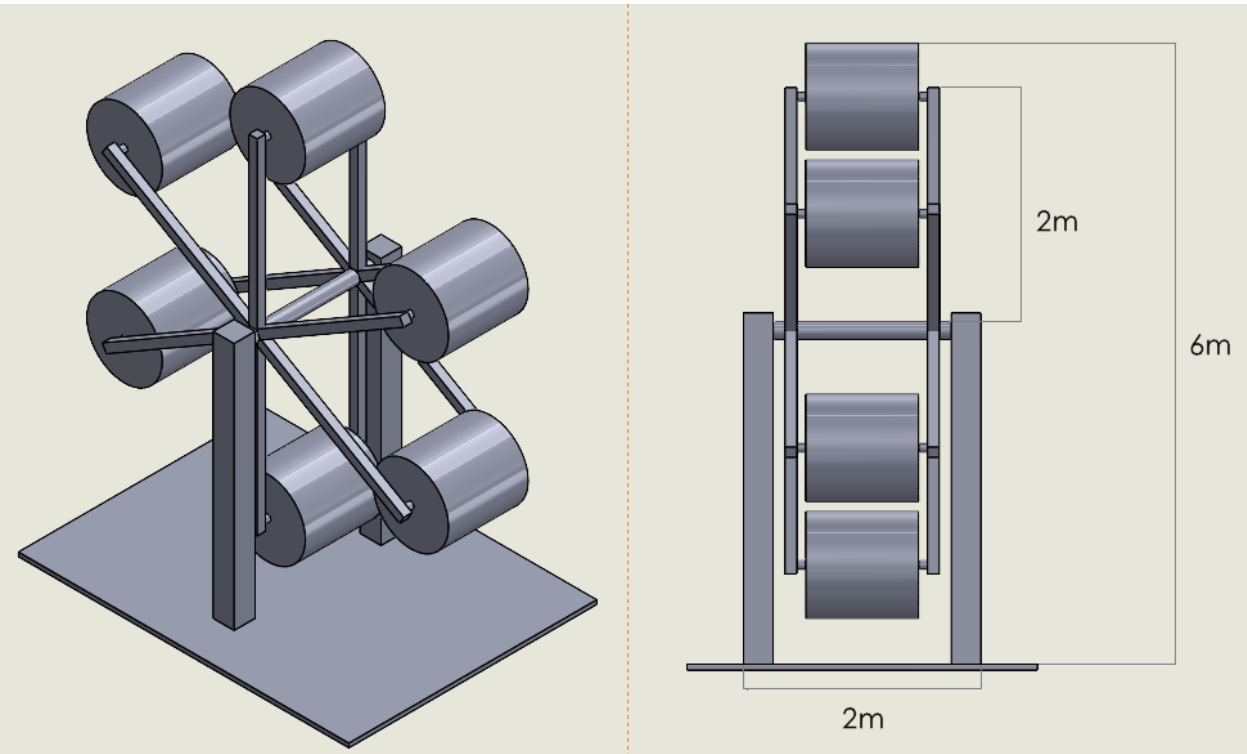

Figure 19: Final Ferris Wheel Design

External Load Analysis

The children, carts, and arms of the ferris wheel all develop a moment about the central axis of the ferris wheel's shaft. The material by which the carts and arms are made of must be decided on first before conducting an external load analysis. The group has decided on using low carbon steel for the arms of the shaft because of its high yield strength that is required to support the load of the cart and the child, and due to its cost in comparison to other commonly used steels. The group also decided that 2 meter long I-beams would be used for the arms to increase overall strength of the design. The carts will be manufactured through a combination of steel and aluminum to provide adequate strength, reduce weight, and minimize costs.

Using the A36 Low Carbon Steel I-beams for the arms and the support structure, we get the following results for the properties of the material:

Yield strength: $50{,}000 \text{ psi } = \ 3.44738 * 10^8 \frac{\text{N}}{\text{m}^2}$

Moment of inertia of arm: $I = \frac{bh^3}{12} = \frac{(0.1016)(0.2032)^3}{12} = 7.104 * 10^{-5}$

Assuming that for each arm, there is a 100kg carriage along with a child of maximum weight 37kg, we get that the largest force applied on the end of the arm would be:

$P = (100kg + 37kg)\left(9.81\frac{m}{s^2}\right) = 1343.97\ N$

Using the properties gathered for the steel being used in the ferris wheel, we concur that the maximum deflection to be observed by each arm would be (assuming a cantilever beam with loading at the unsupported end):

$$Maximum\ Deflection = \frac{PL^3}{3EI} = 1.839 * 10^{-4} m$$

The calculations done to determine the strength of the chosen I beam shows that this material will help increase the overall strength of the design considering that it is more than strong enough to tolerate the applied loads.

The mass of the children riding the ferris wheel was decided during a lab session activity. The masses for the children riding the group's ferris wheel are: 37 kg, 32 kg, 30 kg, 28kg, 23kg, and 15kg.

When evaluating the moments created by the loads that act on the ferris wheel, the group determined that the arrangement of the carts is symmetrical across both the vertical and horizontal axes of the shaft. Therefore, there is no moment created on the shaft by the carts and arms at any instant. For a complete analysis of the system, the group calculated the moment created by an empty cart at any point in time through a MATLAB script. The output of the script shows the moment created versus the angle in degrees which is shown in Figure20. The plot clearly shows that the maximum moment that can be created by a cart around the shaft of the ferris wheel is 1960 Nm.

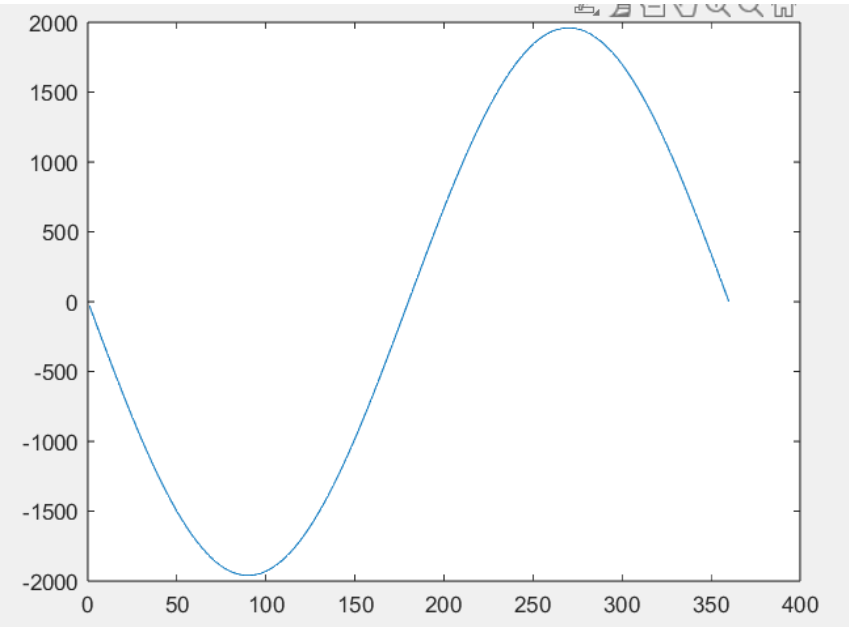

Figure 20: Moment versus angle plot for cart

The group also calculated the moment created by a single arm at any point in time through the MATLAB script. The output of the script shows the moment created versus the angle in degrees which is shown in Figure 21. The plot clearly shows that the maximum moment that can be created by an arm around the shaft of the ferris wheel is 1176 Nm.

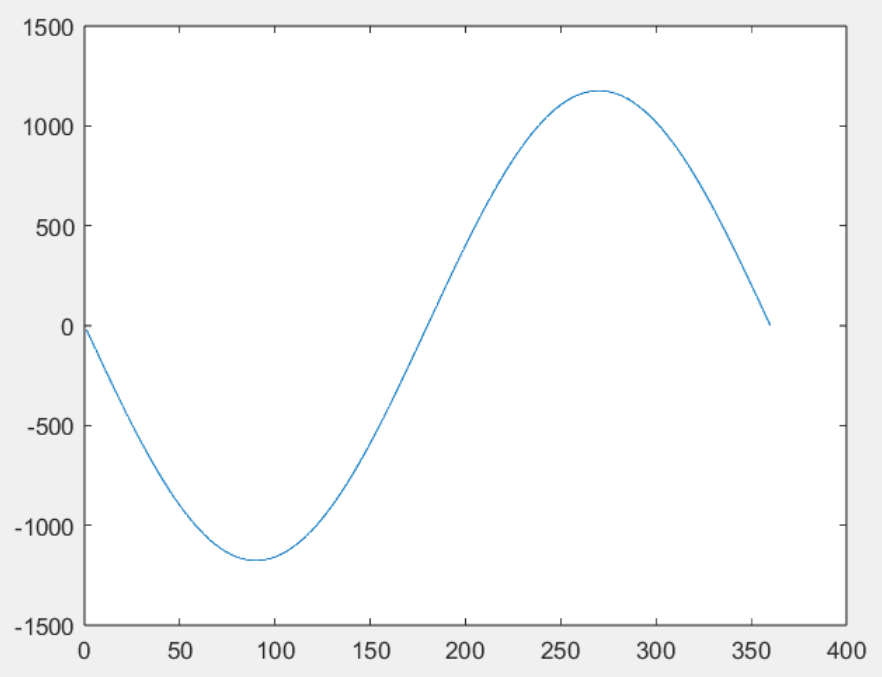

Figure 21: Moment versus angle plot for arm

The group concluded that the arrangement of the children on the ferris wheel will determine the maximum torque that is placed on the rotating shaft. The group investigated a variety of scenarios to compare which loadings would create the maximum moment. The first scenario that was explored was when the children were all loaded on the ferris wheel in no particular order. The free body diagram and corresponding moment calculations are provided for this scenario in Figure22.

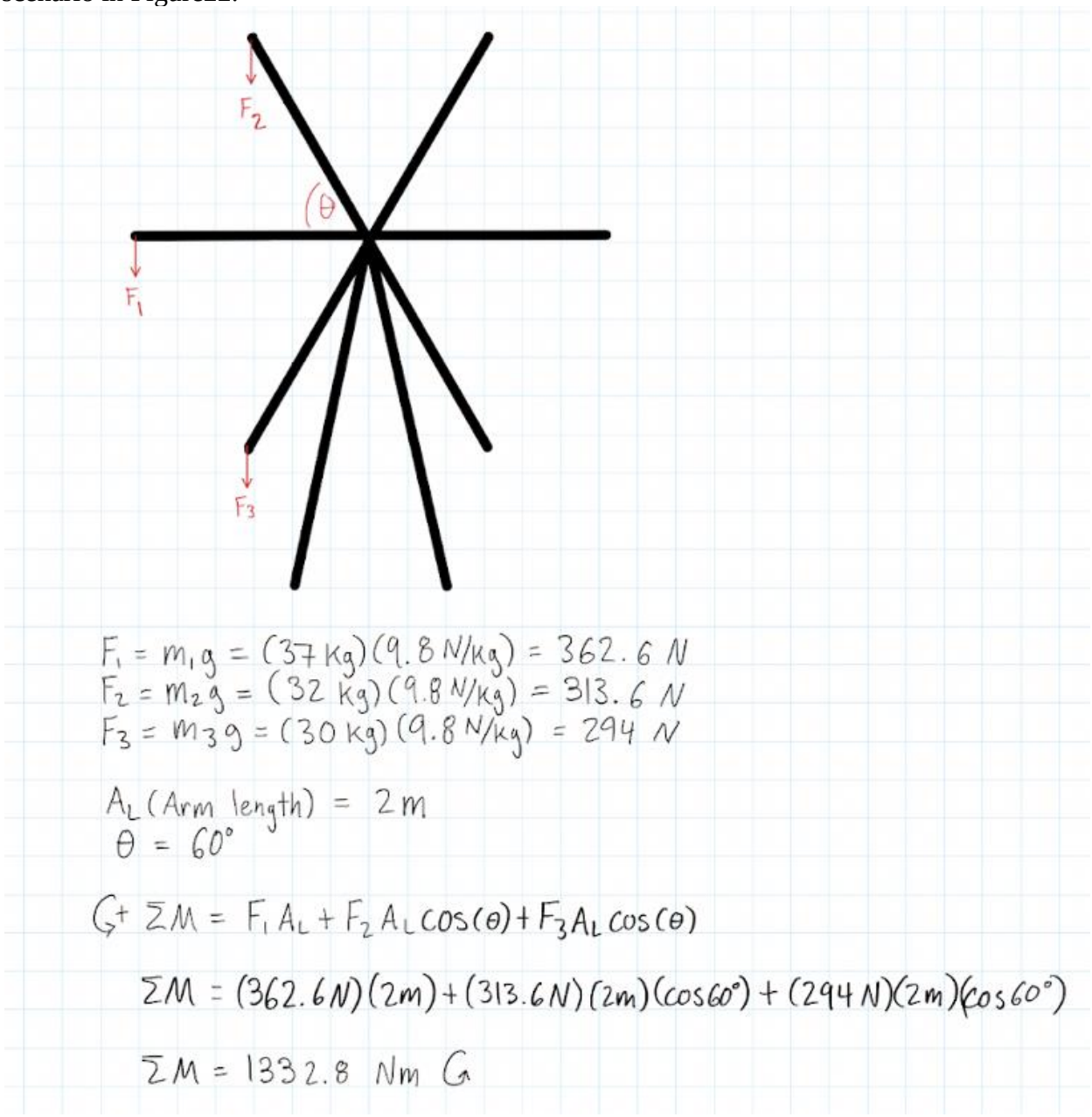

Figure 22: Moment calculations for loading scenario 1

The second scenario considered had all of the children loaded onto the ferris with the heaviest on one side and the lightest on the other side. The free body diagram and calculations for this scenario are shown in Figure 23.

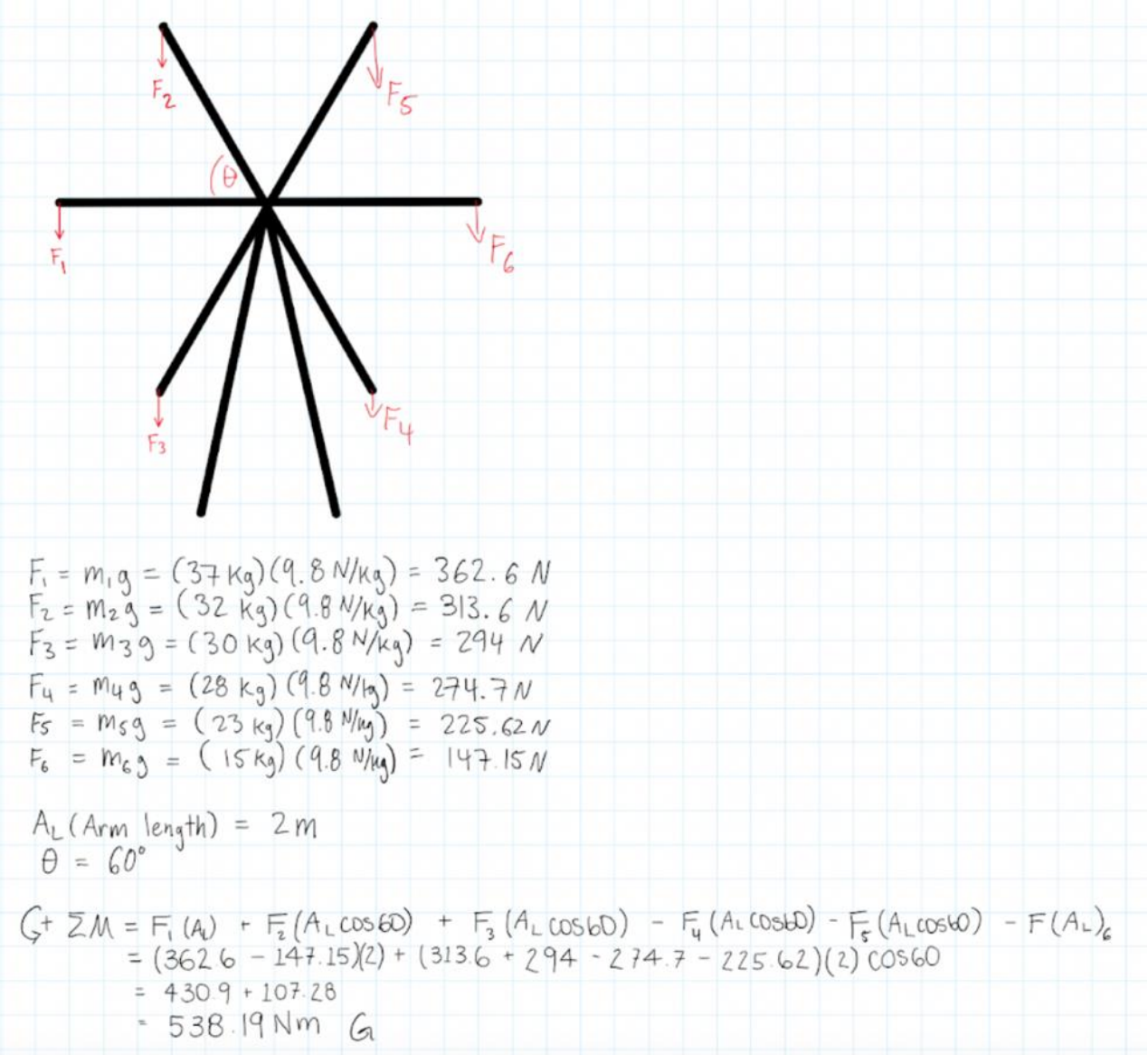

Figure 23: Moment calculations for loading scenario 2

The third scenario considered had all of the children loaded onto the ferris with the heaviest on one side and the lightest on the other side. Unlike the previous, this scenario has two of the arms aligned with the vertical axis of the shaft. The free body diagram and calculations for this scenario are shown in Figure 24.

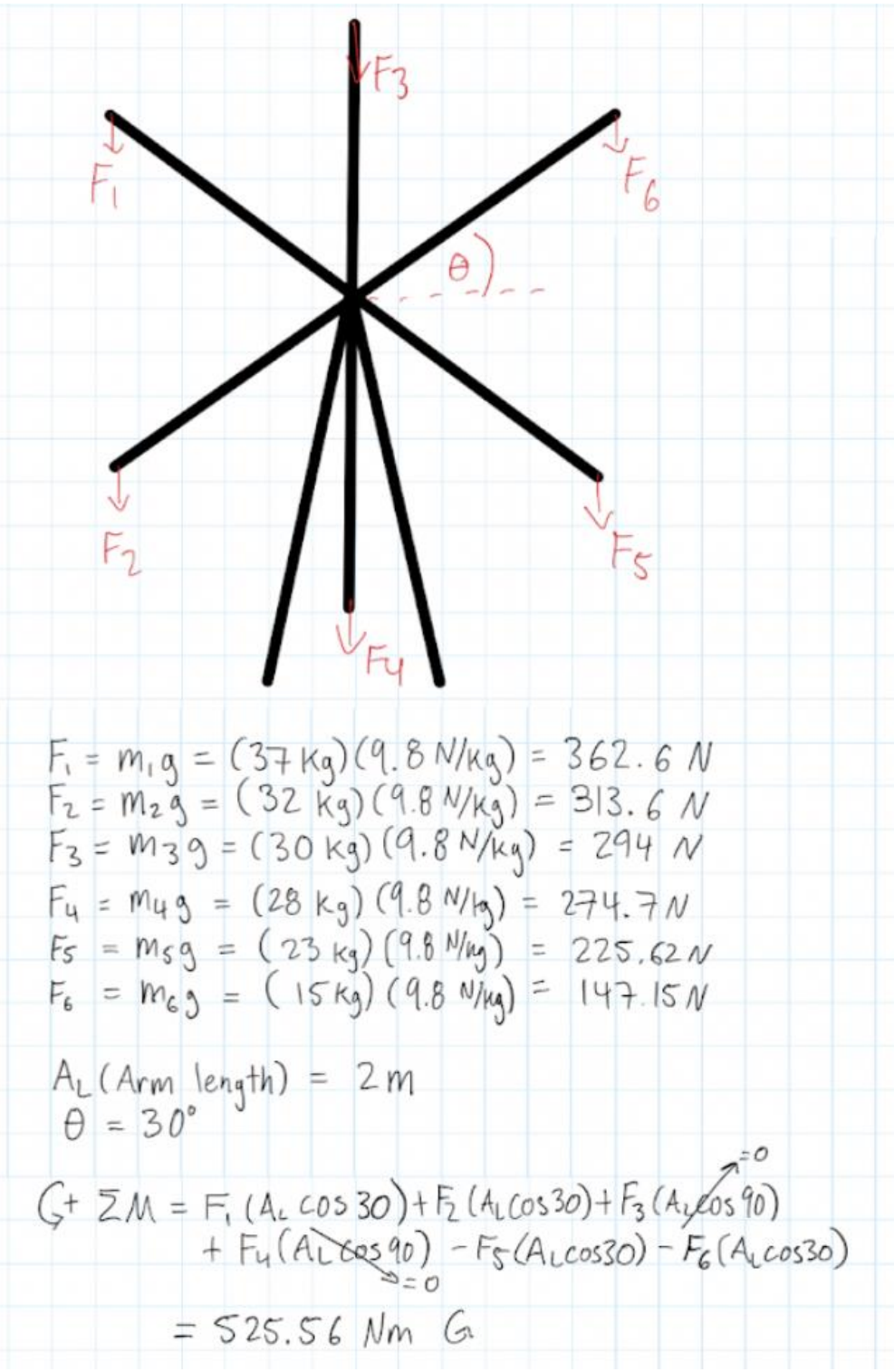

Figure 24: Moment calculations for loading scenario 3

From this analysis we can determine the maximum torque that will be produced when the ferris wheel is fully loaded with kids is in scenario two. In scenario two, the arm with the heaviest

child is aligned with the x-axis of the shaft. The next two heaviest children would be at 60 degrees above and below the arm along the x-axis of the shaft. The other 3 children are located on the other side of the vertical axis of the shaft with the lightest child on the arm along the x-axis of the shaft. However, in the event the ferris wheel is not fully loaded the maximum torque created on the shaft is displayed in scenario 1.

Another type of force that acts on the ferris wheel that must be considered is the centripetal force that is acting on all 6 carriages. Centripetal forces work inwards into the object. This force is also dependant on its displacement from the center of rotation and the velocity of the mass.

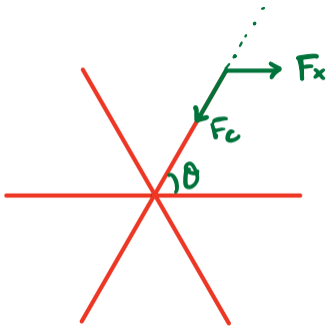

Figure 25: Centripetal force of carriage

To find the magnitude of the force acting on the carriage, the following equation is used:

$$F_{centripetal} = \frac{mv^2}{r}$$

Considering that all the carts weigh the same (100kg) along with the known angular velocity and displacement from the center of rotation – *r*, the magnitude of the centripetal force for each of the carriages is as follows:

$$F_{centripetal} = \frac{(100kg)\left(0.419\frac{rad}{s} * 2m\right)^2}{2m} = 35.11N$$

While there is approximately 35 N of centripetal force acting inwards on each arm of the ferris wheel, since there are 6 individual arms that are equally spaced apart, the forces all cancel out against the centripetal force acting upon the opposite arm as shown in the figure below.

However, since the children on the ferris wheel all have different masses. The sum can be calculated for the worst case scenario as shown in the figure below. In the figure, the opposite arms from one another counteract the centripetal forces of one another. Therefore, the total centripetal force acting on it would just be the residual that does not get cancelled out since the children are all of different masses.

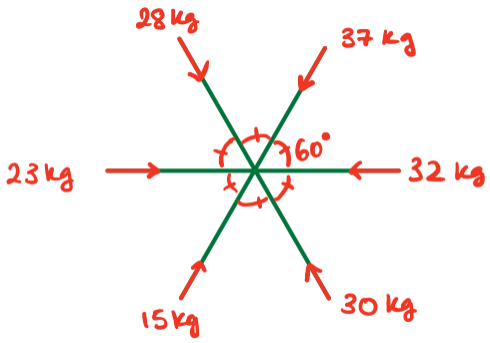

Figure 26: Diagram of centripetal forces working to cancel each other out

$$\Sigma F_c = \left(F_{c,37kg} - F_{c,15kg}\right) + \left(F_{c,32kg} - F_{c,23kg}\right) + \left(F_{c,30kg} - F_{c,28kg}\right)$$
$$\Sigma F_C = 7.724N + 3.160N + 0.702N = 11.586N$$

As seen by the calculations, we find that the total excess centrifugal force acting upon the center of rotation of the ferris wheel is approximately 11.6 N. The value when compared to the gravitational force is negligible. Therefore the centripetal force is not taken into account for the overall torque calculations and such since it has such a minor effect in the grand scheme of the operation of the ferris wheel.

Gearbox Design

Compound gear reduction gearbox: (gear teeth ratios required, can be made compact based on the layout of the shafts and gears)

Overall Gearbox Ratio: 875:1

First, we find the required input Torque needed based on the output torque requirement.

$$\frac{T_{in}}{T_{out}} = \frac{\omega_{out}}{\eta\omega_{in}} = \frac{2[rpm]}{\eta 1750[rpm]} => T_{in} = \frac{T_{out}}{\eta 875} = 0.634[Nm]$$

Based on the required input torque, we can find the required input power.

$$P_{in} = T_{in}\left(s_{rpm} * \frac{2\pi}{60}\right) = 0.615[Nm]\left(1750[rpm]\frac{2\pi}{60}\right) = 112.71\left[\frac{Nm}{s} = W\right] = 0.11271[kW]$$

Next, as the minimum power requirement of the motor is 500W and our necessary input power requirement is 112W, we find the input torque based on the minimum input power requirement of 500W.

$$T_{in}max = \frac{P_{in} * 9.5488}{rpm} = \frac{(500W * 0.97)(9.5488)}{1750rpm} = 2.646[Nm]$$

Finally, we find the output torque based on the 500W input power.

$$\frac{T_{in}}{T_{out}} = \frac{\omega_{out}}{\omega_{in}} => T_{out}max = \frac{T_{in} * \omega_{in}}{\omega_{out}} = \frac{2.646[Nm] * 1750[rpm]}{2[rpm]} = 2315.58[Nm]$$

We found that the input torque based on the minimum motor power requirement of 500W is 2.32[kNm] which is much greater than our maximum output torque requirement of 0.538 [kNm] by a factor of 4.31.

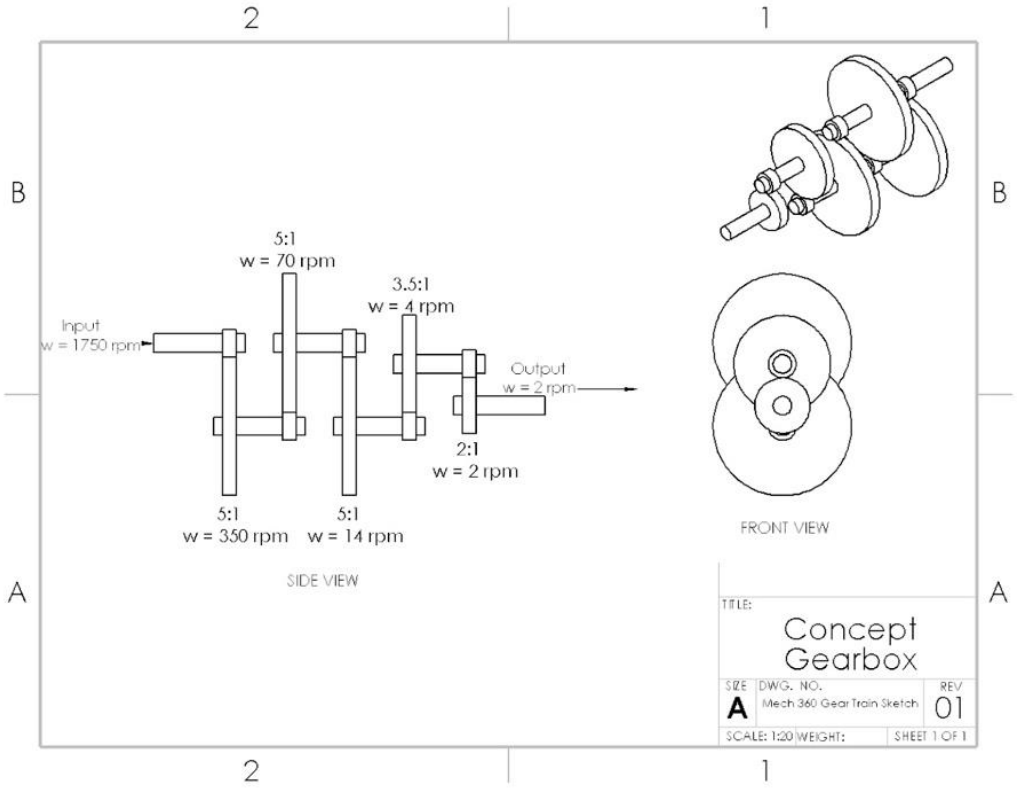

Figure 27: Conceptual Gearbox Sketch

We decided that our input gear would have a diameter of 6 centimeter and we established the necessary gear reduction factors. From there we were able to calculate all subsequent gear diameters, torques, and angular speeds. All of this information has been organized in the table below and a sample calculation is provided.

Our given information for the first gear reduction is:
$D_1 = 6cm\ ;\ \omega_1 = 1750\ rpm\ ;\ T_1 = 2.646Nm\ ;\ gear\ ratio = 5:1$
With this information we can easily find the diameter, speed, and torque of the following gear.

$$D_2 = D_1 * 5 = 6cm * 5 = 30cm$$
$$T_2 = \frac{D_2}{D_1} T_1 = \frac{30cm}{6cm}(2.646Nm) = 13.23Nm$$
$$\omega_2 = \frac{D_1}{D_2} \omega_1 = \frac{6cm}{30cm}(1750rpm) = 350rpm$$

Table 4: Gear sizes for conceptual gearbox

Gear	Diameter (cm)	Number of Teeth	Reduction Ratio	Torque (N•m)	Angular Velocity (rpm)
1 input	6	24	5:1	2.646	1750
2 S1	30	120		13.23	350
3 S1	6	24	5:1	13.23	350
4 S2	30	120		66.15	70
5 S2	9	36	5:1	66.15	70
6 S3	45	180		330.75	14
7 S3	12	48	3.5:1	330.75	14
8 ~~S4~~ output	42	168		1157.63	4
~~9 S4~~	~~12~~	~~48~~	~~2:1~~	~~1157.63~~	~~4~~
~~10 output~~	~~24~~	~~96~~		~~2315.25~~	~~2~~

The group has decided to eliminate the last gear reductions step. This is due to the fact that when the ferris wheel motion was simulated in solidworks, it was determined that the ferris wheel was travelling very slowly – which might not be as enjoyable for the children on the ride if it were travelling that slowly. It was then decided upon further inspection that if the ferris wheel were to travel at four revolutions per minute instead, it would allow for a more enjoyable ride. Therefore, all further calculations conducted were adjusted now been adjusted for this change.

Preliminary gearbox design

The Preliminary gearbox layout is displayed in Figure 28.

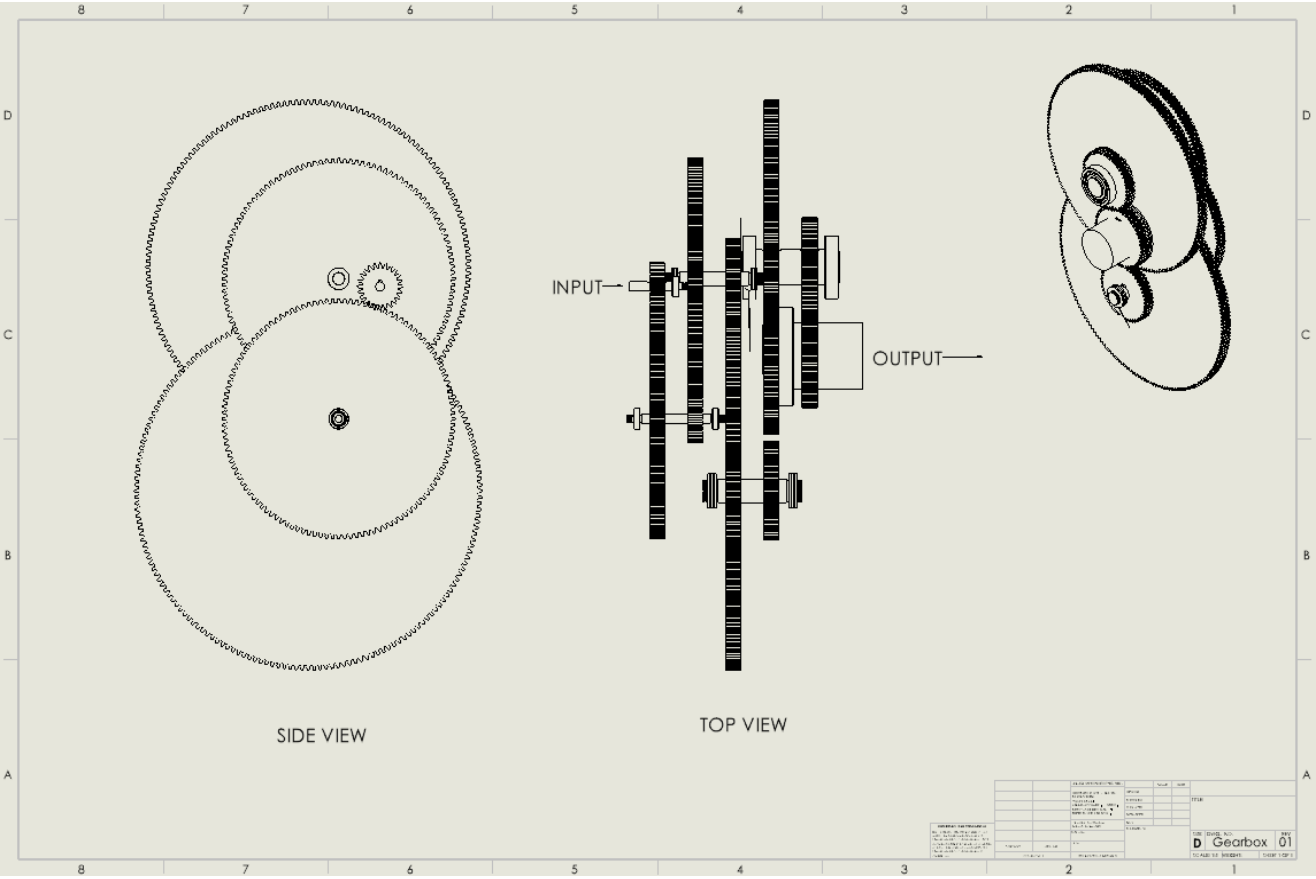

Figure 28: Gear Train

The input shaft is connected to the motor through a coupling and is supported at the other end by a supported bearing. The bearings on all shafts will be fixed to the end, fixated by the shoulders and lock nuts. The gears will be fixated to the shaft through parallel keys; tapered keys and Woodruff keys may be used in later iterations of the design if required.

Assembly Process Flow Chart:

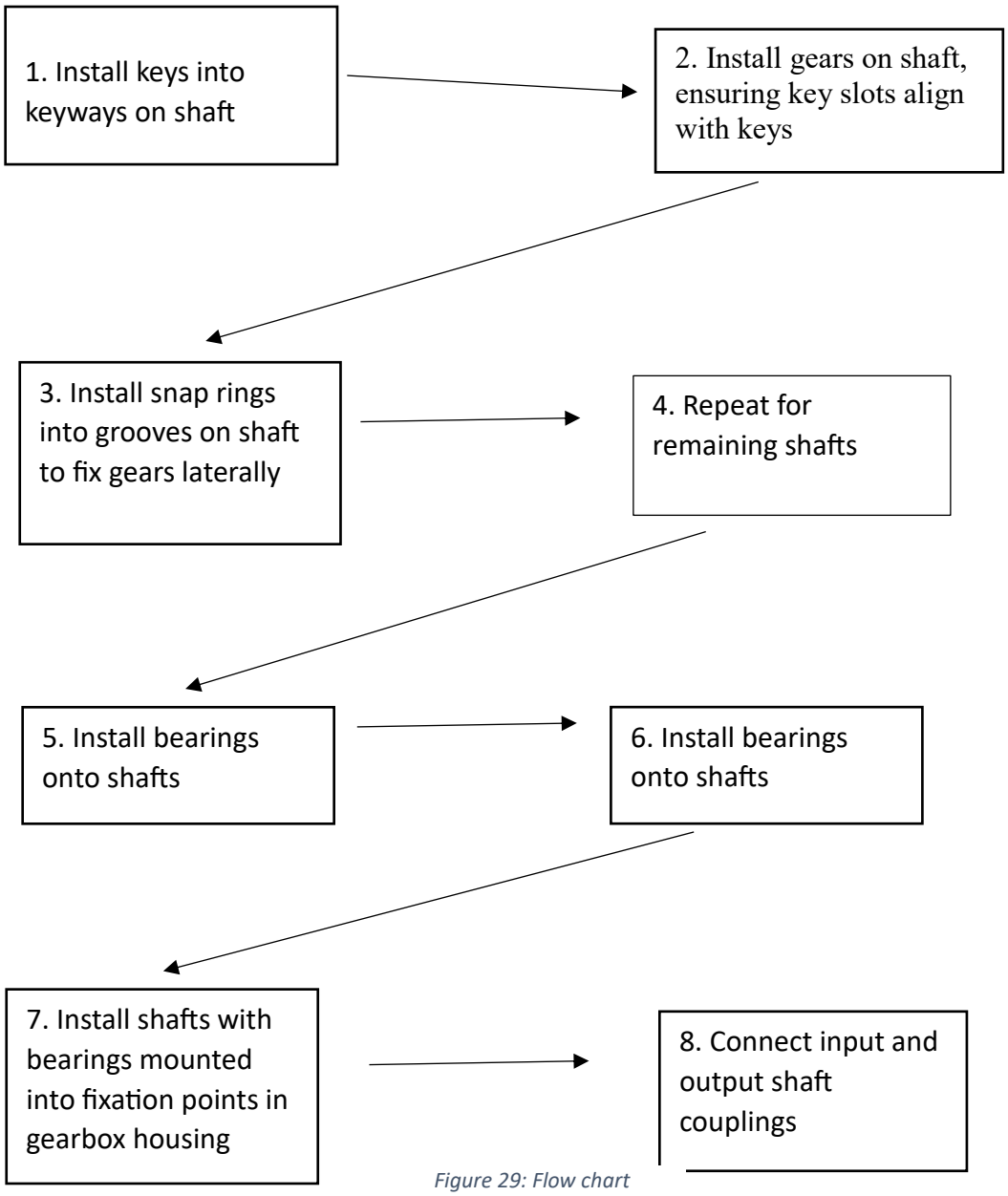

Figure 29: Flow chart

Next, the group must identify locations on the shafts and gears that are potentially critical and where failure analysis will be conducted in the final report. For the shafts, the group believes that the shoulder that fixates the bearings to the ends of the shafts is potentially critical due to change in the diameter. For these shoulders, theoretical stress concentration factors will have to be used to determine what the minimum diameter must to withstand the loads it is subjected to. Another potentially critical location on the shafts is the location of the gears, in particular, the location of the keyways which fixate the gears to the shafts. Due to the large amounts of torque that is being transmitted through gears, large moments will be developed at these locations. The potentially critical locations of the shafts are displayed in the figure below.

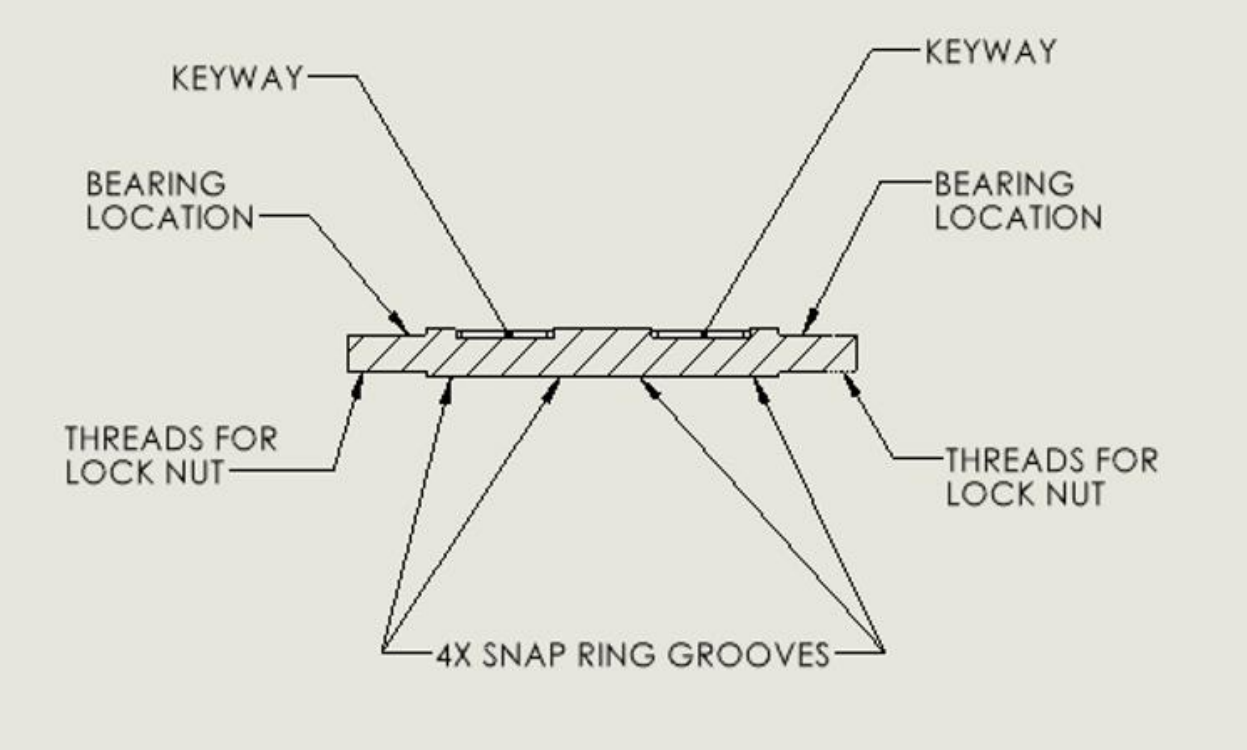

Figure 30: Critical Points on Shaft

The gears in the gearbox will be transmitting large amounts of torque to decrease the given speed of motor to the desired angular velocity of the ferris wheel. The points of gears that are in mesh will be subject to bending stress that can be determined using the AGMA bending stress equation. Later iterations of this report will analyze the bending stress on these gears using this method and the calculated tangential and radial forces to determine an appropriate material for the gears. The location of that gears that is potentially critical is displayed in the figure below.

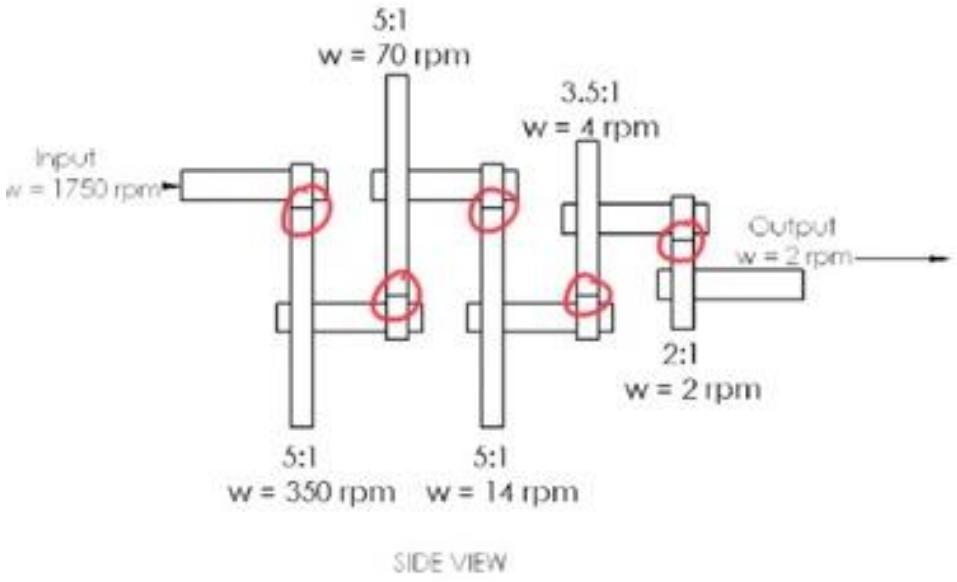

Figure 31: Potential Critical Locations

Gear Design

Final Gear Sizing and Specifications

To begin, the diametral pitch or module must be determined through the following equations:

Module (m) = d/N = 60/24 = 2.5 mm

Diametral pitch (Pd) = N/d = 24/2.362206 = 10.1599in^{-1}

The module and diametral pitch will remain the same throughout the entire gearbox for simplicity. We will be using the diametral pitch for the contact ratio and efficiency calculations below. A standard pressure angle of 20 degrees was chosen as it avoids interference between the set gear and pinion diameters and number of teeth. To find the contact ratio between the pinion and gear we must first find the base pitch diameter Pb using equation 1. Next, we found the pitch diameter for both the pinion and gear using equations 2 and 3 respectively. The addendum can be found using equation 4 based off full depth teeth at a pressure angle of 20 degrees. The center-to-center distance is calculated by the sum of the pinion and gear pitch radii using equation 5. The length of action is then found using the previously calculated pitch radii, center to center distance, addendum, and pressure angle using equation 6. Next, the contact ratio is calculated using equation 7. Finally, the geartrain efficiency is calculated using equation 8.

Gears 1-2, 3-4

Base Pitch

$$P_b = \frac{\pi cos\emptyset}{P_d} = \frac{\pi \cos(20)}{10.1599} = 0.29057in \quad (1)$$

Pitch diameter and radii

$$d_p = \frac{N_p}{P_d} = \frac{24}{10.1559} = 2.36316in, r_p = 1.181103in \quad (2)$$

$$d_g = \frac{N_g}{P_d} = \frac{120}{10.1559} = 11.81579in, r_g = 5.90552in \quad (3)$$

Addendum

$$a = \frac{1.0}{Pd} = \frac{1}{10.1559} = 0.098465in \quad (4)$$

Center to center distance

C= rg + rp = 1.181103 + 5.90552 = 7.086618in (5)

Length of action

$$Z = \sqrt{\left((r_p + a)^2 - (r_p cos\emptyset)^2\right)} + \sqrt{\left((r_g + a)^2 - (r_g cos\emptyset)^2\right)} - csin\emptyset \quad (6)$$

$$Z = \sqrt{((1.181103 + 0.098465)^2 - (1.181103cos(20))^2)} + \sqrt{((5.90552 + 0.098465)^2 - (5.90552cos(20))^2)} - 7.086618sin(20)$$

Z=0.504494in

Contact ratio Gear

$$M_p = \frac{Z}{P_b} = \frac{0.504494}{0.29057} = 1.7362 \quad (7)$$

Efficiency of Gears

$$\eta = 1 - \frac{\mu m_p P_b}{4cos\beta cos\emptyset}\left(\frac{1}{r_p} + \frac{1}{r_g}\right) \quad (8)$$

Where μ is the coefficient of friction, with a lubricant assume μ=0.05, β is the helix angle as this is spur gear β=0, Ø is the pressure angle =20,

$$\eta = \left[1 - \frac{(0.05)(1.7362)(0.29057)}{4\cos(0)\cos(20)}\left(\frac{1}{1.181103} + \frac{1}{5.90552}\right)\right] x\ 100\%$$

$$\eta = 99.318\%$$

Gear train 1-2 and 3-4 have the same pinion and gear diameters and number of teeth resulting in the same contact ratio and efficiency. The contact ratio and efficiency between gears 1-2 and 3-4 was found to be 1.7362 and 99.318% respectively.

Gears 5-6

Base Pitch

$$P_b = \frac{\pi cos\emptyset}{P_d} = \frac{\pi \cos(20)}{10.1599} = 0.29057in$$

Pitch diameter and radii

$$d_p = \frac{N_p}{P_d} = \frac{36}{10.1559} = 3.544738in, r_p = 1.772369in$$

$$d_g = \frac{N_g}{P_d} = \frac{180}{10.1559} = 17.723688in, r_g = 8.8618439in$$

addendum

$$a = \frac{1.0}{Pd} = \frac{1}{10.1559} = 0.098465in$$

Center to center distance

C = rg + rp = 1.772369 + 8.8618439 = 10.634213in

Length of action

$$Z = \sqrt{\left((r_p + a)^2 - (r_p cos\emptyset)^2\right)} + \sqrt{\left((r_g + a)^2 - (r_g cos\emptyset)^2\right)} - csin\emptyset$$

$$Z = \sqrt{((1.772369 + 0.098465)^2 - (1.772369cos(20))^2)} + \sqrt{((8.8618439 + 0.098465)^2 - (8.8618439cos(20))^2)} - 10.634213sin(20)$$

Z=0.5228295in

Contact ratio Gear

$$M_p = \frac{Z}{P_b} = \frac{0.5228295}{0.29057} = 1.7993238$$

Efficiency of Gears

$$\eta = 1 - \frac{\mu m_p P_b}{4cos\beta cos\emptyset}(\frac{1}{r_p} + \frac{1}{r_g})$$

Where μ is the coefficient of friction, with a lubricant assume μ=0.05, β is the helix angle as this is spur gear β=0, Ø is the pressure angle =20,

$$\eta = \left[1 - \frac{(0.05)(1.7993238)(0.29057)}{4\cos(0)\cos(20)}\left(\frac{1}{1.772369} + \frac{1}{8.8618439}\right)\right] x\ 100\%$$

$$\eta = 99.529\%$$

The contact ratio and efficiency between gears 5-6 was found to be 1.799 and 99.529% respectively.

Gears 7-8

Base Pitch

$$P_b = \frac{\pi cos\emptyset}{P_d} = \frac{\pi \cos(20)}{10.1599} = 0.29057in$$

Pitch diameter and radii

$$d_p = \frac{N_p}{P_d} = \frac{48}{10.1559} = 4.7263167in, r_p = 2.363158in$$

$$d_g = \frac{N_g}{P_d} = \frac{164}{10.1559} = 16.148249in, r_g = 8.0741244in$$

Addendum

$$a = \frac{1.0}{Pd} = \frac{1}{10.1559} = 0.098465in$$

Center to center distance

C = rg + rp = 2.363158 + 8.0741244 = 10.4372824in

Length of action

$$Z = \sqrt{\left((r_p + a)^2 - (r_p cos\emptyset)^2\right)} + \sqrt{\left((r_g + a)^2 - (r_g cos\emptyset)^2\right)} - csin\emptyset$$

$$Z = \sqrt{((2.363158 + 0.098465)^2 - (2.363158cos(20))^2)} + \sqrt{((8.0741244 + 0.098465)^2 - (8.0741244cos(20))^2)} - 10.4372824sin(20)$$

Z=0.533863231in

Contact ratio Gear 7-8

$$M_p = \frac{Z}{P_b} = \frac{0.533863231}{0.29057} = 1.8372965$$

Efficiency of Gears 7-8.

$$\eta = \left[1 - \frac{(0.05)(1.8372965)(0.29057)}{4\cos(0)\cos(20)}\left(\frac{1}{2.363158} + \frac{1}{8.0741244}\right)\right] x\ 100\%$$

$$\eta = 99.612\%$$

The contact ratio and efficiency between gears 7-8 was found to be 1.837 and 99.612% respectively.

Gears 9-10

Base Pitch

$$P_b = \frac{\pi cos\emptyset}{P_d} = \frac{\pi \cos(20)}{10.1599} = 0.29057in$$

Pitch diameter and radii

$$d_p = \frac{N_p}{P_d} = \frac{42}{10.1559} = 4.135527in, r_p = 2.0677636in$$

$$d_g = \frac{N_g}{P_d} = \frac{96}{10.1559} = 9.45263345in, r_g = 4.7263167in$$

addendum

$$a = \frac{1.0}{Pd} = \frac{1}{10.1559} = 0.098465in$$

Center to center distance

C = rg + rp = 2.0677636 + 4.7263167 = 6.7940803in

Length of action

$$Z = \sqrt{\left((r_p + a)^2 - (r_p cos\emptyset)^2\right)} + \sqrt{\left((r_g + a)^2 - (r_g cos\emptyset)^2\right)} - csin\emptyset$$

$$Z = \sqrt{((2.0677636 + 0.098465)^2 - (2.0677636cos(20))^2)} + \sqrt{((4.7263167 + 0.098465)^2 - (4.7263167cos(20))^2)} - 6.7940803sin(20)$$

Z=0.51899262in

Contact ratio Gear 9-10

$$M_p = \frac{Z}{P_b} = \frac{0.51899262}{0.29057} = 1.78611906$$

Efficiency of Gears 9-10.

$$\eta = \left[1 - \frac{(0.05)(1.78611906)(0.29057)}{4\cos(0)\cos(20)}\left(\frac{1}{2.0677636} + \frac{1}{4.7263167}\right)\right] x\ 100\%$$

$$\eta = 99.52\%$$

The contact ratio and efficiency between gears 9-10 was found to be 1.786 and 99.52% respectively.

Next, the total gearbox efficiency is obtained through the summation of all the individual gear pair efficiencies using the following formula. The total gearbox efficiency was determined to be ~~97.33%~~ 97.79% for the 4 gear reductions that take place.

$$Gearbox\ efficiency = \eta_1^2\eta_2\eta_3\sout{\eta_4} = (0.99318)^2(0.99529)(0.99612)\sout{(0.9952)} = 97.79\%$$

Table 5: Gearbox Efficiency

Gears	Diametral pitch [in^{-1}]	Contact Ratio	Efficiency [%]	Total Efficiency [%]
1 input	10.1599	1.732	99.318	99.318
2 S1	10.1599			
3 S1	10.1599	1.732	99.318	98.641
4 S2	10.1599			
5 S2	10.1599	1.799	99.529	98.176
6 S3	10.1599			
7 S3	10.1599	1.837	99.612	97.779
8 ~~S4~~ output	10.1599			
~~9 S4~~	~~10.1599~~	~~1.786~~	~~99.52~~	~~97.33~~
~~10 output~~	~~10.1599~~			

Gear Failure Analysis

To determine materials, face widths, and safety factors of our gears, the group ran a thorough gear failure analysis by creating and implementing a MATLAB script. To do so, the group made a function which took various parameters including gear specifications and material properties and returned the minimum acceptable face width and safety factors against bending and surface stresses. This allowed the group to easily iterate through various materials to determine what the minimum face width of a gear could be to achieve our desired safety factors.

To pick a material, we iterated through multiple different materials using the final gear contact as input, to determine the minimum acceptable face width at the final gear reduction. Because the final gear reduction has the highest torque input, it will require the largest face width, meaning that once that is determined, we know that material and width will be suitable for the rest. From there we are able to determine the minimum face widths for each of the other gears in our gear train.

The first step in our gear failure analysis was to calculate the load transmitted by the input gear (gear 7 in this case). Given an input torque, pressure angle, and the diameter of the input gear, we could calculate the tangential force (W_t), the radial force (W_r), and the total force (W).

$T_{in} = 330.75\ N \cdot m = 2927.37\ lb \cdot in$
$\emptyset = 20°$
$d_{in} = 4.724in$

$$W_t = \frac{T_{in}}{(\frac{d_{in}}{2})} = \frac{2927.37\ lb \cdot in}{(\frac{4.724in}{2})} = 1239.37\ lb$$

$$W_r = W_t tan\emptyset = (1239.37\ lb)\tan(20°) = 451.05\ lb$$

$$W = \frac{W_t}{cos\emptyset} = \frac{1239.37\ lb}{\cos(20°)} = 1318.77\ lb$$

The next step was to determine the appropriate correction factors for our gears to allow us to accurately calculate the bending stress on the gear teeth. To find our dynamic factor K_v, we first needed to calculate the pitch velocity and A B factors. Given the speed of rotation, the gear quality number Qv was determined to be 8.

$$V_t = \frac{d_{in}}{2}\omega_{in} = \frac{4.724in}{2} \cdot 1.466\frac{rad}{s} \cdot (\frac{60s}{1\text{min}})(\frac{1ft}{12in}) = 17.316\frac{ft}{min}$$

$$B = \frac{(12 - Q_v)^{\frac{3}{2}}}{4} = \frac{4^{\frac{3}{2}}}{4} = 0.63\ ; since\ 6 \le Q_v \le 12$$

$$A = 50 + 56(1 - B) = 50 + 56(0.37) = 70.722$$

$$K_v = \left(\frac{A}{A + \sqrt{V_t}}\right)^B = \left(\frac{70.722}{70.722 + \sqrt{17.316}}\right)^{0.63} = 0.965$$

The other applicable correction factors were determined as follows:

Load distribution factor K_m was determined to be 1.6, according to table 12-16 of Norton's Textbook [16]. This holds true as long as our face width is below 5cm, which is the goal.

The application factor K_a is 1.0 for the purposes of our application. This factor is appropriate for a uniform machine such as ours, and driven by a uniform motor, such as the motor being implemented in our design as seen in Table 12-17 in Norton's textbook [16].

The size factor K_s was determined to be 1.0, as is standard given that our teeth are of a reasonable size.

The rim thickness factor K_B was found to be 1.0 given that the gears used will have suitable material between the shaft and teeth meaning the gears will be essentially solid discs.

Since the proposed gear train contains no idler gears, the idler factor K_I is 1.0.

Finally, before the stress due to bending can be calculated, the appropriate geometry factor J must be determined. For the gears being examined, the pressure angle is 20° and the teeth are full depth, therefore using Table 12-9 of *Machine Design: An Integrated Approach* [16], the appropriate geometry factor can be extrapolated. In the case of gears 7-8, the geometry factor is 0.47.

With the correction factors determined, the stress due to bending can be calculated. Using the equation below.

$$\sigma_b = \frac{W_t P_d K_a K_m K_s K_B K_I}{F J K_v}$$

However, since the MATLAB script was designed to output the minimum acceptable face width that would meet our desired safety factor (for these purposes >1.5), an initial face width of 1cm was set and the program then iterated through, increasing it by 1mm until the goal was met. Therefore, before calculating bending stress, the corrected fatigue strength due to bending must be calculated using the following equation.

$$S_{fb} = S'_{fb} \cdot \frac{K_L}{K_T K_R}$$

The fatigue strength due to bending is dependent on specific material properties. For these calculations we are examining 4340–Normalized (870°C) steel which has a Brinell Hardness (HB) of 363 and a grade of 2. The HB and grade of the material allows us to calculate the uncorrected bending fatigue strength of the material. The equation below was obtained from figure 12-25 of Norton's *Machine Design: An integrated Approach* [16] and is valid for grade 2 materials.

$$S'_{fb} = 6235 + 124HB - 0.126HB^2$$
$$= 6235 + 124(363) - 0.126(363)^2 = 52794.11\ psi$$

The life factor K_L varies depending on the amount of use the gear will be subject to. This can be calculated using:

$$K_L = 1.3558\ N^{-0.0178}\ ; for\ commercial\ applications$$

Where N is the expected number of cycles. This was calculated using the input speed as well as the expected time of use.

$$N = (14\ rpm)\left(60\frac{min}{hour}\right)\left(8\frac{hour}{day}\right)\left(180\frac{day}{year}\right)(20\ years) = 2.42 \times 10^7$$

$$K_L = 1.3558\ N^{-0.0178} = 1.3558(2.42 \times 10^7)^{-0.0178} = 1.002$$

The temperature factor K_T was determined to be 1.0 considering that for the applications being examined the temperature is assumed to remain below 120°C.

The reliability factor was obtained from Table 12-9 of *Machine Design: An integrated Approach* [16], and for a chosen reliability of 99%, $K_R = 1.0$.

The corrected fatigue strength due to bending can now be calculated:

$$S_{fb} = S'_{fb} \cdot \frac{K_L}{K_T K_R} = (52794.11\ psi) \cdot \frac{1.002}{1} = 52887.34\ psi$$

Finally, the safety factor can be determined by taking the ratio of fatigue strength to applied bending stress. Since our minimum acceptable safety factor against bending was determined by the group to be 1.5, the only unknown remaining in the equations above is the face width. Therefore, by having MATLAB iterate through the calculations and slowly incrementing the initial face width of 1cm, until the required safety factor is met.

It is important to note that the surface stresses must also be considered, and therefore the program created by the group executes the bending and surface-fatigue stress calculations simultaneously to ensure that an acceptable safety factor is met for both forms of stresses. The surface-fatigue stresses were calculated as follows.

To calculate the surface-fatigue stress, we implement the equation:

$$\sigma_c = C_p\sqrt{\frac{W_t C_a C_m C_s C_f}{FIdC_v}}$$

$$where, C_a = K_a, C_m = K_m, C_v = K_v, C_s = K_s, C_f = 1$$

With F being the face width (which will be iterated through), and d being the diametral pitch, the only remaining unknowns are the elastic coefficient C_p and the surface geometry factor I. C_p can be found as follows:

$$C_p = \left(\frac{1}{\pi\left(\frac{1-v_{in}^2}{E_{in}} + \frac{1-v_{out}^2}{E_{out}}\right)}\right)^{1/2}$$

Because both the input and output gear are made of the same material, the expression above can be simplified to the following:

$$C_p = \sqrt{\frac{1}{2\pi(\frac{1-v^2}{E})}}$$

$$C_p = \sqrt{\frac{1}{2\pi(\frac{1-(0.29)^2}{2.9\times 10^7})}} = 2244.84$$

To calculate the value for the geometry factor, the surface fatigue values for ρ_{in} and ρ_{out} must first be determined:

$$\rho_{in} = \left(\left(r_{in} + \frac{1+x_p}{P_d}\right)^2 - \left(r_{in}cos(\phi)\right)^2\right)^{1/2} - \frac{\pi cos(\phi)}{P_d}$$

$$where\ x_p = 0\ since\ teeth\ are\ full\ depth$$

$$\rho_{in} = \left(\left(2.36 + \frac{1}{10.1599}\right)^2 - \left(2.36cos(20°)\right)^2\right)^{1/2} - \frac{\pi cos(20°)}{10.1599} = 0.771in$$

$$\rho_{out} = (r_{in} + r_{out})sin(\phi) - \rho_{in}$$

$$\rho_{out} = (2.366 + 8.268)sin(20°) - 0.771in = 2.864in$$

The geometry factor I can now be calculated:

$$I = \frac{cos(\phi)}{\left(\frac{1}{\rho_{in}} + \frac{1}{\rho_{out}}\right) * d_{in}} = \frac{\cos(20°)}{\left(\frac{1}{0.771} + \frac{1}{2.864}\right) * 4.724} = 0.121$$

The surface fatigue stress can now be calculated assuming a face width is known. Once again because we are looking for a minimum face width, given a required safety factor, we will first solve for the surface fatigue strength.

The corrected surface fatigue strength can be calculated using the following equation:

$$S_{fc} = \frac{C_L C_H}{C_T C_R} S_{fc'}$$

$$from\ bending\ analysis: C_T = K_T = 1; C_R = K_R = 1$$

With the Brinell hardness factor and the grade known, we can implement a similar equation as we did to find are used to find $S_{fb'}$ to find the uncorrected surface fatigue strength ($S_{fc'}$). This can be found using the equation below, found in figure 12-27 of Norton's textbook [16].

$$S_{fc'} = 27{,}000 + 364(HB)$$

$$S_{fc'} = 27{,}000 + 364(363) = 159{,}132 \text{ psi}$$

To find the surface-life factor (C_L), we can use figure 12-26 from the textbook [16]. Given the intended application of this design, and the expected number of cycles ("N" found in bending analysis) we will be using the following formula, applicable for commercial applications:

$$C_L = 1.4488N^{-0.023}$$

$$C_L = 1.4488(2.42 \times 10^7)^{-0.023} = 0.952$$

Additionally, the factor C_H in this case is equal to 1.0 since in this gearbox all the gears involved will be made of the same material.

The surface fatigue strength can now be calculated.

$$S_{fc} = \frac{C_L C_H}{C_T C_R} S_{fc'} = \frac{(0.952)(1.0)}{(1.0)(1.0)}(159{,}132) = 151{,}448.5 \text{ psi}$$

The equation below illustrates the relationship between the surface-fatigue strength and the surface-fatigue stress.

$$N_c = \left(\frac{S_{fc}}{\sigma_c}\right)^2 > 1.5$$

With the fatigue strength is calculated, and the minimum acceptable safety factor against surface failure determined. We once again have only the face width unknown, and can iterate through to find the minimum acceptable face width which meets our required safety factors.

When the program is run with information for the final gear contact and the material 4340– Normalized (870°C) steel, the result is a minimum face width of 3.2cm. At this face width, the safety factor against bending failure is 1.50, and the safety factor against surface failure is 1.59. This was the material we decided on, as it provided us the smallest acceptable face width.

The material properties and gear specifications inputted into MATLAB script are shown in the tables below [17].

Table 6. Gear specifications inputted into MATLAB script

Gears	# of Teeth Driving	# of Teeth Driven	Input Torque (Nm)	Input Speed (RPM)	Bending Geometric factor –J
7-8	48	168	330.75	14	0.47
5-6	36	180	66.15	70	0.48
3-4	24	120	13.23	350	0.34
1-2	24	120	2.646	1750	0.34

Table 7. Gear material specifications

Material	Young's Modulus E (psi)	Brinell Hardness	Grade	Poisson's Ratio	Min Face Width Gears 7-8 (cm)
1020– Hot rolled	27,000,000	163	2	0.29	5.5
1020– Cold drawn	27,000,000	121	2	0.29	7.0
1020– Annealed (870°C)	27,000,000	111	2	0.29	7.5
4340– Annealed (810°C)	27,800,000	217	2	0.29	4.5
4340– Normalized (870°C)	29,000,000	363	2	0.29	3.2
303 Stainless Steel	27,990,000	228	2	0.25	4.5

The table above shows various materials and their respective properties that were analyzed as well as the minimum resultant face width of the critical gear contact (7-8). As shown, our minimum acceptable face width is 3.2cm and is achieved using 4340 Normalized (870°C) Steel.

The following table shows the minimum acceptable face widths of the other gear contacts for our chosen material 4340 Normalized (870°C) Steel. Note that the iterations start at 1cm as no gears will be less than that.

Table 8. Minimum face width and safety factor of gears

Gear Contact	1-2	3-4	5-6	7-8
Minimum Face Width (cm)	<1.0	<1.0	1.28	3.2
Safety Factor Against Bending	15.84	3.68	2.16	1.50
Safety Factor Against Surface-Fatigue	7.21	1.95	1.51	1.59

In our final design, the group decided to give gears 7 and 8 a face width of 3.2cm, whereas all other gears are set as 2cm for consistency, ease of manufacturing, and added strength.

Shaft Design and Load Analysis

Preliminary Shaft design

Preliminary drawings were developed for each shaft, displaying features such as shoulders, threads, grooves, and keyways. The locations of these key features are labelled in each of shaft drawings. Threads are located on either end of the shafts to secure the bearing between the end of the shaft and the shoulder. Keyways are shown at the location of the gears with locations for snap ring grooves to be incorporated in the next iteration of this project. The preliminary drawings for all shafts displayed in the figures below.

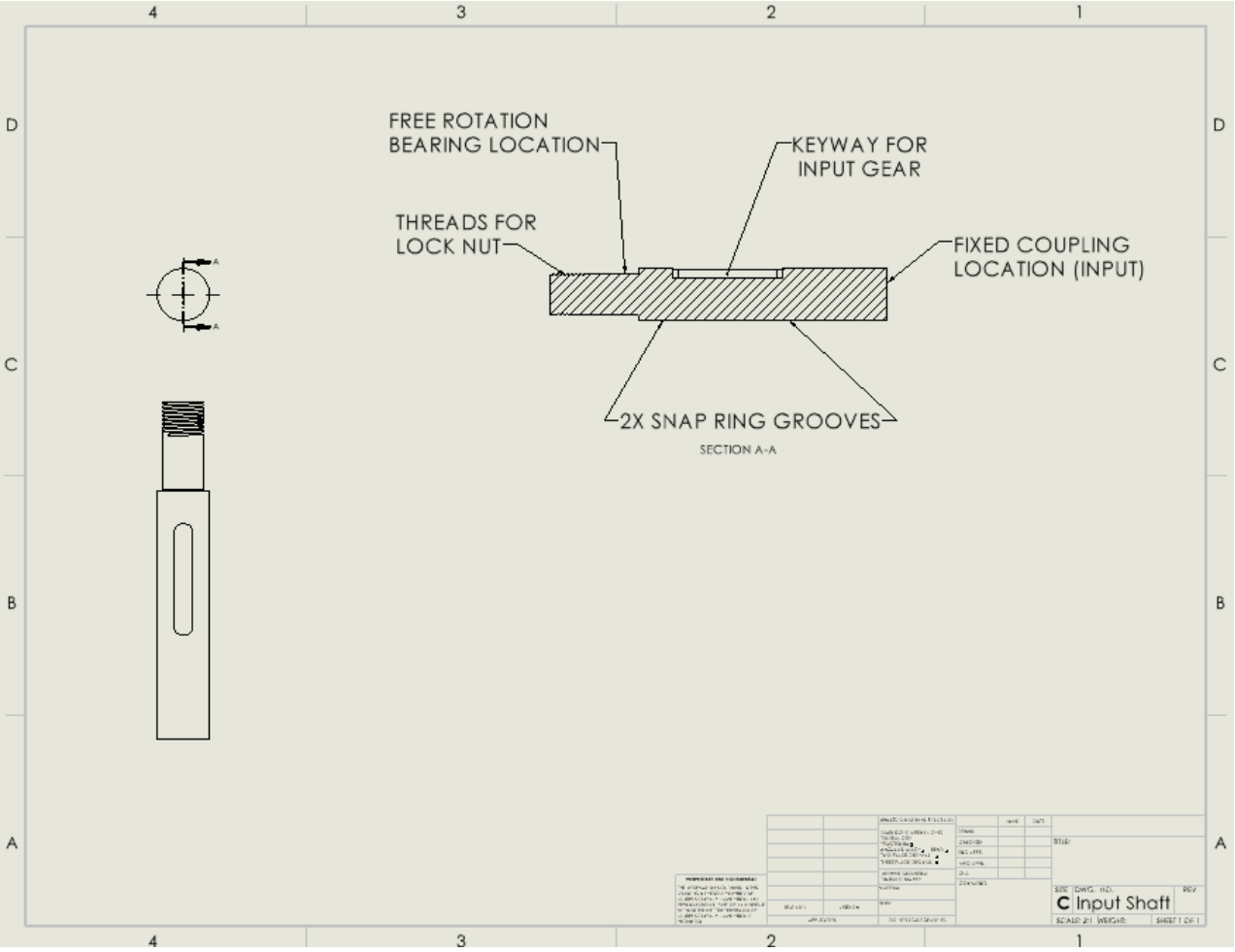

Figure 32: Input Shaft

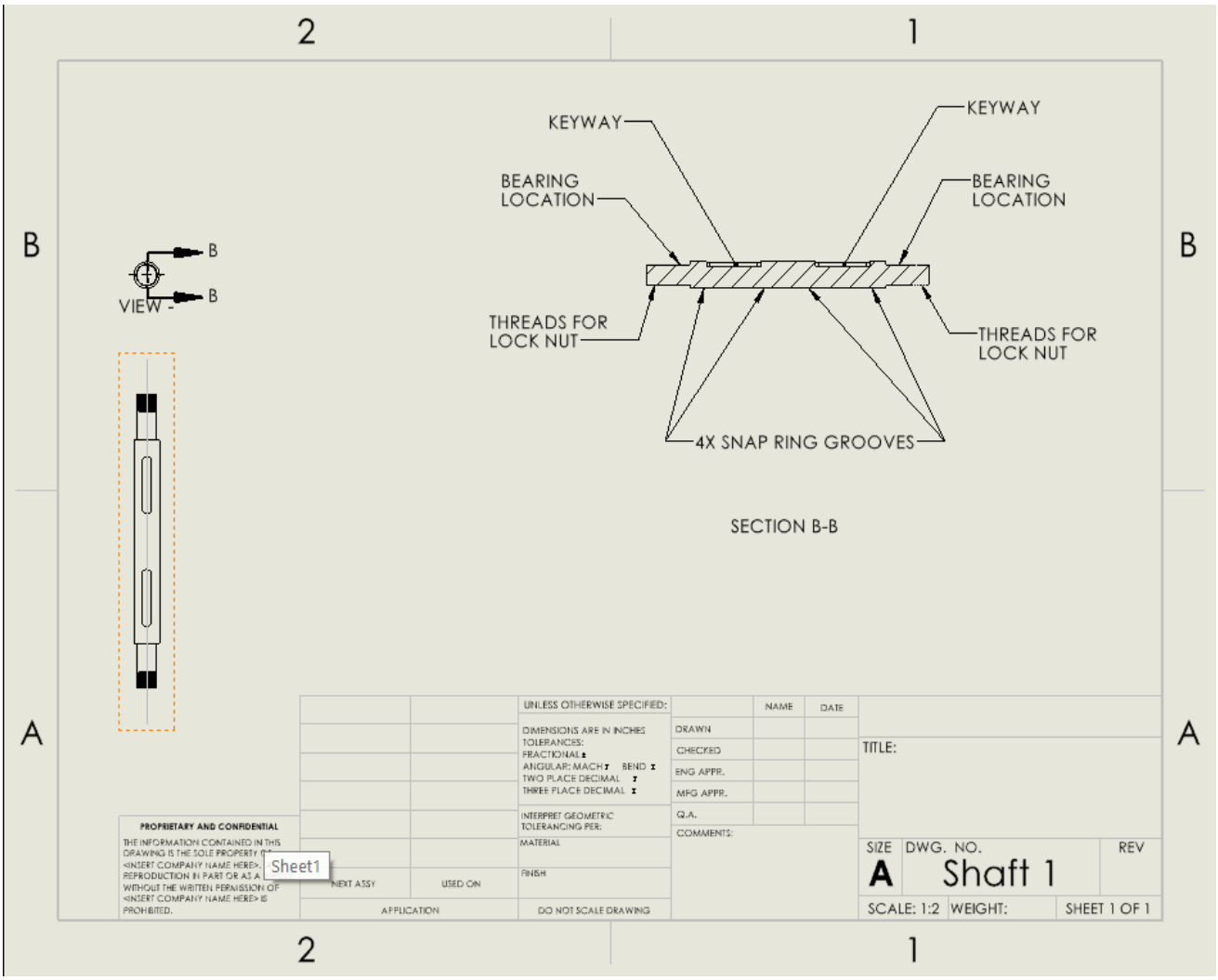

Figure 33: Shaft 1

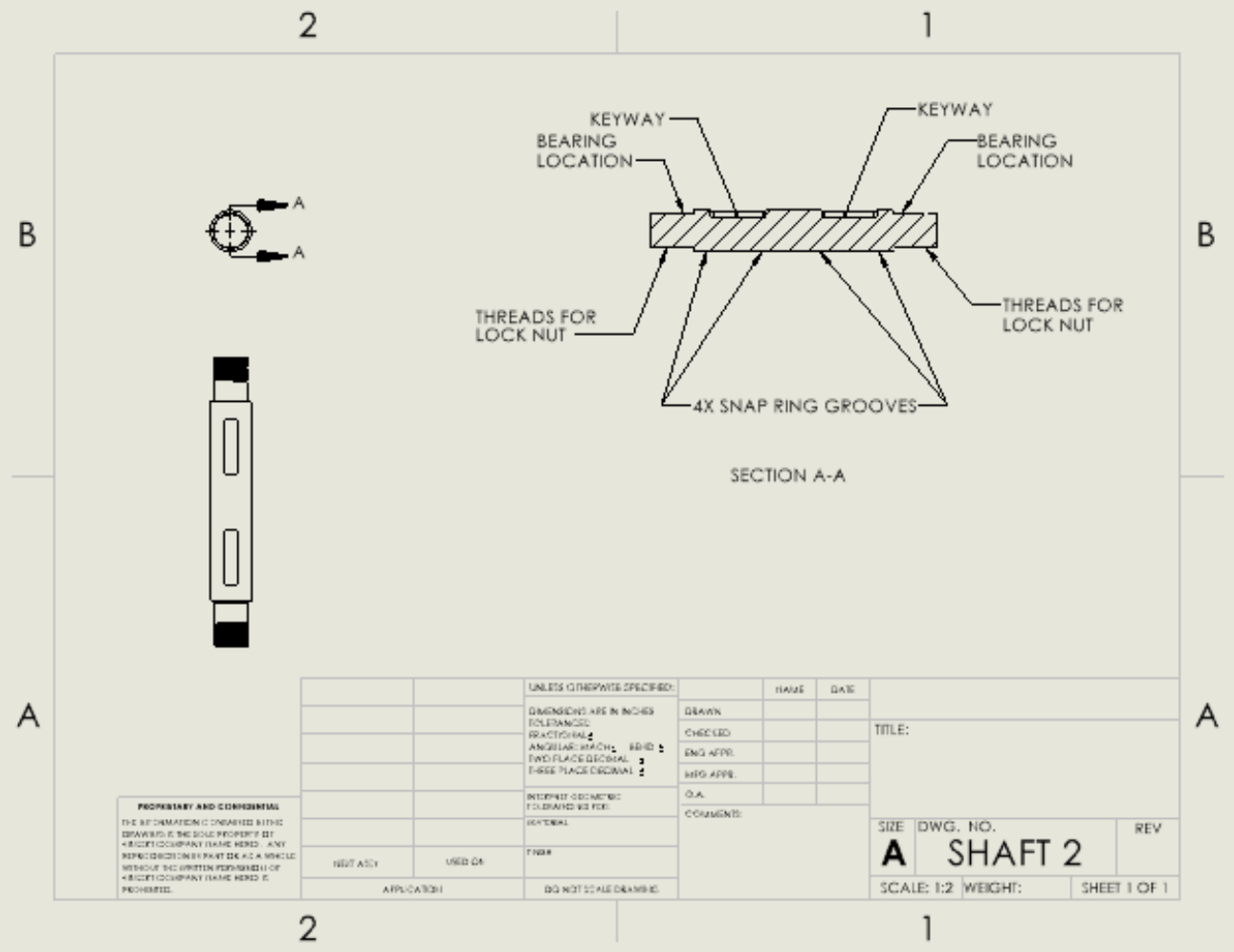

Figure 34: Shaft 2

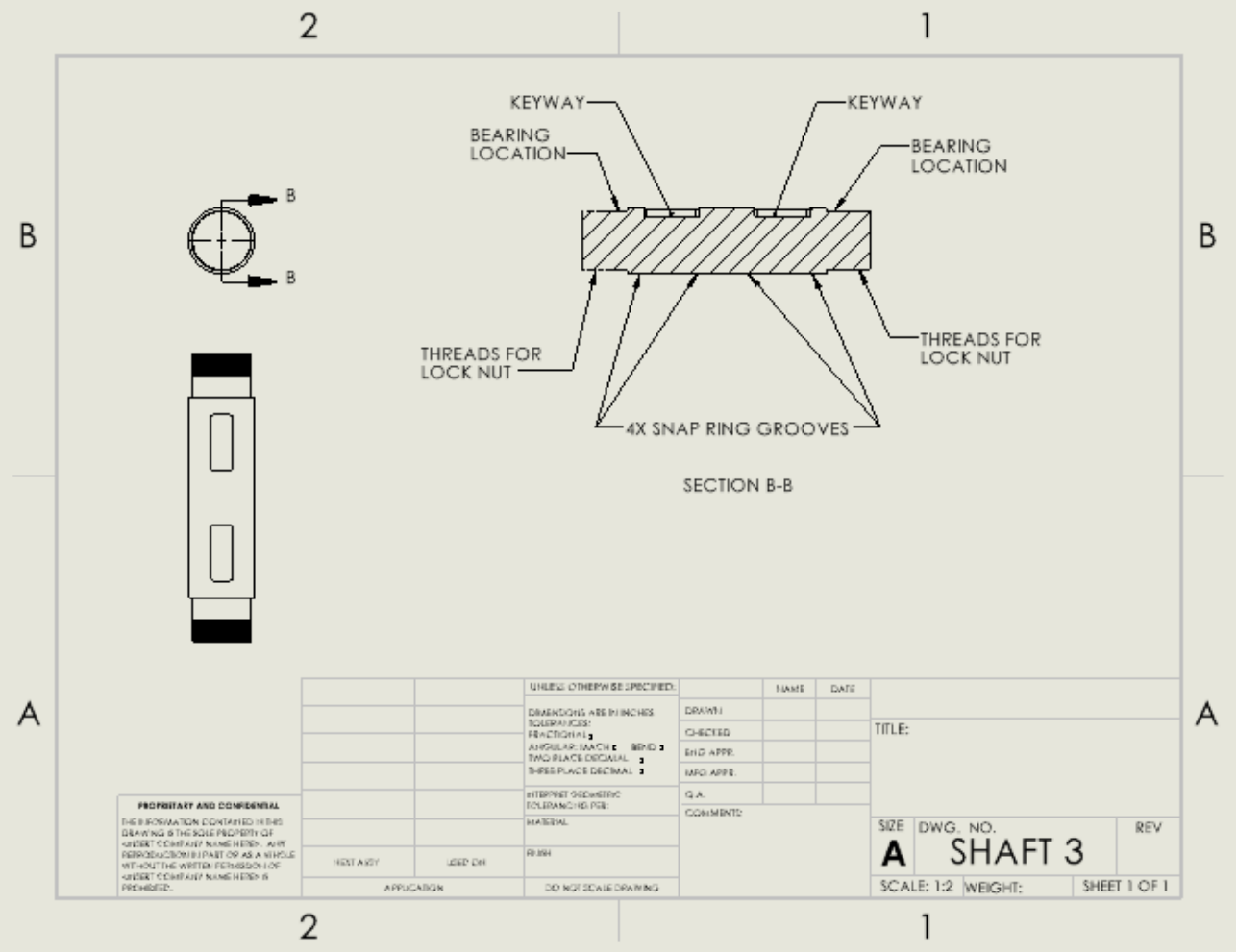

Figure 35: Shaft 3

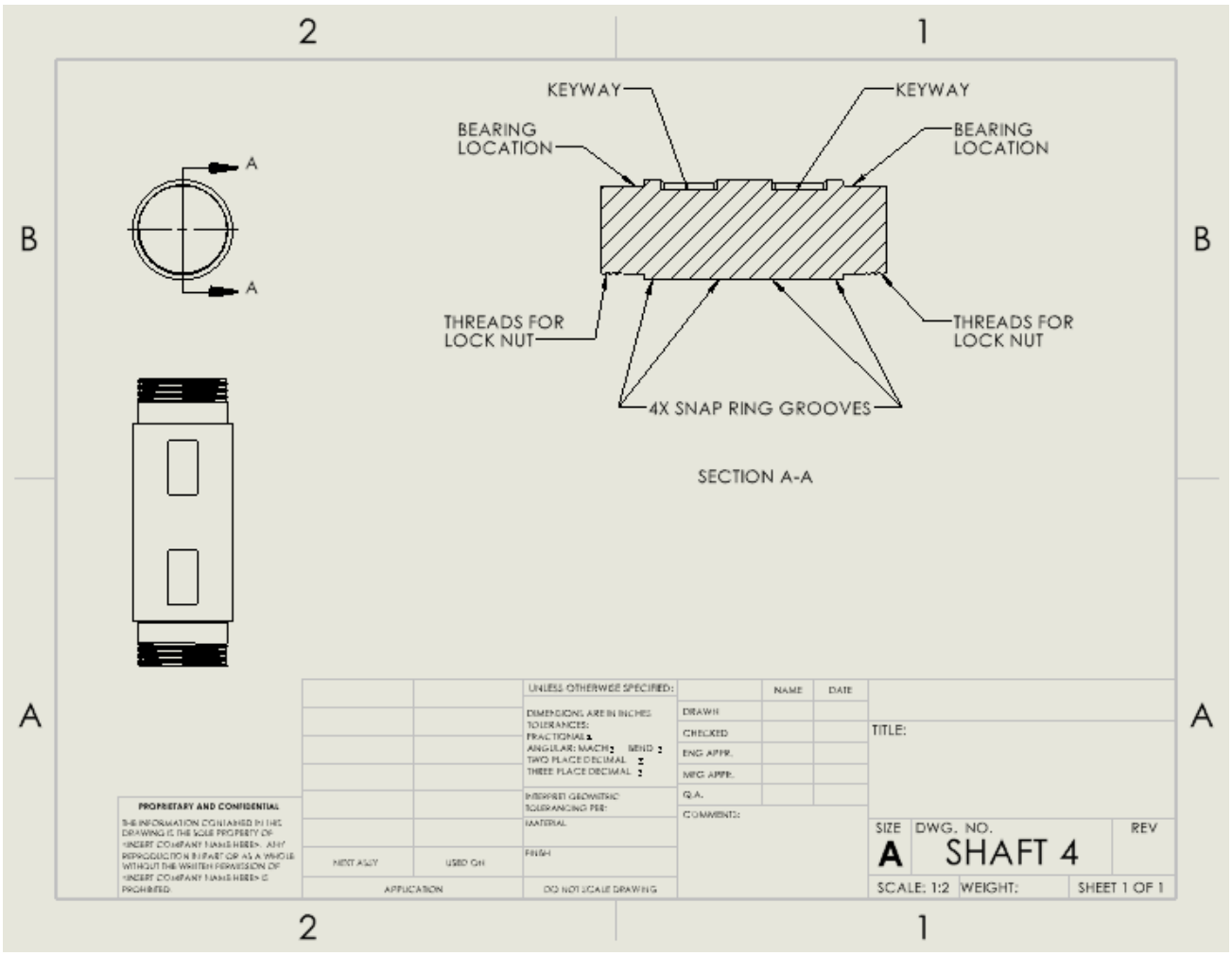

Figure 36: Shaft 4

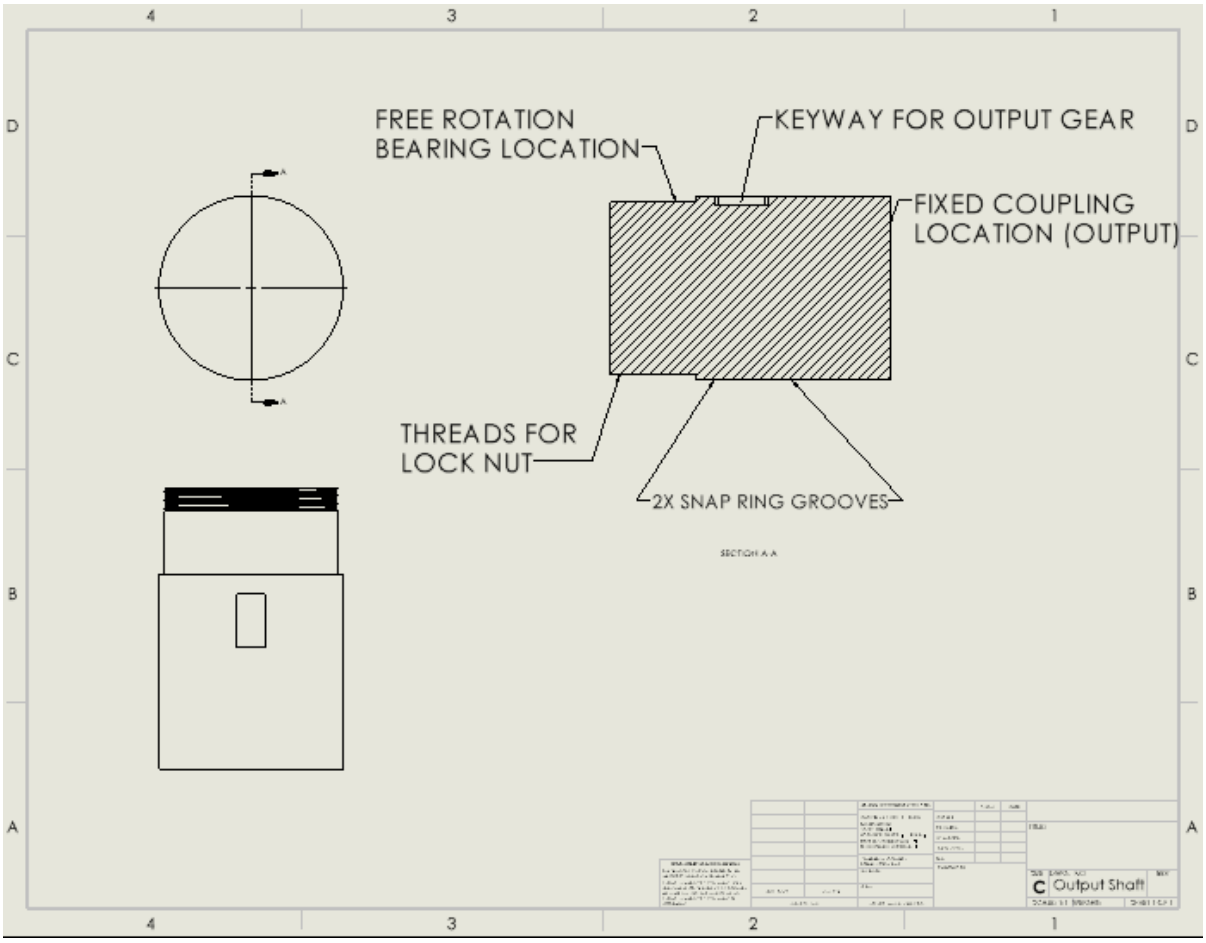

Figure 37: Output Shaft

Based on the free body diagrams (FBDs) for each of the shafts, we can develop equations to determine the reaction forces at the bearings.

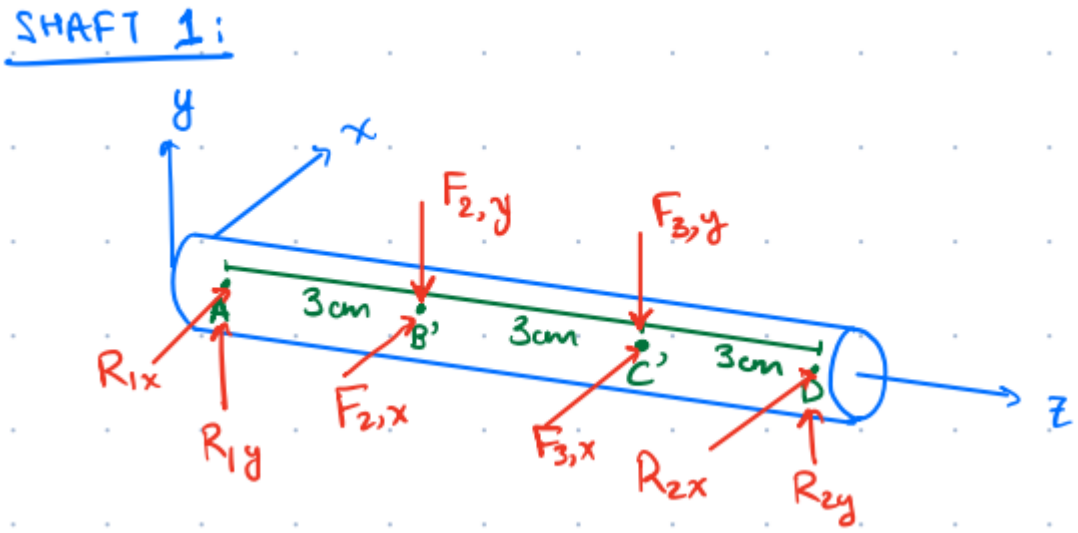

Figure 38: Shaft 1 FBD

First off, the forces exerted by the gears are determined – using our contact angle of 20°:

$$F_{2y} = \frac{\tau}{r} = \frac{13.23}{0.15} = 88.2N \; ; \; F_{3y} = \frac{\tau}{r} = \frac{13.23}{0.03} = 441N$$
$$F_{2x} = F_{2y}tan(\phi) = 32.1N \; ; \; F_{3x} = F_{3y}tan(\phi) = 160.51N$$

From there, assuming static equilibrium, we can use the sum of the moments about point A being set to zero:

$$\Sigma M_A = 0 = \overrightarrow{r_{A/B'}} x \overrightarrow{F_2} + \overrightarrow{r_{A/C'}} x \overrightarrow{F_3} + \overrightarrow{r_{A/D}} x \overrightarrow{R_2}$$

$$\begin{bmatrix} 0 \\ 0 \\ z_1 \end{bmatrix} x \begin{bmatrix} F_2x \\ -F_{2y} \\ 0 \end{bmatrix} + \begin{bmatrix} 0 \\ 0 \\ z_2 \end{bmatrix} x \begin{bmatrix} F_{3x} \\ -F_{3y} \\ 0 \end{bmatrix} + \begin{bmatrix} 0 \\ 0 \\ z_3 \end{bmatrix} x \begin{bmatrix} R_{2x} \\ R_{2y} \\ 0 \end{bmatrix} = \begin{bmatrix} 0 \\ 0 \\ 0 \end{bmatrix}$$

$$\begin{bmatrix} z_1F_{2y} + z_2F_{3y} - z_3R_{2y} \\ z_1F_{2x} + z_2F_{3x} + z_3R_{2x} \\ 0 \end{bmatrix} = \begin{bmatrix} 0 \\ 0 \\ 0 \end{bmatrix}$$

From here, we can isolate for the unknown reaction forces to be:

$$z_1F_{2y} + z_2F_{3y} - z_3R_{2y} = 0 \Rightarrow R_{2y} = \frac{z_1F_{2y} + z_2F_{3y}}{z_3}$$
$$z_1F_{2x} + z_2F_{3x} + z_3R_{2x} = 0 \Rightarrow R_{2x} = \frac{-z_1F_{2x} - z_2F_{3x}}{z_3}$$
$$R_{2y} = \frac{(0.03m)(88.2N) + (0.06m)(441N)}{0.09m} = 323.4N$$

$$R_{2x} = \frac{-(0.03m)(32.1N) - (0.06m)(160.51N)}{0.09m} = -117.208\ N$$

Using the reaction forces for the bearing at point D found using the sum of the moments, another equation is used to determine the other bearing's reaction forces.

$$\Sigma F_x = 0 = R_{1x} + F_{2x} + F_{3x} + R_{2x} \Rightarrow R_{1x} = -F_{2x} - F_{3x} - R_{2x}$$
$$R_1x = -(32.1N) - (160.51N) - (-117.208N) = -74.9051N$$

$$\Sigma F_y = 0 = R_{1y} - F_{2y} - F_{3y} + R_{2y} \Rightarrow R_{1y} = F_{2y} + F_{3y} - R_{2y}$$
$$R_{1y} = (88.2N) + (441N) - (323.4N) = 205.8N$$

Using all the acting forces that were calculated, the shear force and bending moment diagrams must be made to perform further calculations regarding the shaft.

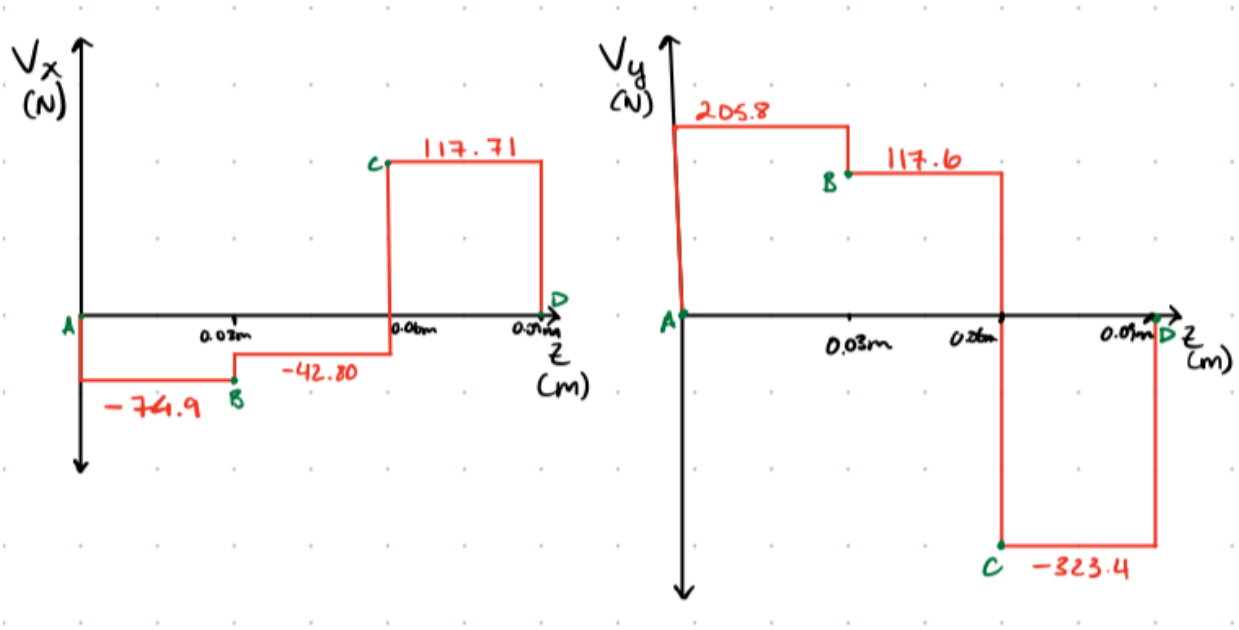

Figure 39: Shear force diagram for shaft 1

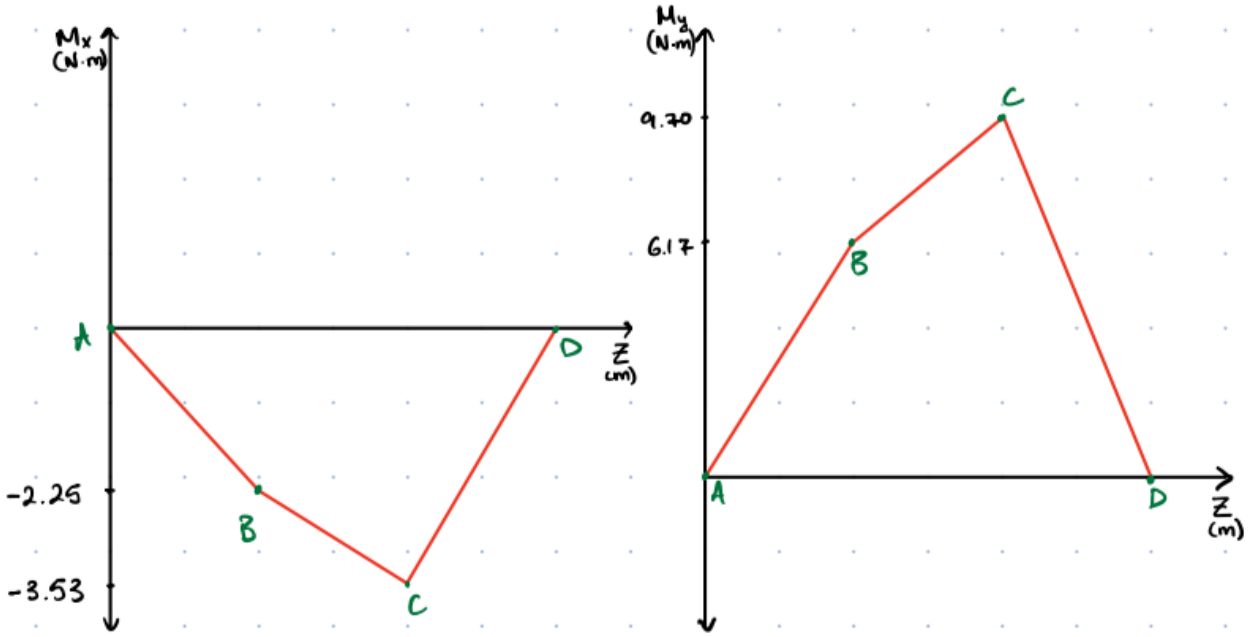

Figure 40: Bending moment diagrams for shaft 1

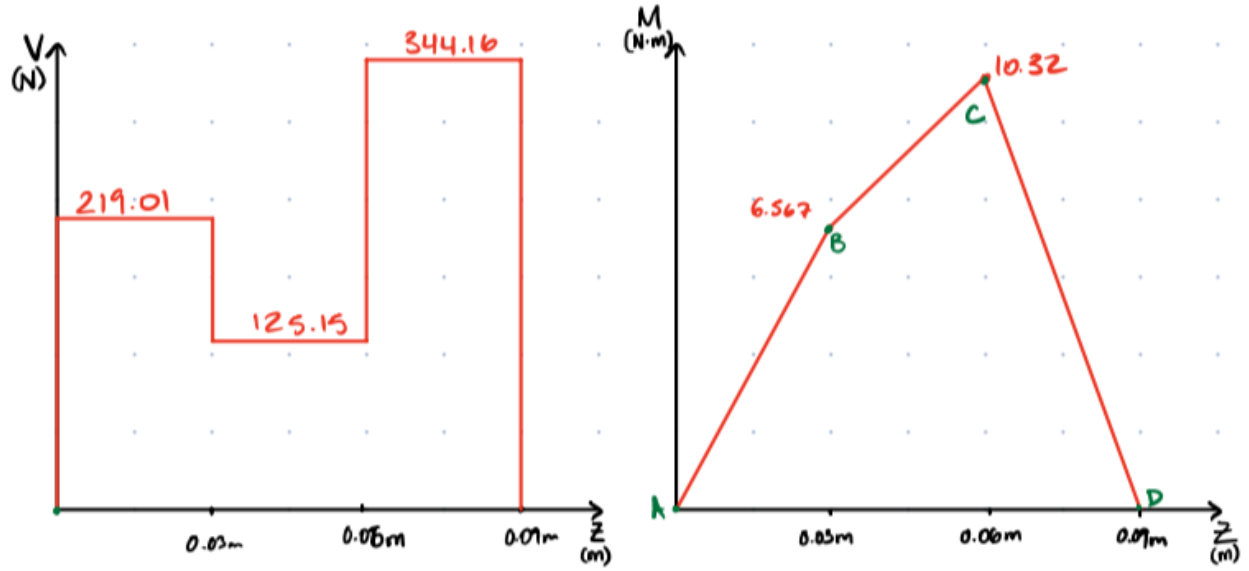

Figure 41: Combined Shear force and Moment Diagrams for Shaft 1

The FBDs, shear force diagrams, and bending moment diagrams for the other three shafts can be found in Appendix A.

The next step in the design process is to select a material. For our first iteration, the group will use SAE 1020 cold-rolled carbon steel. Later iterations will use other materials with varying

ultimate and yield strengths to observe the effect it has on the critical diameters. Given that the steel has an ultimate strength of 448 MPa and a yield strength of 262MPa, the uncorrected endurance limit can be determined.

$$Se' = 0.5S_{ut}$$
$$Se' = 224MPa$$

To find the correct endurance limit we must use correction factors through the following equation:

$$Se = C_{load}C_{size}C_{surf}C_{temp}C_{reliab}Se'$$

Since the group is still in the preliminary design stage, some assumptions must be made on these correction factors that may be adjusted later.

- C_{load} = 1 (bending and torsion)
- C_{size} = 1 (the size unknown at this stage, this can be adjusted later)
- C_{Surf} can be determined by, $A(S_{ut})^B$, where A and B are constants determined by the finish of the material. For the material used in this sample calculation, C_{surf} = 0.89
- C_{temp} = 1 (assuming that the temperature is below 450 °C)
- C_{reliab} = 1 (assuming 50% reliability, which can be altered later)

$$Se = (1)(1)(0.89)(1)(1)(224\ MPa)$$
$$Se = 200.37\ MPa$$

The next step of this analysis is to calculate the notch sensitivity and stress concentrations. Given that the group is in the preliminary design stage, theoretical stress concentration factors can be assumed an adjusted in later iterations of this analysis.

- K_t = 3.5 (bending)
- K_{ts} = 2 (torsion)
- K_t = 4 (keyways)
- Notch radius, r =0.001in (this parameter will be kept in imperial units as it will be evaluated with the Neuber constant

Using Table 6-6: Neuber's Constant for Steels, the Neuber's constant can be determined. At an ultimate strength of 448 MPa, the Neuber constant can be evaluated to be 0.1. The bending notch sensitivity can be determined through the following relationship:

$$q = \frac{1}{1 + \frac{\sqrt{a}}{\sqrt{r}}}$$

$$q = \frac{1}{1 + \frac{0.1}{\sqrt{0.01}}} = 0.5$$

The torsional notch sensitivity can be evaluated using the same equation, however for torsional loading an ultimate strength that is 20% higher than the original value is used. At an S_{ut} of 537.6 MPa, the Neuber constant can be evaluated to be 0.083.

$$q = \frac{1}{1 + \frac{0.083}{\sqrt{0.01}}}$$

$$q = 0.55$$

Having calculated the notch sensitivities, the fatigue concentration factors can be calculated.

- $K_f = 1 + q(K_t - 1) = 1 + 0.5(3.5 - 1) = 2.25$
- $K_f = 1 + q(K_{ts} - 1) = 1 + 0.55(2 - 1) = 1.55$
- $K_{fsm} = K_{fs} = 1.55$

Given that the shaft is subject to fully-reversed loading for bending and a steady torque, the ASME method is appropriate to be applied to this problem. The shaft diameters can be determined through the following equation:

$$d = \sqrt[3]{\frac{32N_f}{\pi}\left[\left(K_f \frac{M_a}{S_e}\right)^2 + \frac{3}{4}\left(K_{fsm}\frac{\tau_m}{S_y}\right)^2\right]^{\frac{1}{2}}}$$

The minimum required diameter at the shoulders of the shaft can be determined using the fatigue concentration factors calculated:

$$d = \sqrt[3]{\frac{32(1.5)}{\pi}\left[\left(2.25\frac{0}{200.37\ x\ 10^6}\right)^2 + \frac{3}{4}\left(1.55\frac{13.23}{262\ x\ 10^6}\right)^2\right]^{\frac{1}{2}}}$$

$$d = 0.90\ cm$$

At the locations of the gears, keyways are placed to secure the gears to the shaft. At the location of the keyways, the theoretical concentration factor is greater, thus it must be considered. Given that the moment at point C is higher than at point B, point C is deemed to be critical and the diameter must be evaluated. The fatigue concentration factors can be for the keyways can be calculated through the following:

- $K_f = 1 + q(K_t - 1) = 1 + 0.5(4 - 1) = 2.50$
- $K_{fs} = 1 + q(K_t - 1) = 1 + 0.55(4 - 1) = 2.65$

The minimum required diameter of the shaft at the gears can be determined using the fatigue concentration factors calculated:

$$d = \sqrt[3]{\frac{32(1.5)}{\pi}\left[\left(2.50\frac{10.32}{200.37\ x\ 10^6}\right)^2 + \frac{3}{4}\left(2.65\frac{13.23}{262\ x\ 10^6}\right)^2\right]^{\frac{1}{2}}}$$

$$d = 1.18\ cm$$

This process can be repeated for the other shafts in the gearbox. The critical diameters were calculated using a MATLAB script that was developed so that parameters could easily be changed. In summary of these results are presented in table 9 below.

Table 9: Critical diameters of shafts with SAE 1020 cold-rolled carbon steel

	Bearing step-down diameter (cm)	Gear shaft diameter (cm)	Torque (Nm)	Key dimensions (cm) base x height
Shaft input	1cm	1cm	2.646	
Shaft 1	0.90	1.18	13.23	0.4 x 0.4
Shaft 2	1.55	1.85	66.15	0.6 x 0.6
Shaft 3	2.64	2.98	330.75	1.0 x 0.8
Shaft ~~4~~ [output]	4.02	4.53 [5.5]	1157.63	1.4 x 0.9
~~Shaft output~~	~~8cm~~	~~8cm~~	~~2315.25~~	

[13]

Now, other materials can be tested to see how the critical diameters of the shaft are impacted. To do this, some constants in the MATLAB script were changed. The ultimate and yield strength values need to be updated as well as the surface correction factors. Additionally, the Neuber's constant must also be updated to the newly established ultimate strength. By iterating through different materials, the group can optimize the design of gearbox by choosing appropriate shaft lengths and determining which materials satisfy the force requirements to make the design cost effective.

Many different materials can be used for gears and gear trains depending on the intended use and operating conditions of the gears. For the purposes of a Ferris wheel, it is important for the gears to be durable, capable of supporting high loads, and easily machinable for cost purposes. Based on these requirements, we will be looking at iron alloys, and comparing different types of steel.

Table 10: Strength of different materials

Material	Yield Strength (MPa)	Ultimate Strength (MPa)	Neuber's Constant$(\sqrt{in})$
A36– Hot rolled	250	500	0.098
1020– Hot rolled	210	380	0.113
1020– Cold drawn	350	420	0.104
1020– Annealed (870°C)	295	395	0.109
4340– Annealed (810°C)	472	745	0.054
4340– Normalized (870°C)	862	1,280	0.019

[14][15]

The materials listed above were evaluated using the MATLAB code to determine the critical diameters if the given material was used for the shafts in the gearbox. By iterating through a variety of materials, the group was able to determine which material was optimal to satisfy design, safety, and cost requirements.

Table 11: MATLAB script material results

Material	Shaft 4 Bearing step-down diameter (cm)	Shaft 4 Gear shaft diameter (cm)
A36– Hot rolled	4.08	4.73
1020– Hot rolled	4.80	5.18
1020– Cold drawn	4.07	4.59
1020– Annealed (870°C)	4.29	4.87
4340– Annealed (810°C)	3.80	4.65
4340– Normalized (870°C)	3.15	4.50

Potential materials were iterated through to determine the critical diameters for shaft 4 because it is the location of the maximum torque. After analyzing the results, the group concluded that there are many materials that can handle the loads required. For this preliminary design material selection, the group has decided to go SAE 1020 cold-rolled carbon steel as it satisfies the design, safety, and cost requirements.

Final Shaft Design

For the final shaft designs, adjustments were made due to the addition of c-clips to prevent axial motion of the gears, presence of selected bearings, and changes in gear width determined by the gear failure analysis. The final design drawings for each shaft display the critical features: shoulders, grooves, and keyways. Grooves for c-clips are located on either end of the shafts to secure the bearing between the end of the shaft and the shoulder. Keyways are shown at the location of the gears with grooves for snap rings on either side to prevent axial motion of the gears. The final drawings for all shafts are displayed in figures 42 to 46 below.

Input

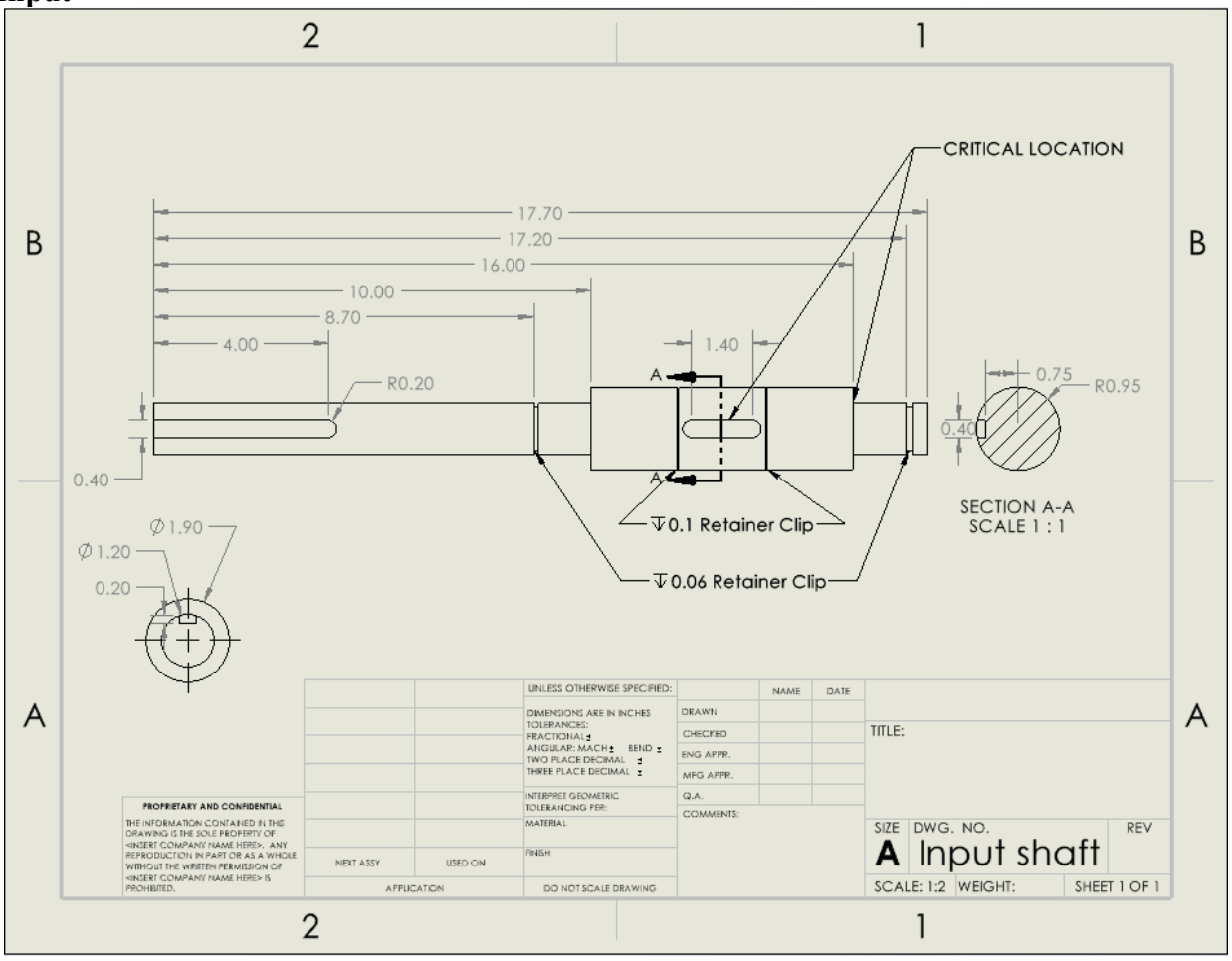

Figure 42. Input shaft

Shaft 1

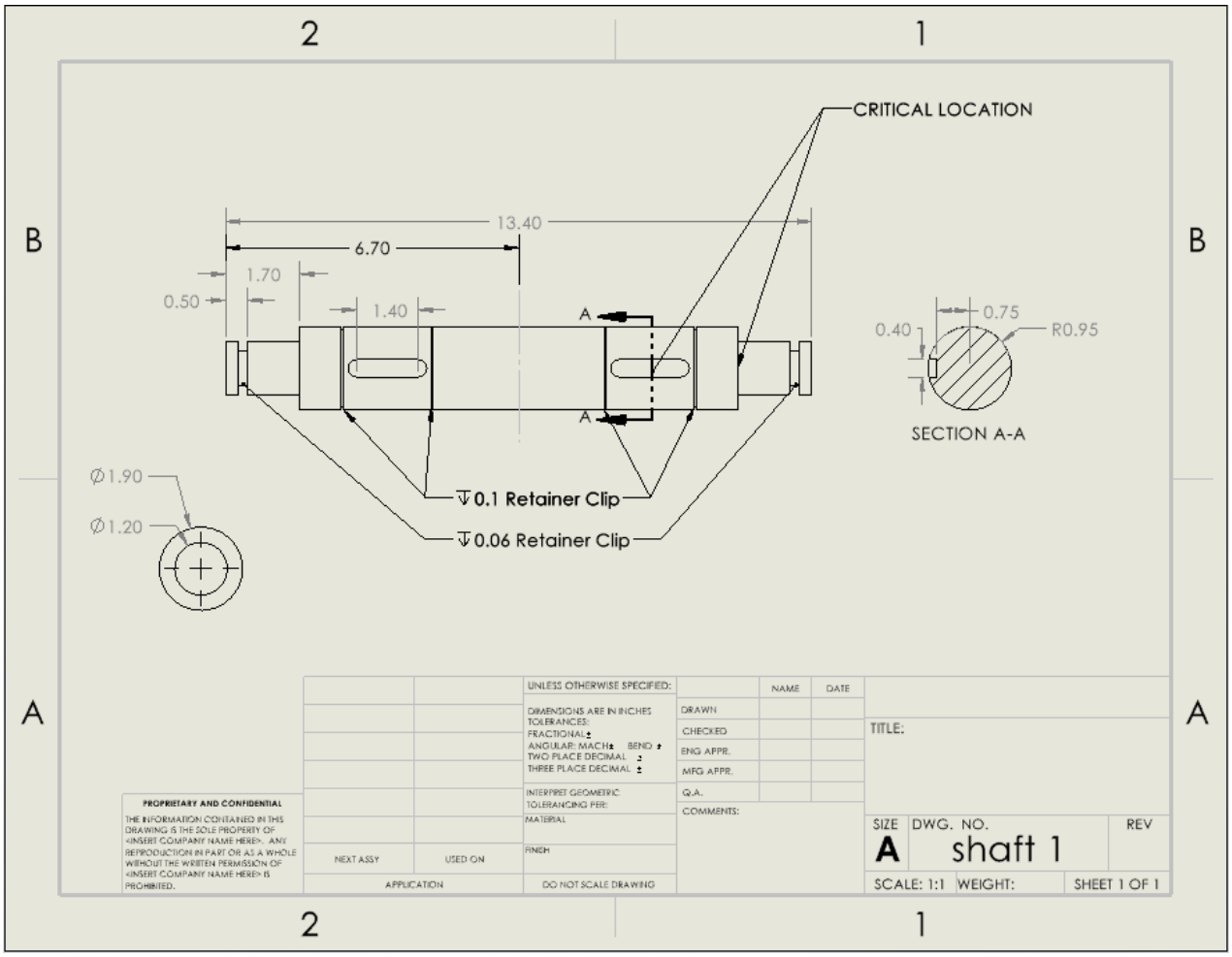

Figure 43. Shaft 1

Shaft 2

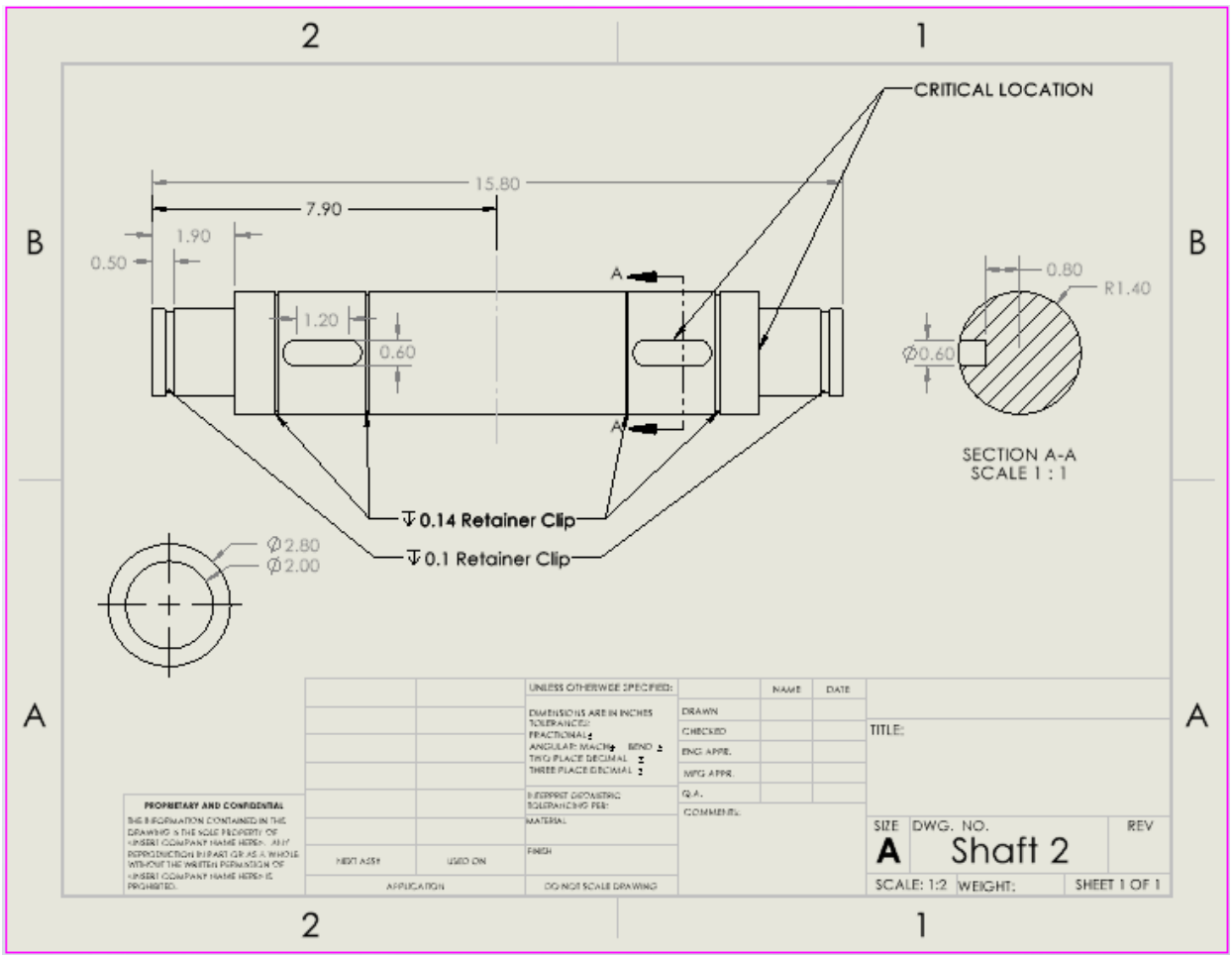

Figure 44. Shaft 2

Shaft 3

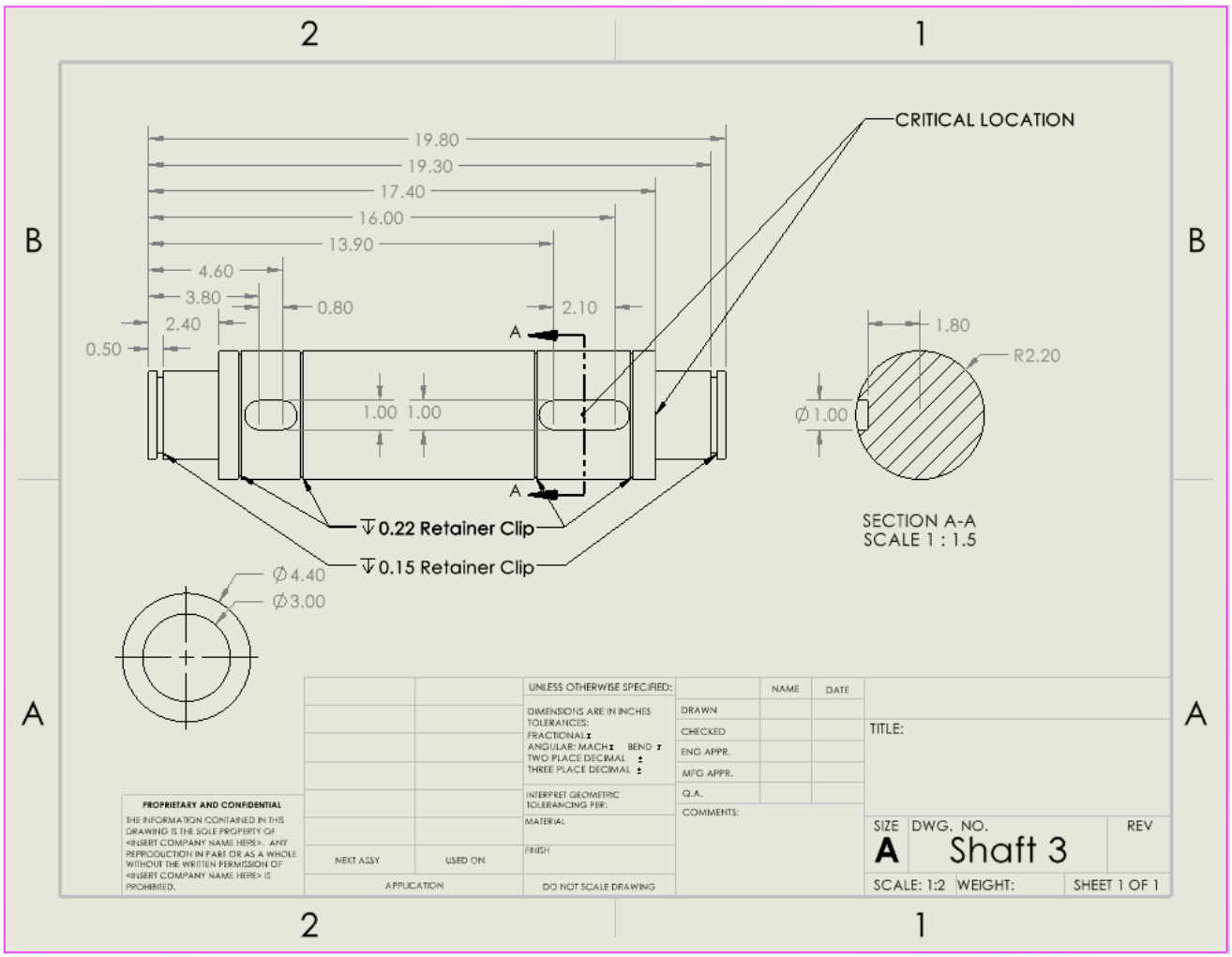

Figure 45. Shaft 3

Output

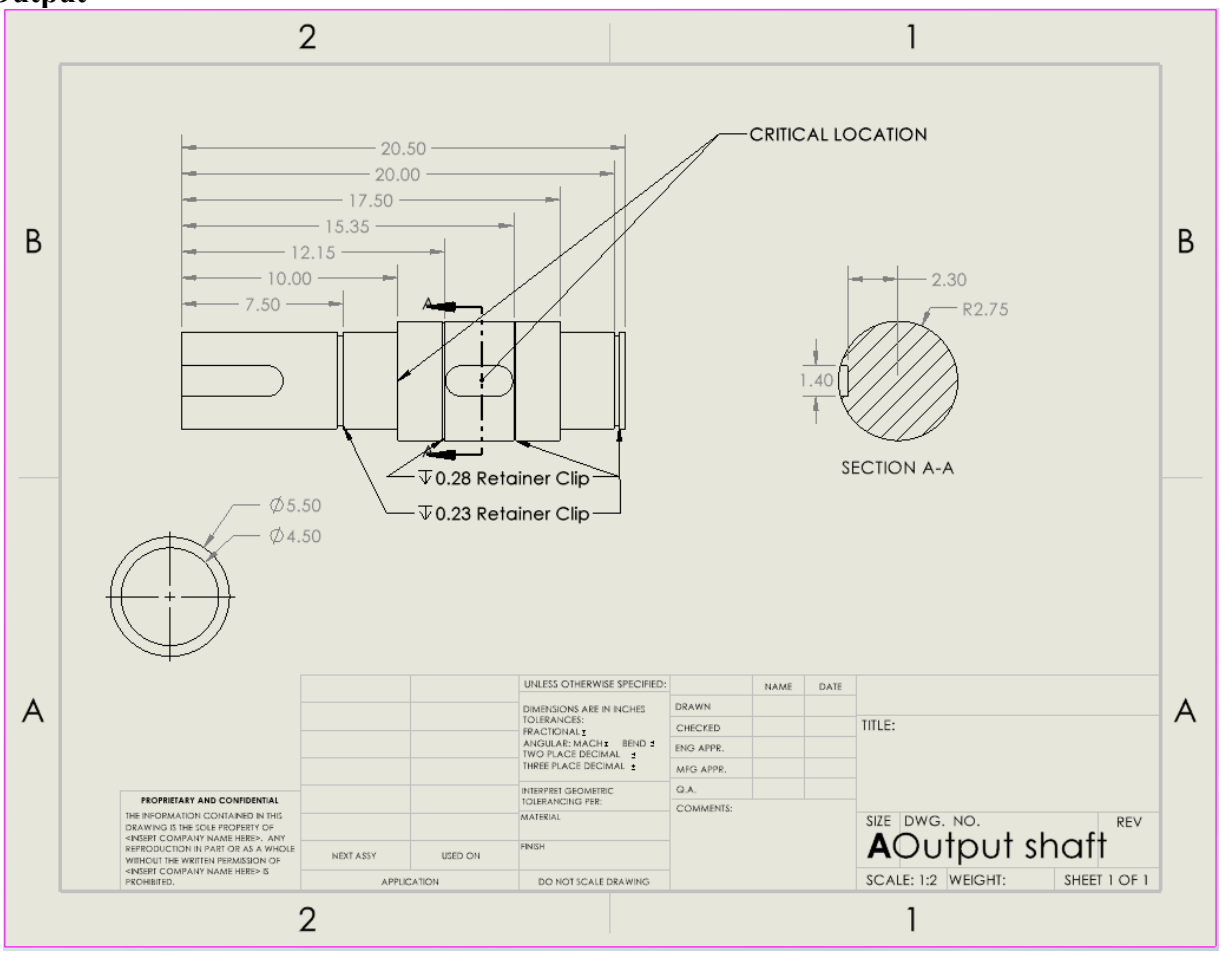

Figure 46. Output shaft

Updated free body diagrams (FBDs) for each of the shafts were developed, from which we can develop equations to determine the reaction forces at the bearings.

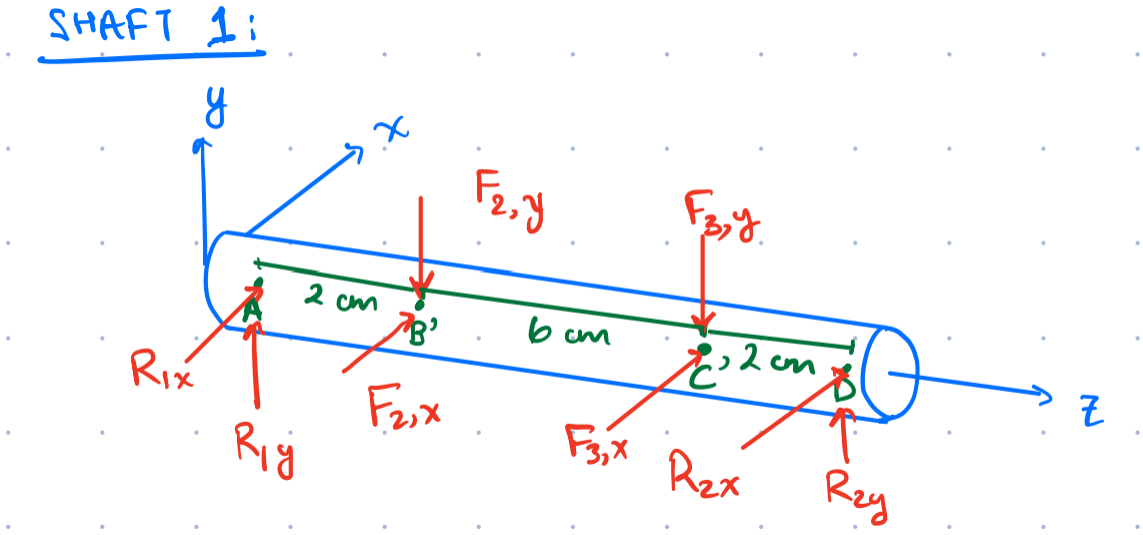

Figure 47. Shaft 1 FBD

Using all the acting forces that were calculated, the shear force and bending moment diagrams must be made to perform further calculations regarding the shaft. The shear and bending moment diagram for shaft 1 is displayed in the figure below.

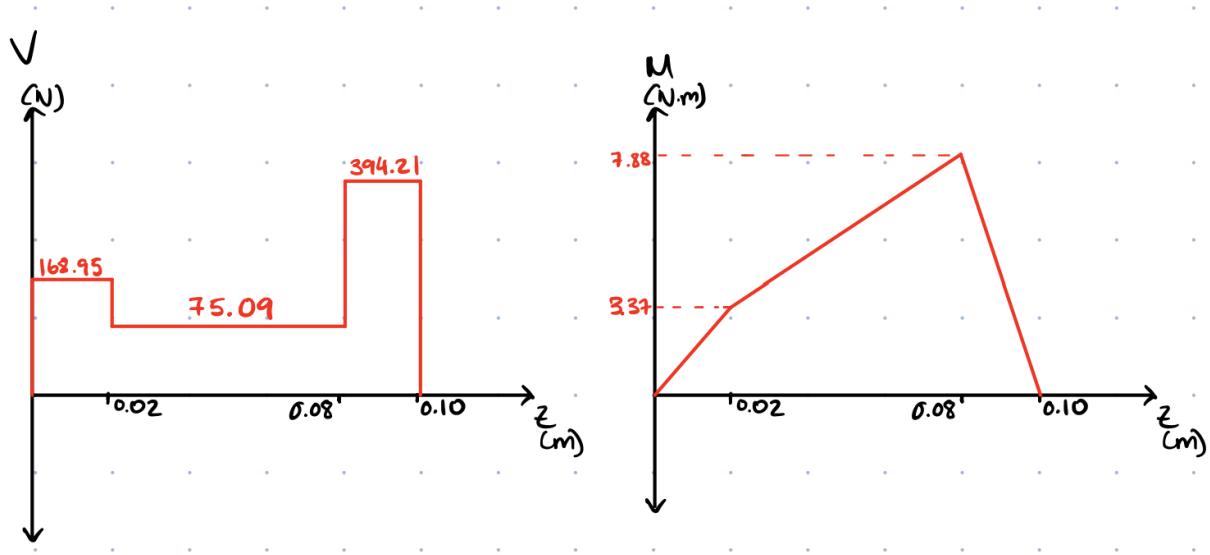

Figure 48. Shear and bending diagram for shaft 1

From the moment diagrams, we can apply similar triangles to obtain the moments at both shoulders. The moment developed at the first shoulder of shaft 1 can be obtained through the following:

$$M_{shoulder} = \frac{0.006}{0.02}(3.37) = 1.011\ Nm$$

As demonstrated in the preliminary shaft design, the ASME method can be used to determine the minimum required diameter at the shoulder:

$$d = \sqrt[3]{\frac{32N_f}{\pi}\left[\left(K_f\frac{M_a}{S_e}\right)^2 + \frac{3}{4}\left(K_{fsm}\frac{\tau_m}{S_y}\right)^2\right]^{\frac{1}{2}}}$$

The minimum required diameter at the shoulders of the shaft can be determined using the fatigue concentration factors calculated in the preliminary shaft design:

$$d = \sqrt[3]{\frac{32(1.5)}{\pi}\left[\left(2.25\frac{1.011}{200.37\ x\ 10^6}\right)^2 + \frac{3}{4}\left(1.55\frac{13.23}{262\ x\ 10^6}\right)^2\right]^{\frac{1}{2}}}$$

$$d = 1.00\ cm$$

In the final shaft design, grooves were added to both ends of each keyway to prevent axial motion of the gears. These grooves will develop a stress raiser which can be evaluated using Appendix C of *Machine Design: An Integrated Approach*]. When analyzing a grooved shaft in bending, the stress concentration factor, K_t, is determined through the following:

$K_t = A\left(\frac{r}{d}\right)^b$ where A and b are determined by D/d

At a D/d ratio of 1.05, the constants A and B can be determined to be 0.98755 and -0.24134 respectively. Assuming an *r* of 0.01, the theoretical stress concentration can be calculated:

$$K_t = 0.98755\left(\frac{0.01}{1.01}\right)^{-0.24134} = 3.01$$

The fatigue concentration factors can be for the grooves can be calculated through the following:

- $K_f = 1 + q(K_t - 1) = 1 + 0.5(3.01 - 1) = 2.50$
- $K_{fs} = 1 + q(K_t - 1) = 1 + 0.55(3.01 - 1) = 2.1055$

Similar to the earlier critical shoulder diameter calculations, similar triangles can be used to determine the moments developed at the grooves.

$$M_{groove} = \frac{0.016}{0.02}(3.37) = 2.696\ Nm$$

The minimum required diameter of the shaft at the gears can be determined using the fatigue concentration factors calculated:

$$d = \sqrt[3]{\frac{32(1.5)}{\pi}\left[\left(2.05\frac{2.696}{200.37\ x\ 10^6}\right)^2 + \frac{3}{4}\left(2.1055\frac{13.23}{262\ x\ 10^6}\right)^2\right]^{\frac{1}{2}}}$$

$$d = 1.13\ cm$$

As the keyways for the gears and the groove for the snap ring to prevent axial motion are on the part of the shaft, the critical diameters at the keyways will be used to determine the minimum allowable diameter. Before proceeding, the critical diameters at the shoulders and gears were recalculated using the appropriate size correction factor. Given that all the shafts will be between 8 mm and 256 mm the size correction factor can be altered to the following:

$$C_{size} = 1.189d^{-0.097}$$

The updated critical diameters are summarized in table 12 below.

Table 12. Updated critical diameters summarized

	Bearing step-down diameter (cm)	Gear shaft diameter (cm)	Torque (Nm)	Key dimensions (cm) base x height
Input Shaft	1.00	1.00	2.646	
Shaft 1	1.01	1.06	13.23	0.4 x 0.4
Shaft 2	1.73	1.78	66.15	0.6 x 0.6
Shaft 3	2.95	3.01	330.75	1.0 x 0.8
Output Shaft	4.02	4.53	1157.63	1.4 x 0.9

Now that the minimum required diameters have been established, the group can select bearings that can handle the loading required for this project. The shaft will be sized up to ensure the requirements are met.

Table 13. Bearing step-down and gear shaft diameters

	Bearing step-down diameter (cm)	Gear shaft diameter (cm)
Input Shaft	1.20	1.90
Shaft 1	1.20	1.90
Shaft 2	2.00	2.80
Shaft 3	3.00	4.30
Output Shaft	4.50	5.5

Next, the group must calculate the lifetime of each shaft using the stress-life method. First, we must identify the critical locations of the shaft which requires analyzing the stresses at multiple points. The group has previously developed the shear and bending moment diagrams for each of the shafts which will be used to determine the critical locations.

$$\sigma_c = K_f \frac{M_c r_c}{I_c} = 2.50 \frac{(7.88)(0.019/2)}{\pi \frac{0.019^4}{64}} = 29.26\ MPa$$

$$\sigma_D = K_f \frac{M_D r_D}{I_D} = 2.2255 \frac{(2.364)(0.012/2)}{\pi \frac{0.012^4}{64}} = 31.01\ MPa$$

For shaft 1, the stress developed at the gears and at the shoulder that experience the greatest moment are very close. This means that both values should be assessed for all shafts. The material used for the shafts is SAE 102 cold-rolled carbon steel which has an ultimate strength of 448 MPa and a yield strength of 262MPa, the uncorrected endurance limit can be determined.

$$Se' = 0.5 S_{ut}$$
$$Se' = 224\ MPa$$

$$S_m = 0.9 S_{ut}$$
$$S_m = 403.2\ MPa$$

To find the correct endurance limit we must use correction factors through the following equation:

$$Se = C_{load} C_{size} C_{surf} C_{temp} C_{reliab} Se'$$

Given that each of the shafts have different diameters, the corrected endurance limit will be different for each shaft. All correction factors other than the size correction factor will be assumed to be the same as the ones used in the final shaft design analysis.

Next, to estimate the life of each shaft the group must develop an empirical model:

$$S = aN^b$$

$$b = \frac{\log\left(\frac{S_m}{S_e}\right)}{\log\left(\frac{10^3}{10^6}\right)}$$

$$a = \frac{S_m}{1000^b}$$

For shaft 1 at the gears, a and b were calculated to be 4.65 x 10^8 and -0.0205. At the shoulder, a and b were calculated to be 4.44 x 10^8 and -0.0141.

The life of the shaft can be calculated through the following:

$$\log(N) = \frac{\log(\sigma_{a)} - \log(a)}{b}$$

$$N = 10^{\log(N)}$$

When evaluating at the gears we get 3.46 x 10^{58} cycles and when evaluating at the shoulder 1.68 x 10^{82} cycles. This is a lot of cycles! However, given we are using steel this is reasonable.

For shaft 2, evaluating at the gears we get 1.89 x 10^{43} cycles and when evaluating at the shoulder 2.77 x 10^{55} cycles. For shaft 3, evaluating at the gears we get 1.27 x 10^{34} cycles and when evaluating at the shoulder 1.01 x 10^{40} cycles.

As the Shaft material was chosen to be 1020 cold drawn steel with a yield strength Sy=350 MPa, and the Gear material was chosen to be 4340 Normalized (810°C) steal with a yield strength Sy=862 MPa. The material chosen for the keys is 1020 Annealed (870°C) steel with an Sy=295 MPa to ensure the key will be the first to fail. The minimum key length was calculated using the following formula:

$L_{min} = \frac{4TN}{DWS}$, Where T is the torque applied to the shaft, N is the chosen safety factor of 3, D is the shaft diameter, W is the key width, and Sy is the keys material yield strength (Sy=295MPa).

For Shaft 1; T=13.23 Nm, D=0.019m, W=0.004

$$L_{min} = \frac{4TN}{DWS} = \frac{(4)(13.23)(3)}{(0.019)(0.004)(295x10^6)} = 0.00708m$$

The keys length will be extended to match the width of the gears at 0.018m

For Shaft 2: T=66.15 Nm, D=0.028m, W=0.006m

$$L_{min} = \frac{4TN}{DWS} = \frac{(4)(66.15)(3)}{(0.028)(0.006)(295x10^6)} = 0.016m$$

The keys length will be extended to match the width of the gears at 0.018m

For shaft 3: T=330.75 Nm, D=0.043m, W=0.01m

$$L_{min} = \frac{4TN}{DWS} = \frac{(4)(330.75)(3)}{(0.043)(0.01)(295x10^6)} = 0.0257m$$

For Output shaft: T=1157.63 Nm, D=0.055m, W=0.014m

$$L_{min} = \frac{4TN}{DWS} = \frac{(4)(1157.63)(3)}{(0.055)(0.014)(295x10^6)} = 0.0311m$$

For each Shaft the key selection is shown in Table 14 below:

Table 14. Key specifications and selection

Shaft #	Key Dimensions Width x Height [cm]	Key Length [cm]
Input	0.4 x 0.4	1.8
1	0.4 x 0.4	1.8
2	0.6 x 0.6	1.8
3	1.0 x 0.8	2.57
Output	1.4 x 0.9	3.11

Carriage shaft Analysis

The group also performed shaft analysis on the shafts connecting the carriage to the arms on either side of the cart. While the force put on these shafts is only the downwards force incurred by the weight of the carriage and the child, it is considered to be half the force applied on each shaft since the group is using a design where there are supports on either side of the arms. The proper schematic of the load distribution can be seen in the figure below.

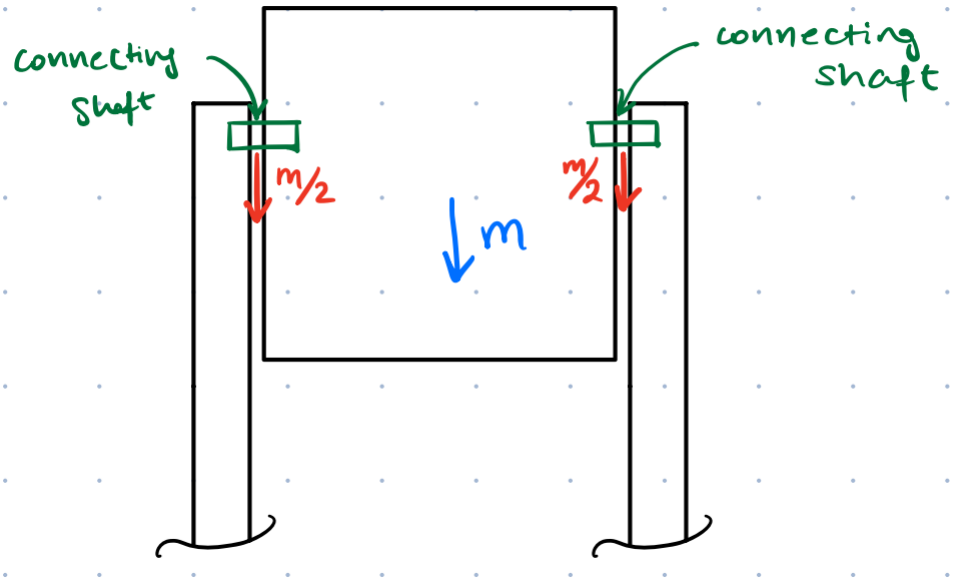

Figure 49. Load distribution of carriage

For these shafts, the group has decided to use the same material as is used for the shafts in the gearbox – 4340 Normalized Steel. Additionally, the endurance limit for the material was found to be 6.89 MPa along with an ultimate strength of 1110 MPa.

Since the downward force induced by the mass of the carriage and the child are the only forces acting on the shaft, the reaction forces on either side of the shafts is seen to be as shown in the figure below.

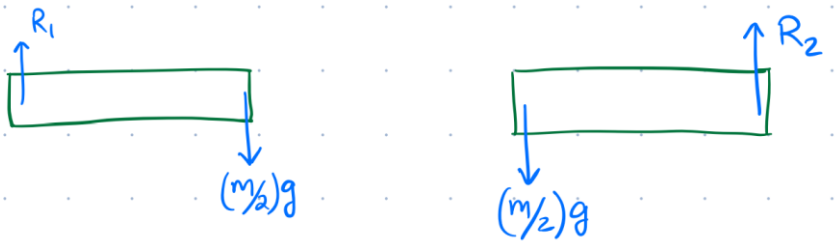

Figure 50. Reaction forces induced by mass of carriage and child

Therefore, we find that:

$$\Sigma F_y = 0 \Rightarrow R_1 = R_2 = \left(\frac{mg}{2}\right)$$

Following this, the shear force acting on each of these shafts is found to be as seen below with which the mean and alternating von misses stresses can be calculated as well:

$$\tau_m = \tau_a = \left(\frac{mg}{2}\right) * \frac{1}{2A}$$

$$\sigma'_a = \sqrt{3\tau_a^2} = \sqrt{3}\tau_a = \sqrt{3} * \left(\frac{mg}{2}\right) * \frac{1}{2A}$$

$$\sigma'_m = \sqrt{3\tau_m^2} = \sqrt{3}\tau_m = \sqrt{3} * \left(\frac{mg}{2}\right) * \frac{1}{2A}$$

Using the values found for the von misses stresses, the safety factor equation can be readjusted to find the cross-sectional area of the shaft used. Through this, the required diameter of the shaft is also calculated as shown through the steps taken in the following equations. In these calculations, the group has decided to go with a safety factor of 2 to ensure the safety of the children.

$$N_f = \frac{S_e S_{ut}}{\sigma'_a S_{ut} + \sigma'_m S_e} = \frac{S_e S_{ut}}{\sqrt{3} * \left(\frac{mg}{2}\right) * \frac{1}{2A} S_{ut} + \sqrt{3} * \left(\frac{mg}{2}\right) * \frac{1}{2A} S_e}$$

$$A = \frac{N_f \sqrt{3}(mg/2)(S_e + S_{ut})}{2 * S_e * S_{ut}}$$

$$A = \frac{\pi D^2}{4} \Rightarrow D = \sqrt{\frac{4A}{\pi}}$$

After inputting the actual values for the variables seen in the equations above, the proper required diameter can be seen to be:

$$A = \frac{(2)\sqrt{3}\left(137kg * 9.81\left(\frac{m}{s^2}\right)/2\right)\left((6.89MPa) + 1110MPa\right)}{2 * (6.89MPa) * (1110MPa)} = 0.0001699m^2$$

$$D = \sqrt{\frac{4 * 0.0001699}{\pi}}$$

$$D = 0.0147\, m = 14.7mm$$

Therefore, with these calculations, the group found that the minimum required diameter of the shaft connecting the carriage and the ferris wheel arms must be approximately 15mm.

Bearing Design and Analysis

Advantages and disadvantages of Ball Bearings Vs Roller Bearings

Types of Bearings

Ball Bearings

Advantages:

- Lower friction, Ball bearings generally have lower friction than roller bearings, leading to smoother operation and reduced energy consumption.
- High-speed capacity, Ball bearings are well suited for high-speed applications due to their low friction and ability to handle radial loads.
- Compact design, typically more compact than roller bearings, making them suitable for applications with limited space.
- Lower cost, In general ball bearings tend to be more cost-efficient then roller bearings, making them a popular choice for many applications.

Disadvantages:

- Limited load capacity, Ball bearings have a lower load-carrying capacity compared to roller bearings. They may not be well suited for heavy duty applications with high radial or axial loads.
- Lower tolerance for misalignment, Ball bearings are less tolerant to misalignment than roller bearings. Improper alignment can lead to increased wear and reduced lifespan.
- Lower shock resistance, Ball bearings may be more susceptible to shock loads and impacts compared to roller bearings.

Roller Bearings

Advantages:

- Higher Load Capacity, Roller bearings, such as cylindrical or tapered roller bearings, generally have a higher load carrying capacity, making them suitable for heavy duty applications.
- Greater misalignment tolerance, roller bearings can tolerate higher levels of misalignment than ball bearings, providing more flexibility in certain applications.
- Increased shock resistance, Roller bearings are often more robust and can handle higher shock loads, making them suitable for applications with variable or heavy loads.

Disadvantages:

- Higher friction, Roller bearings generally have higher friction than ball bearings, which can lead to increased energy consumption and heat generation.
- Limited high-speed capacity, while roller bearings can handle heavier loads, they may not be as well suited for high-speed applications as ball bearings.
- Larger size, Roller bearings are typically larger and may require more space compared to ball bearings. This can be a limitation in applications with tight space constraints.
- Higher cost, Roller bearings, especially specialized designs, can be more expensive than ball bearings, which may impact the overall cost of the system.

Bearing Selection

The choice between ball and roller bearings depends on the specific requirements of the application, including load, speed, available space, and cost considerations. After careful consideration of the advantages and disadvantages we have decided to use deep groove ball bearings.

The magnitude of the reaction forces for each shaft can be determined through the following relationships:

$$R_1 = \sqrt{{R_{1x}}^2 + {R_{1y}}^2}$$

$$R_2 = \sqrt{{R_{2x}}^2 + {R_{2y}}^2}$$

The reactions forces occurring at the bearings for each shaft were determined using the Matlab script. The reaction forces at the bearings for shaft 1 can be calculated as follows:

$$R_1 = \sqrt{(-57.78)^2 + (158.76)^2} = 168.95\ N$$

$$R_2 = \sqrt{(-134.8)^2 + (370.44)^2} = 394.22\ N$$

The minimum required diameters for the section of the shaft where the bearing is fixated are summarized in the final shaft design. Thus, the bearing must have a minimum bore diameter of the required shaft diameter; the shaft diameters will be increased to fit a reasonable bearing.

For intermediate shaft 1, the group decided to use 6301-2Z deep groove ball bearings on both ends. The critical characteristics of the bearing are listed in the table below.

Table 15. Critical characteristics of intermediate shaft 1

Dynamic Loading	10.1 kN
Static Loading	4.15 kN
Limiting Speed	22000 rpm
Bore Diameter	12 mm
Shoulder diameter	19.51 mm
Width	12 mm

As calculated earlier, the magnitude of the largest reaction force is 394.22 N, which is less than the static loading limit. Additionally, given that this shaft will be rotating at 375 rpm, which is less than the limiting speed. For all bearing calculations, 95% reliability was used, giving a reliability factor of 0.62. To calculate the expected lives of each bearing, the following relationship is used:

$$L_P = K_R \left(\frac{C}{R}\right)^3 * 10^6$$

For intermediate shaft 1, the expected lives of both bearings can be calculated to be:

$$Bearing\ 1 \quad L_P = 0.62\left(\frac{10{,}100}{168.95}\right)^3 * 10^6 = 1.32\ x\ 10^{11}$$

$$Bearing\ 2 \quad L_P = 0.62\left(\frac{10{,}100}{394.22}\right)^3 * 10^6 = 1.04\ x\ 10^{10}$$

The expected lives for all bearings were calculated and the results are summarized in table 16.

Table 16. Life expectancy of bearings with regards to reaction force

Bearing	Reaction Force (N)	Expected Life (Revolutions)
1	168.95	$1.32 * 10^{11}$
2	394.22	$1.04 * 10^{10}$
3	651.8	$5.51 * 10^{9}$
4	1381.8	$5.78 * 10^{8}$
5	2333.5	$1.26 * 10^{9}$
6	5097.2	$1.21 * 10^{8}$
Output	5866.3	$5.19 * 10^{8}$

Engineering drawings and specifications for each are shown in the following figures and tables.

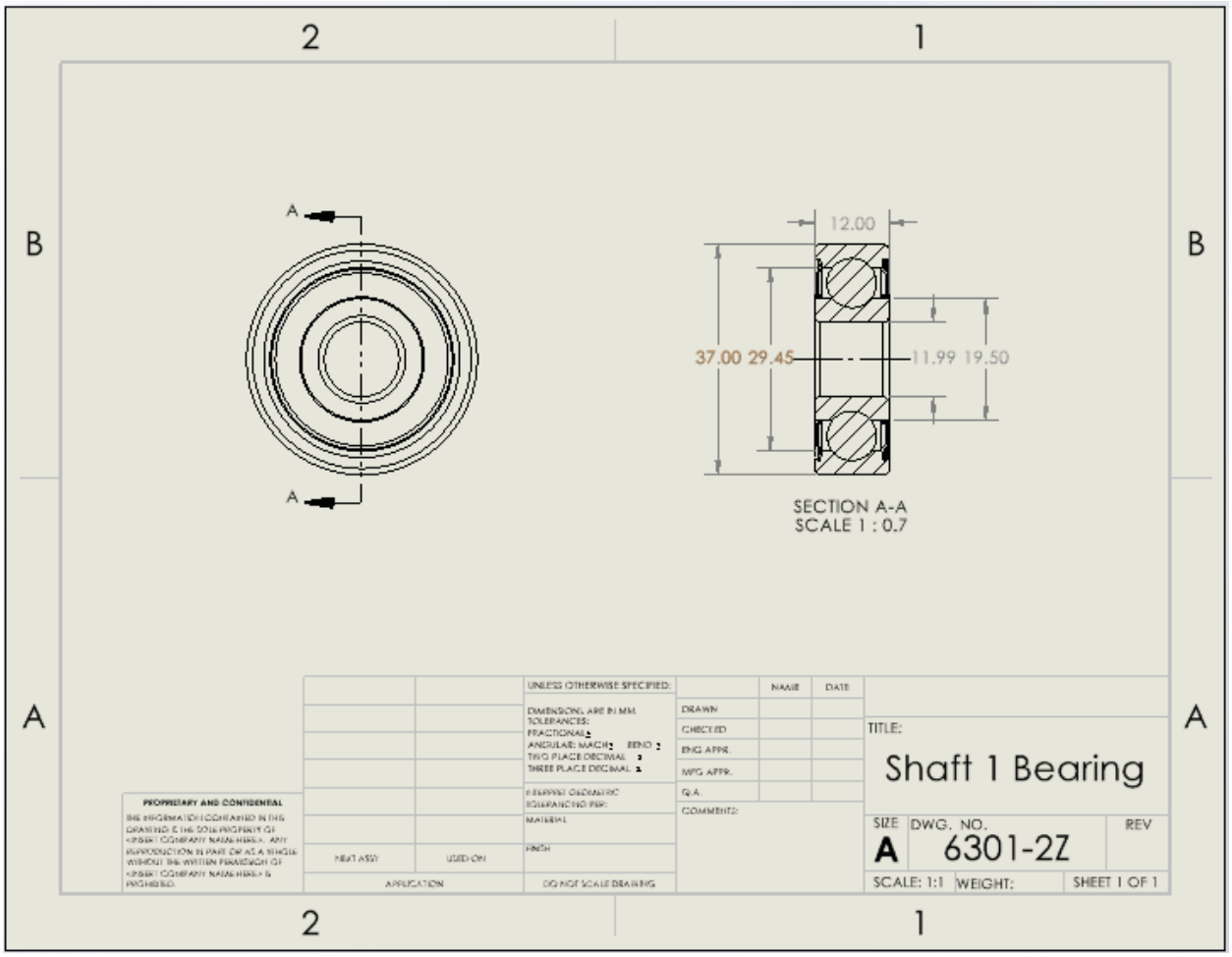

Figure 51. Shaft 1 bearing

For intermediate shaft 2, 6204 deep groove ball bearings on both ends

Table 17. Critical characteristics of intermediate shaft 2

Dynamic Loading	13.5 kN
Static Loading	6.55 kN
Limiting Speed	20000 rpm
Bore Diameter	20 mm
Shoulder diameter	28.8 mm
Width	14 mm

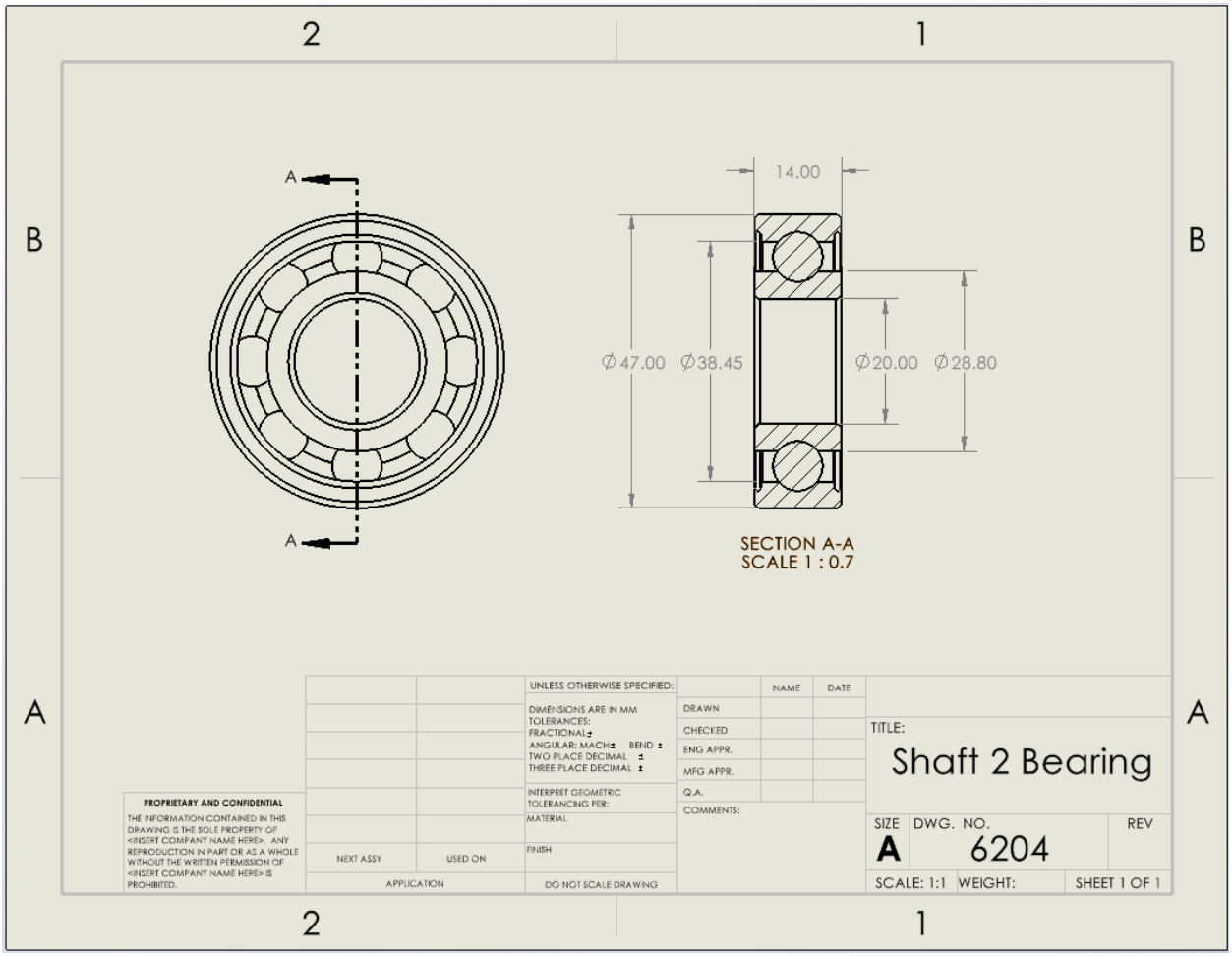

Figure 52. Shaft 2 bearing

For intermediate shaft 3, 6306 deep groove ball bearings on both ends

Table 18. Critical characteristics of intermediate shaft 3

Dynamic Loading	29.6 kN
Static Loading	16 kN
Limiting Speed	13000 rpm
Bore Diameter	30 mm
Shoulder diameter	44.6 mm
Width	19 mm

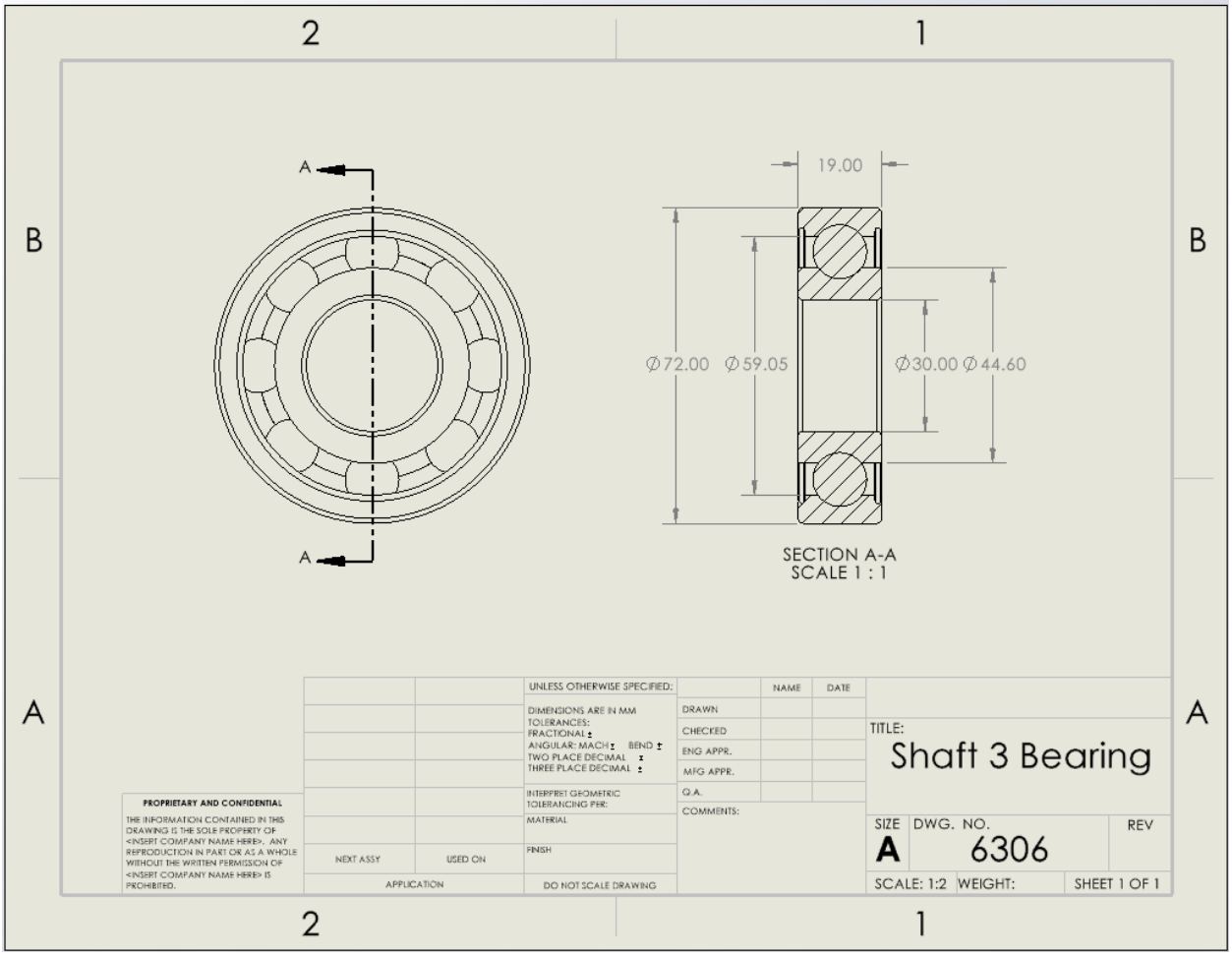

Figure 53. Shaft 3 bearing

For the output shaft, 6309-2RSH deep groove ball bearing on both ends

Table 19. Critical characteristics of output shaft

Dynamic Loading	55.3 kN
Static Loading	31.5 kN
Limiting Speed	4500 rpm
Bore Diameter	45 mm
Shoulder diameter	58.256 mm
Width	25 mm

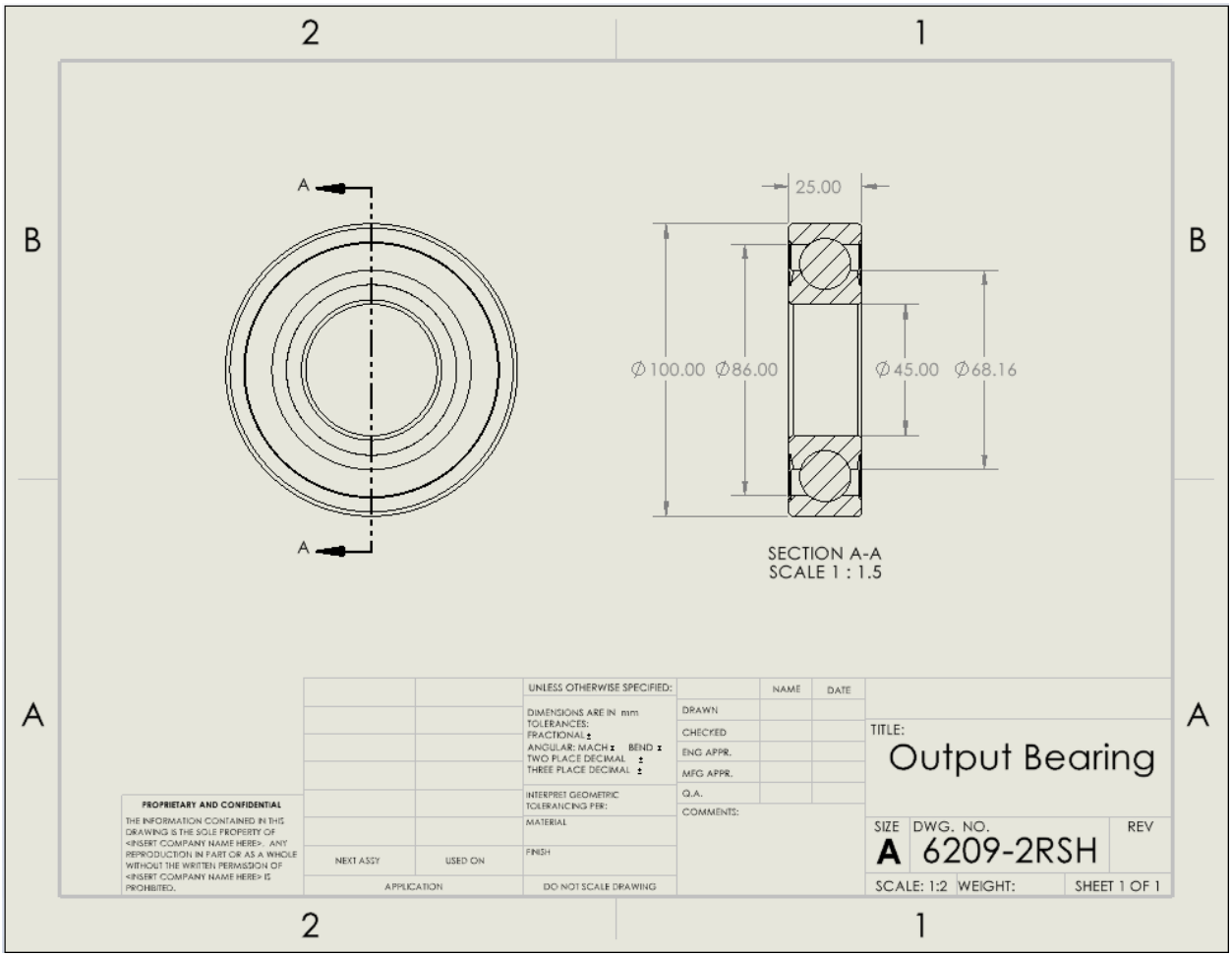

Figure 54. Output bearing

Final Gearbox Design

Couplings, Fasteners, and Seals

Due to the low pressure and compression in the gearbox case, it does not require a complicated gasket. For this gearbox case, a simple non-metallic gasket will suffice in sealing the upper and lower portion of the case. A great material for this task is rubber due to its cost-efficiency and availability. It is also very easy to work with when assembling and disassembling the gearbox case compared to other forms of sealing, for example silicon, which requires scraping and chemicals to remove it. Additionally, rubber does not retain dirt, bears no risk of pieces falling into the case, and creates an even seal along the mating surfaces.

As for the input and output, the gearbox case will be fitted with spring-loaded rotary shaft seals with wiper lip, which are designed for many purposes, including gearboxes. Both seals will be obtained from McMaster-Carr. The input will use the 1199N11 seal with an inner diameter of 12 mm and a bore diameter of 22 mm. The output will use the 5154T868 seal with an inner diameter of 45 mm and an outer diameter of 62 mm. The seals will be press-fit into the bored-out part in the gearbox case. Figure 55 and Figure 56 illustrate the input and output seals, respectively.

The Output shaft will be mated to a High-Torque keyed screw flexible shaft coupling sourced from McMaster-Carr, capable of withstanding 1580 Nm or torque at speeds of 6000 rpm, this results in a safety factor of 1.36. This is a three-piece coupler comprised of a steel hub (1), Urethane Split Spider (2), and Steel Split Spider Cover (3).

The input shaft will be mated to a High-Torque keyed flexible shaft coupling sourced from McMaster-Carr, capable of withstanding 92 Nm or torque at speeds of 12000 rpm, this results in a safety factor of 42. This is a three-piece coupler comprised of a 303 stainless steel hub (4), Urethane Split Spider (5), and 303 stainless Steel Split Spider Cover (6).

McMaster-Carr Part numbers:

1) 3565N9
2) 3565N52
3) 3565N64
4) 3565N1
5) 3565N43
6) 3565N61

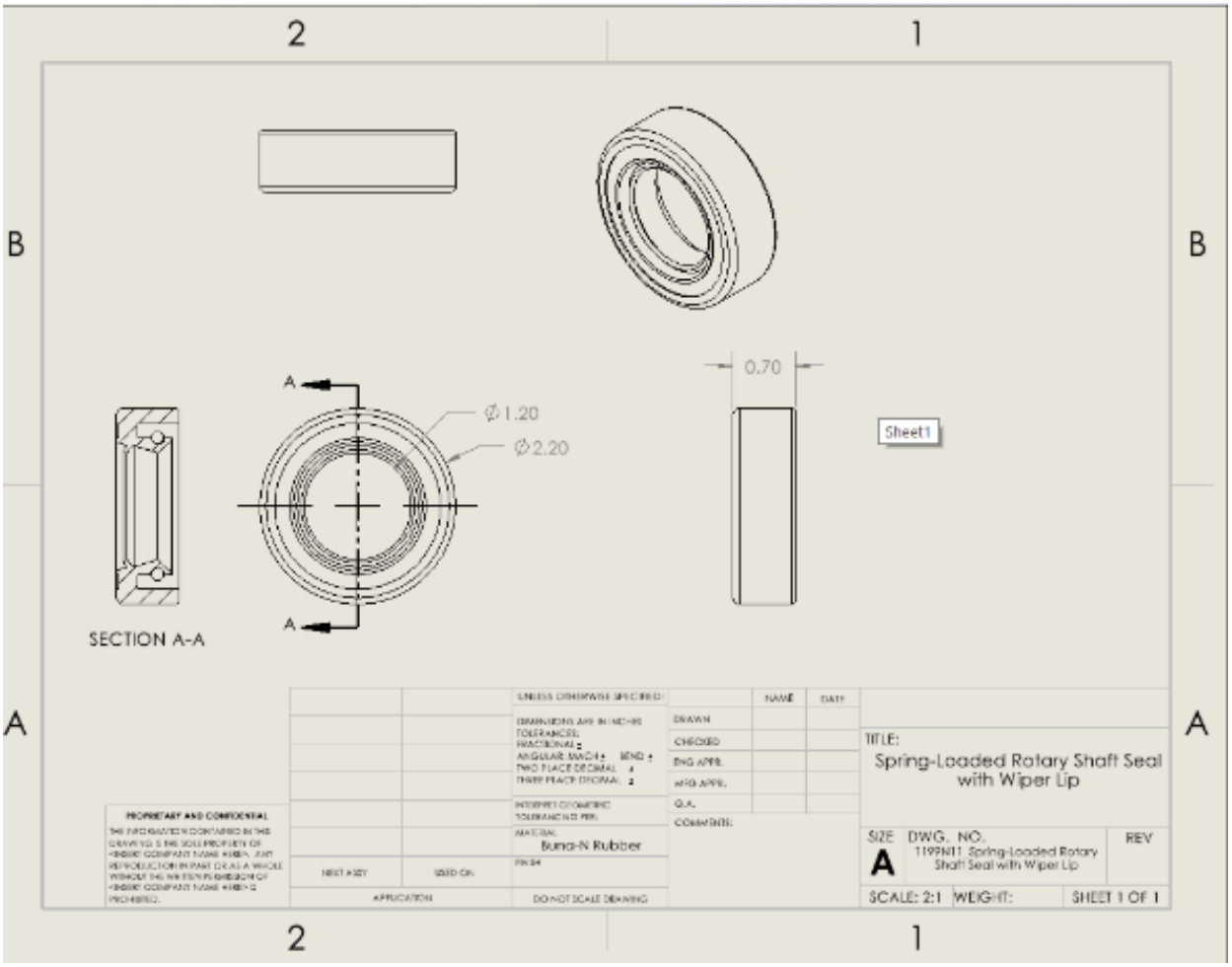

Figure 55. Input shaft spring-loaded rotary shaft seal drawing

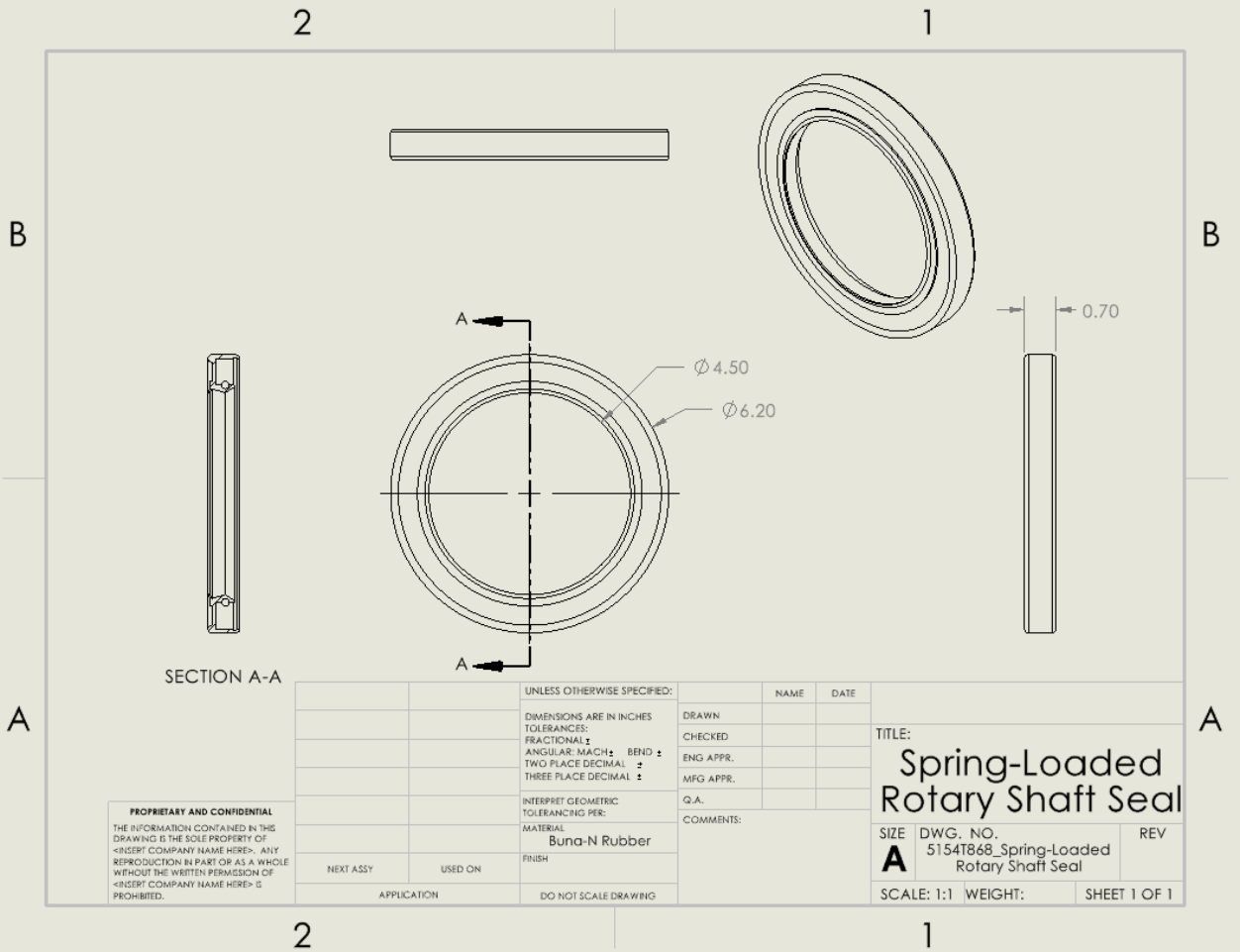

Figure 56. Output shaft spring-loaded rotary shaft seal drawing

The fasteners that will be used to hold the upper and lower parts of the gearbox case together will be bolts add part number with washers add part number. The bolts will be spaced out evenly along the flange that connects the two parts of the gearbox case.

The gears used are as specified in the preliminary gearbox design. The final gear sizing and gear failure analysis were completed in the gear design portion of this report. The detailed drawing for the first gear is found in figure 57 below. The remaining detailed gear drawings can be found in Appendix C.

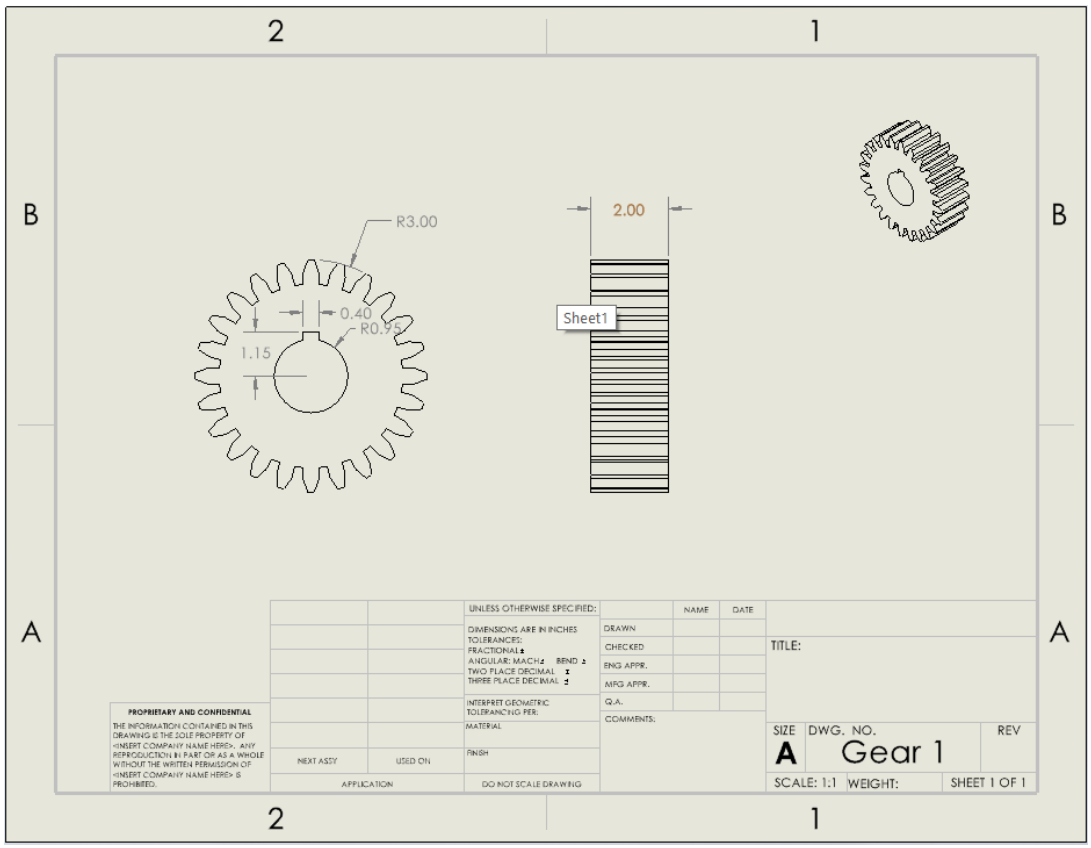

Figure 57. Gear 1 drawing

Next, with the basic shaft layout chosen, the group performed a load analysis to evaluate forces acting on the shafts by creating shear and moment diagrams. By solving for the critical diameter algebraically we were able to create a Matlab script which takes in parameters of tensile strength and Neuber's constant and returns critical diameters. This allowed us to easily test many different material options and find one that best fit the scope of the project.

With shaft lengths and diameters established, we were able to determine bearing support, and keyhole placements on the shafts. The shafts and gears were then modeled on SolidWorks and the group was able to create preliminary gearbox layout drawings. In this stage, the final bearings were chosen for modeling purposes.

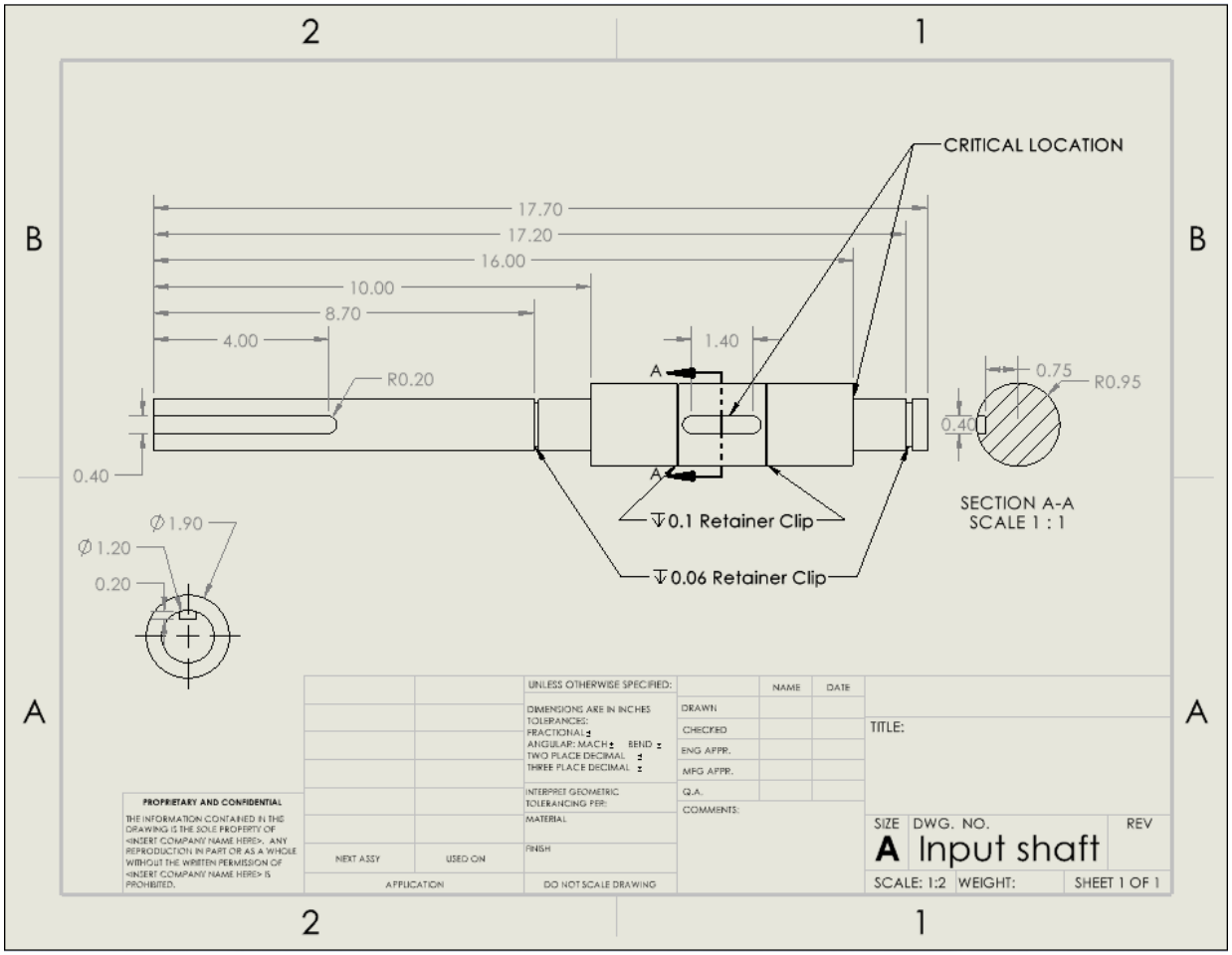

Figure 58: Shaft 1 Design

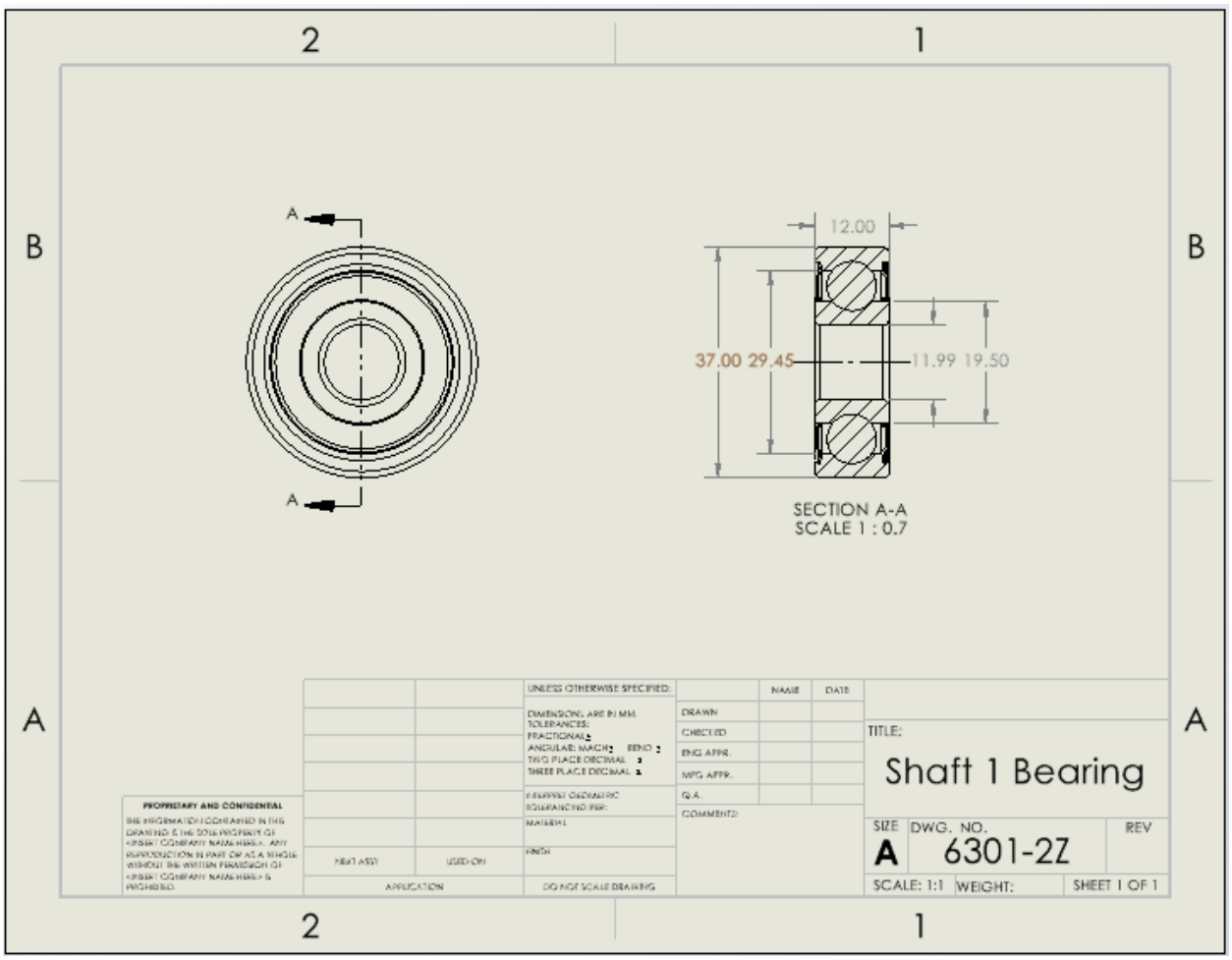

Figure 59: Shaft 1 Bearing overview

Final Gearbox Assembly Layout

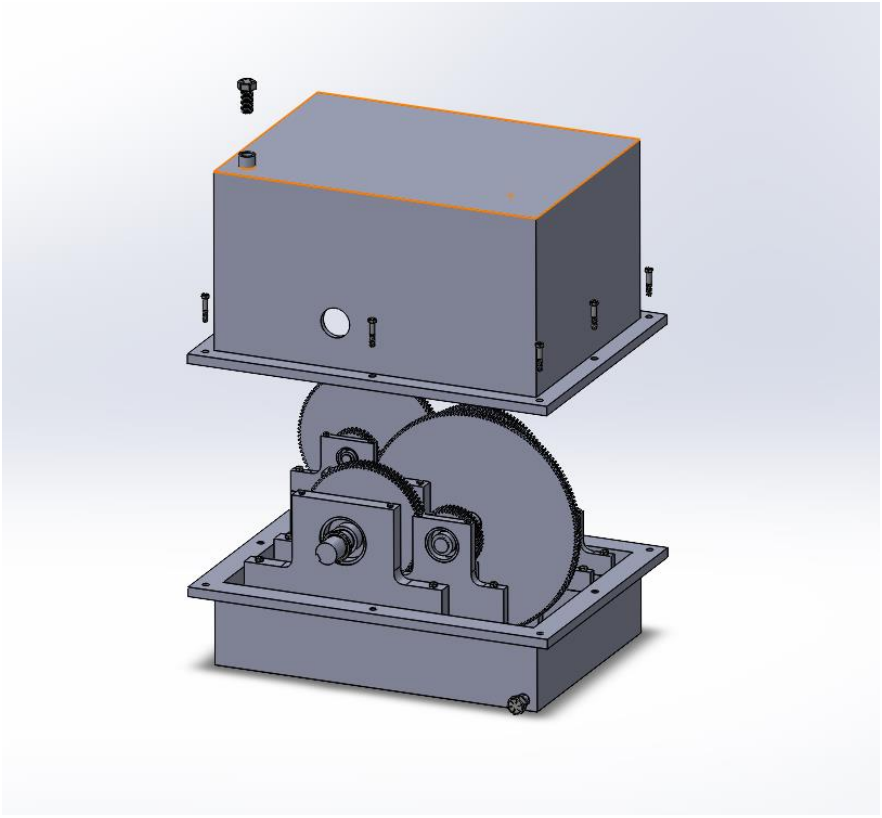

Figure 60: Exploded Casing View of Gearbox

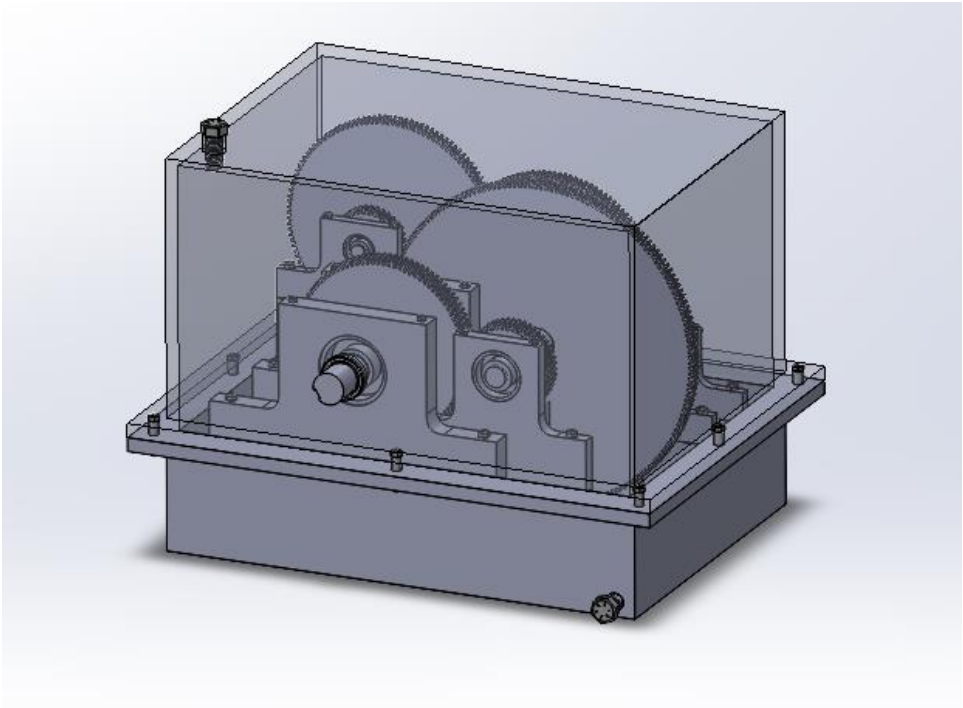

Figure 61: Transparent top Full Housing View

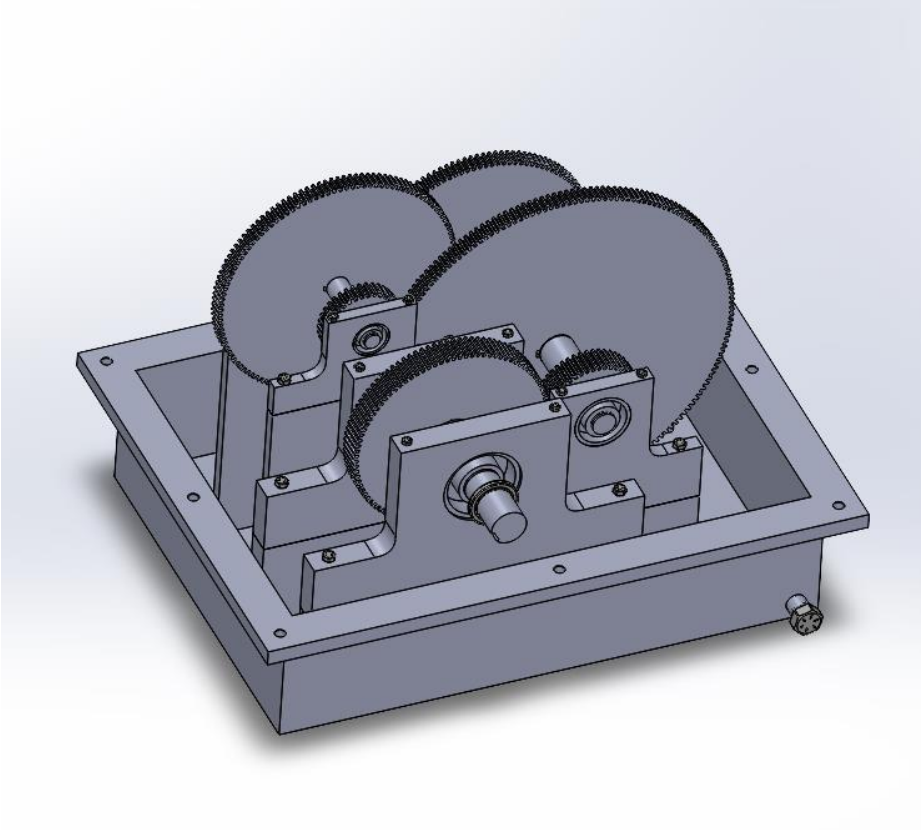

Figure 62: Isometric view with upper casing removed

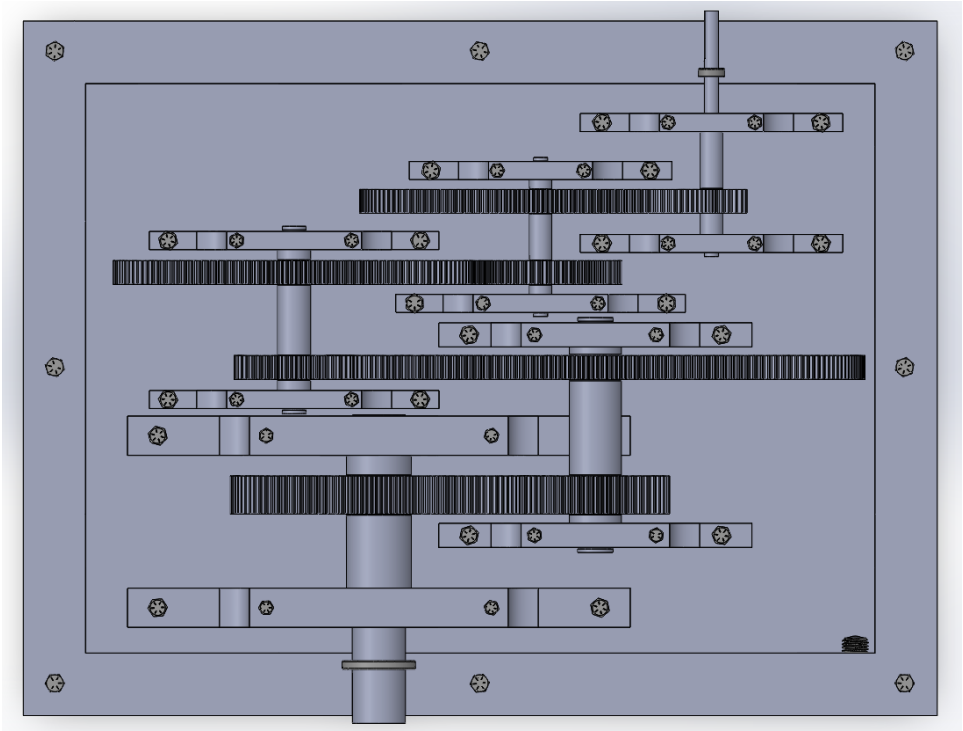

Figure 63: Top View of Gearbox

Figure 64: Additional Features

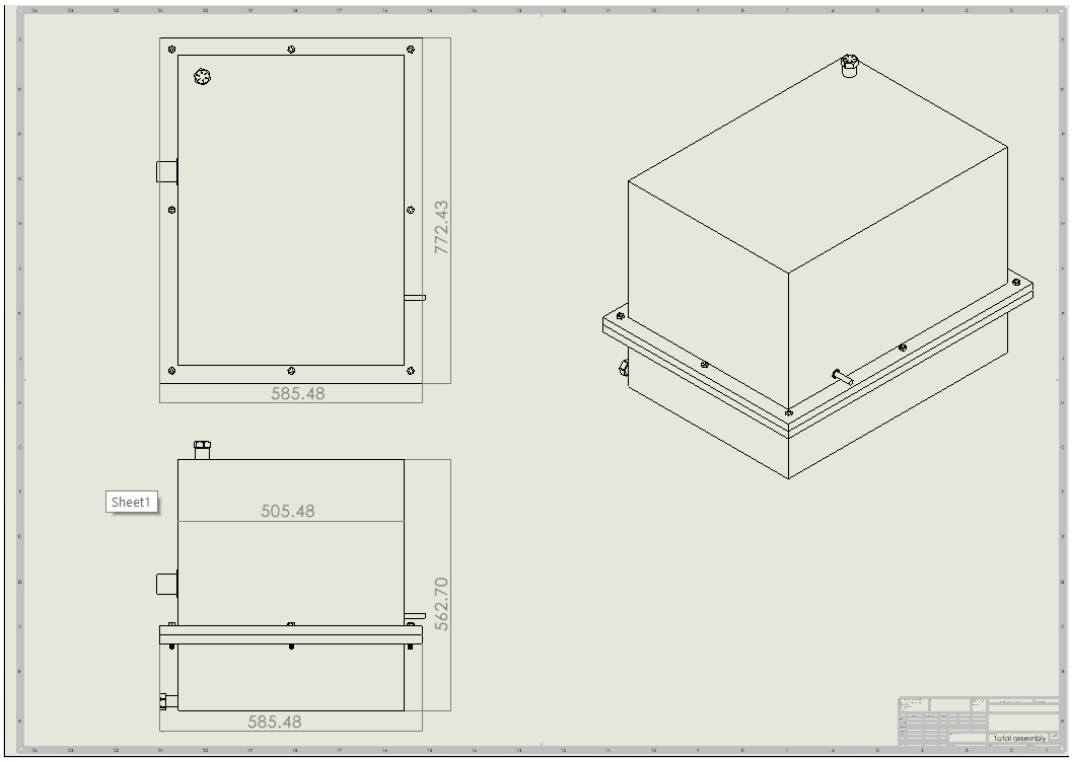

Figure 65: Overall Casing dimensions

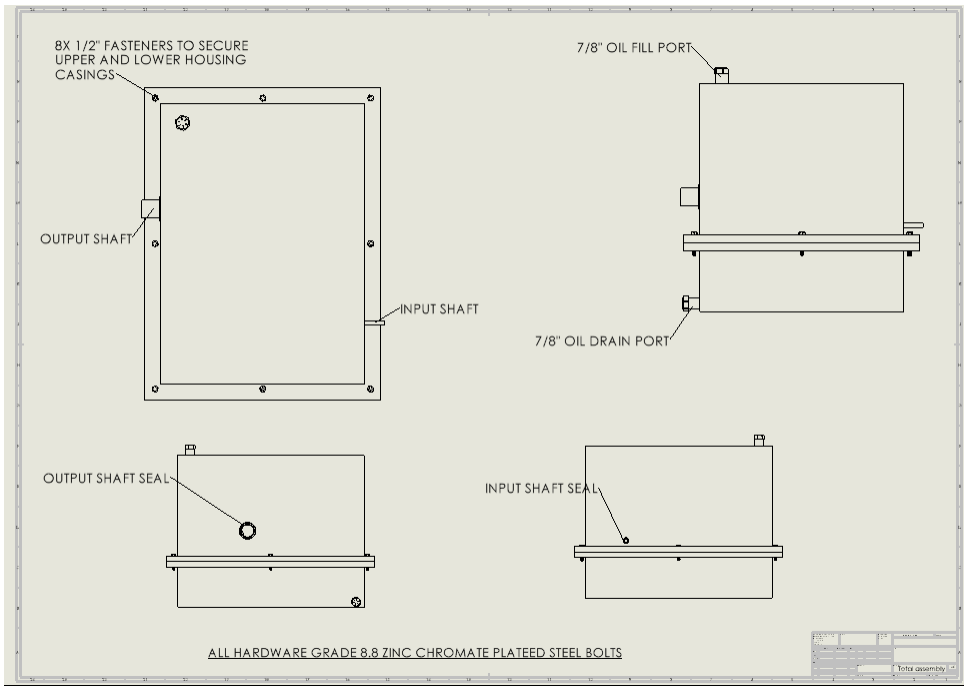

Figure 66: Gearbox Serviceable features

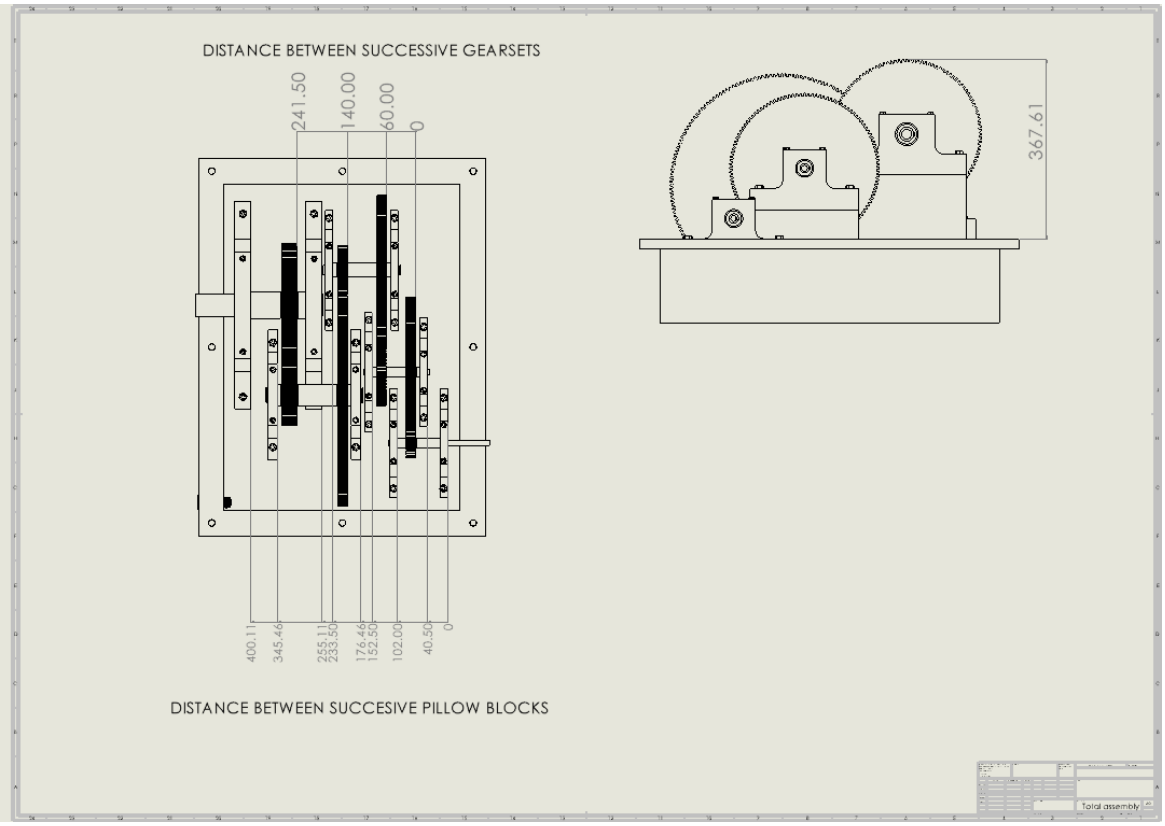

Figure 67: Pillow Block and Gear face separation dimensions

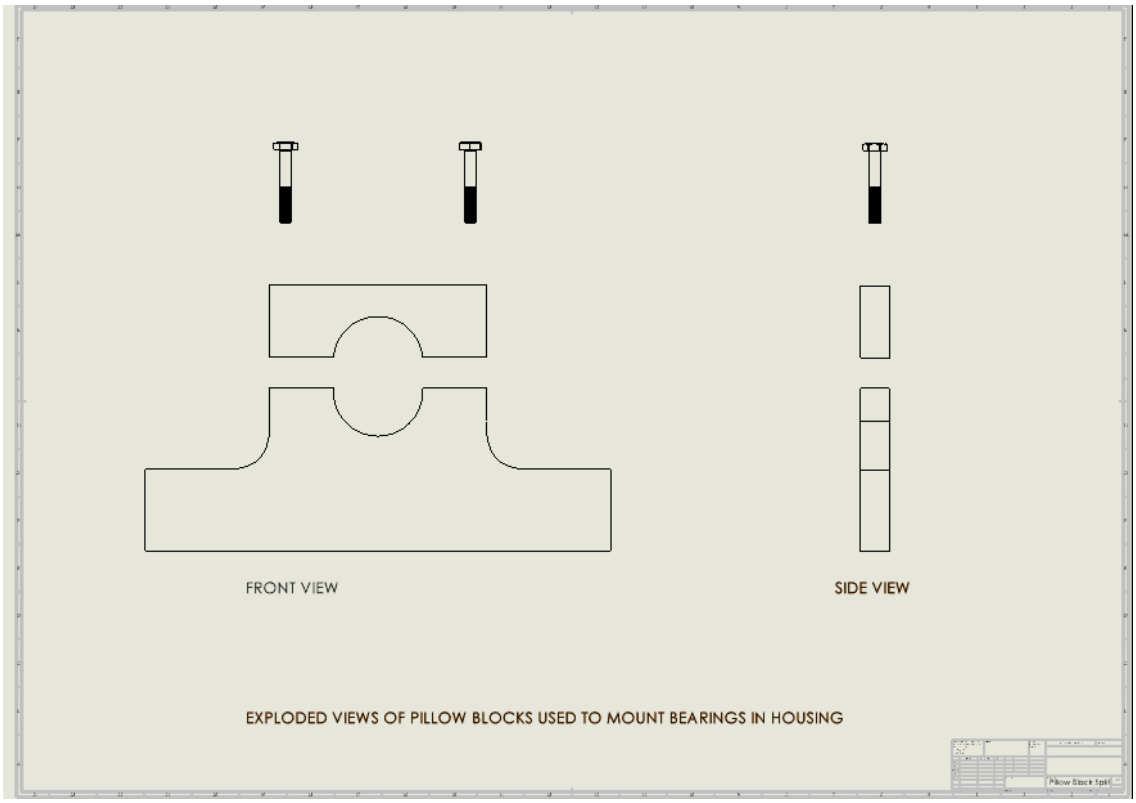

Figure 68: Pillow Block Schematic

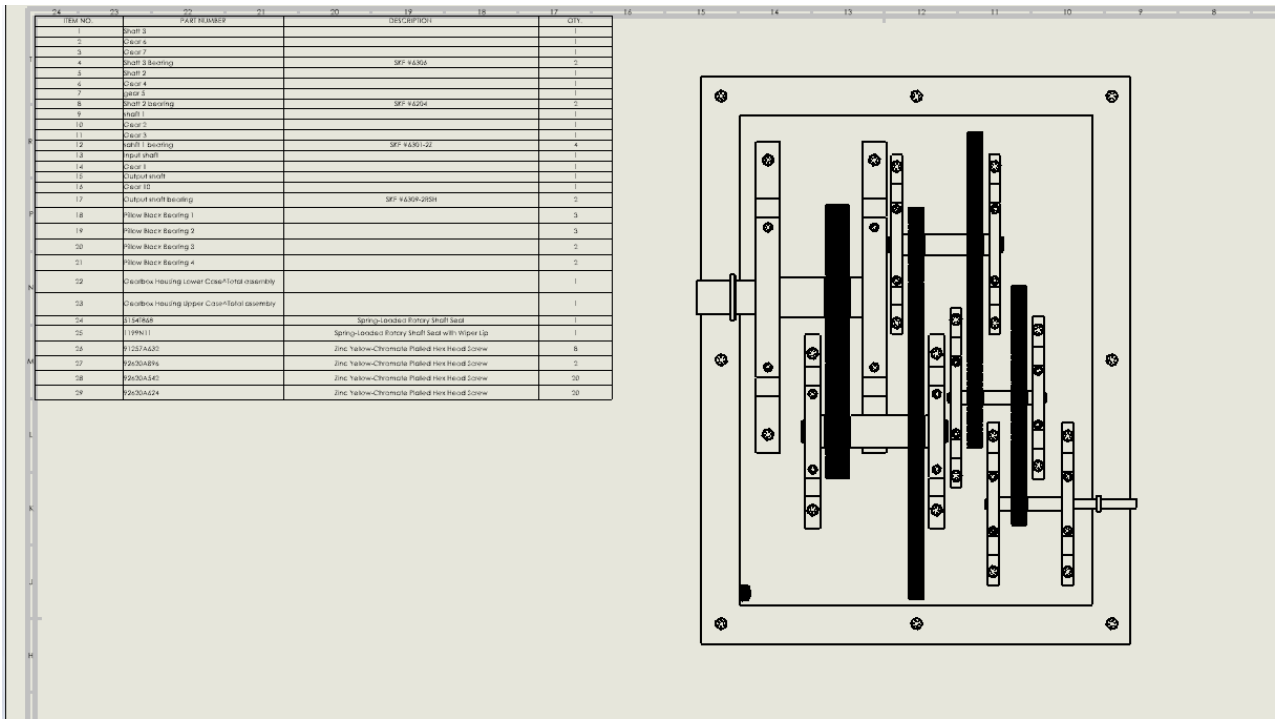

ITEM NO.	PART NUMBER	DESCRIPTION	QTY.
1	Shaft 3		1
2	Gear 6		1
3	Gear 7		1
4	Shaft 3 Bearing	SKF W6306	2
5	Shaft 2		1
6	Gear 4		1
7	Gear 5		1
8	Shaft 2 Bearing	SKF W6204	2
9	Shaft 1		1
10	Gear 2		1
11	Gear 3		1
12	Shaft 1 Bearing	SKF W6301-2Z	4
13	Input shaft		1
14	Gear 8		1
15	Output shaft		1
16	Gear 10		1
17	Output shaft Bearing	SKF W6308-2RSH	2
18	Pillow Block Bearing 1		3
19	Pillow Block Bearing 2		3
20	Pillow Block Bearing 3		2
21	Pillow Block Bearing 4		2
22	Gearbox Housing Lower Case-Total assembly		1
23	Gearbox Housing Upper Case-Total assembly		1
24	6154K68	Spring-Loaded Rotary Shaft Seal	1
25	1199N11	Spring-Loaded Rotary Shaft Seal with Wiper Lip	1
26	91257A630	Zinc Yellow-Chromate Plated Hex Head Screw	8
27	92630A896	Zinc Yellow-Chromate Plated Hex Head Screw	2
28	92630A540	Zinc Yellow-Chromate Plated Hex Head Screw	20
29	92630A624	Zinc Yellow-Chromate Plated Hex Head Screw	20

Figure 69: Bill of Materials

Lubrication

The gearbox will be lubricated with heavy duty truck manual transmission fluid called Delo® Syn-Trans HD. This fluid is “formulated to deliver outstanding protection against gear wear and all-weather, year-round performance. This fluid will provide us with ease of use throughout the year and will help to reduce the rate of maintenance because of its protection.

Maintenance

Maintenance is a crucial part of any moving system. For this gearbox system, since all involved parts have a high safety factor, the inspections required can be conducted on a seasonal basis. During the inspections, the main things to look for would be the to check for signs of wear and damage to the gears, shafts and keys. Additionally, another thing to look for would be the gear misalignment, which - if not perfect – may lead to a catastrophic failure of the gearbox. As shown in Table 16, the bearings all have incredibly high lifetimes exceeding 100 years under the current operating conditions, however, one thing to look for on regular inspections would be signs of overheating, unconventional wear or damage.

Cleanliness of the gearbox is another factor that may greatly affect the performance of the gearbox. Debris within the gearbox could have an effect on the friction between the gears and cause unnecessary wear and tear within the system. Therefore, using proper sealing and filtration system for the fluid within is an essential part of the gearbox maintenance.

Design Reflections

Throughout the design process of this gearbox the group went through many different design iterations, before finally landing on this design. When conducting a simulation of the Ferris wheel in SolidWorks it became clear to the group that an output speed of 2 rpm was slower than the group had wanted. This led to the removal of the final gear reduction as we still had more than double the required torque without it. With this removed it may make more sense to change the other gear ratios to further reduce the amount of gear reductions and lower manufacturing costs.

When conducting the gear failure analysis, the group initially created a program that required a face width as a parameter and returned only the safety factors against bending and surface fatigue. This required the group to manually iterate through face widths and material properties which was a poor use of time and very difficult to get an accurate minimum face width. This lead us to modify the program into what it is now, where material properties are used as input and a minimum face width and associated safety factors are returned. To further optimize the design process of the entire gearbox it may be worthwhile to modify all of our programs to return critical values. This would make modifications to things like materials, size of gearbox, output requirements, input requirements, and manufacturing costs very easy to do if problems in manufacturing become apparent.

The current design implements standard spur gears. It may be optimal to run analysis to determine whether switching to helical gears would improve overall efficiency and smoothness of operation given our purposes. To further decrease costs and improve ease of manufacturing it may also be worthwhile to have the design accommodate off the shelf gears as opposed to custom. This would also make repairs easier in the event that a gear needs to be replaced. In order to mount the gears to the shafts the group opted to use keys. Upon further research, it may be preferable to switch to splined shafts given the load requirements of our application. This could improve the longevity and durability of the shafts.

Although not critical to the performance of the gearbox, the housing and layout of the gears could likely be optimized to decrease the weight and amount of space the gearbox will require. With the gearbox in its current form, the housing is made of cast iron which will be very heavy at the current size. The casting process could likely leave the housing with further clean up and machining needing to be done to accommodate precision parts. Finally, the cast iron housing will need to be coated in something to protect it from rusting as proposed Ferris wheel is set to be operating outdoors in peak seasons at Butchart Garden’s which are summer and winter. Given that west coast winters are very wet, protection against moisture is key to the lifespan of the gearbox.

There are many different types of bearings readily available to purchase and for the purpose of this project the group decided to use standard ball bearings as they will accommodate the scope of the project. In further iterations of design, it may be worth looking into different types of bearings on input and output shafts. In the case of the input shaft, it will be constantly spinning at 1750 rpm and a specific high speed bearing such as angular contact bearings may be optimal for this application. The output shaft however will be subject to high loads of torque and low speeds, in this case it may be better to use something like a roller bearing to improve the durability.

Conclusions

The conceptual design process of creating a ferris wheel has many stages along with multitudes of components which all need to be controlled when making decisions regarding the design. Every decision that is made in this process has to be adhered to in order to create a suitable concept. The most significant parts of this process have to do with choosing the support structure, the arms, carriages, and most importantly the gearbox to be used in the system to provide optimal results. While there are a vast number of potential ferris wheel mechanisms to take into account, each group member came up with a design of their own, which were then compared with one another to select the best and most plausible with our provided conditions regarding the power consumption, the chosen speed reduction within the gearbox, and the overall ferris wheel structural limitations.

Using the weighted objectives chart, the final design that was chosen was the animal-themed ferris wheel by Jack Martin. Each design was put through the design concept weighted objectives chart and the final design was chosen based on its presumed performance of the following: ease of maintenance, durability, gearbox design, and structural design. The chosen design excelled at the structural design and durability because of its support system. The wheel is supported on both sides with an I-beam frame, making it very strong and stable for the safety of the children on the ride. Each of the carts also have an I-beam arm attached on each side, contributing to the structural integrity of the design. Another benefit of having supports on both sides of the wheel is that it reduces the forces on the structure. Compared to a single-sided design, this design cancels the moment and reduces the displacement on the wheel. The ferris wheel is designed to be located at Butchart Gardens and hold carts themed as local animals (rabbit, squirrel, deer, bear, cougar, and eagle).

During the external load analysis, details such as the materials used for the arms and the carriages were determined to have a suitable estimate of the forces and moments to be experienced by the arms and the shaft to aid in the gearbox and motor calculations conducted further into the design process.

Due to the symmetrical nature of the ferris wheel with six carts coming off the shaft with identical weights and arm supports - at the length of 2 meters, we find that there is no net moment on the system when there are no children in the carts. Therefore, we find that the only moment produced is from the weights of the various children in the carriages. After considering multiple different loading scenarios of the ferris wheel, the maximum possible torque on the shaft was calculated to be 538.19 Nm with it fully loaded. Furthermore, using the maximum torque, the maximum power required of the motor (accounting for the 97% efficiency) was found to be 0.113 kW, which led to us choosing 0.5 kW to be our motor power output allowing for excess power if any variables were to change.

For the gearbox design, the group decided on using a compound gear reduction gearbox with an overall reduction ratio of 875:1 producing an output speed of 2 rpm. The torques, angular velocities, and gear ratios were all calculated as well, as seen in Table 4. This design on the gearbox investigates the use of spur gears in the gearbox design described; however, future

analysis of the gearbox will investigate the use of helical gears since they produce lower noise and conduct smoother movement.

This report is a conceptual design report for a ferris wheel in the Greater Victoria District. The final design is very stable, has a durable and efficient gearbox, and is a great way for children to enjoy an amusing and safe ferris wheel ride at Butchart Gardens. Future considerations are to replace the spur gears in the gearbox with helical gears due to their low noise production and smooth movement, both of which are crucial for a ride for children.

The preliminary design report of this project delves deeper into the specifics of the gearbox. Factors discussed and chosen include the pressure angle and the preliminary shaft lengths. Parameters, such as contact ratios, pitch, length of action, and overall efficiency of the gearbox were then calculated.

With the shaft layout chosen, shear and moment diagrams were then created to determine the forces acting on shafts. The critical diameters were then algebraically solved which allowed the group to be able to create a MATLAB script. The MATLAB script solved for critical diameters using parameters of tensile strength and Neuber's constant which allowed the group to be able to test different materials and determine the material that best fit for the scope of the project. The material that was chosen was 1020 cold rolled steel based on the results of the MATLAB code but also because of its accessibility, ease of manufacturing, and durability.

With the shaft length and diameters determined, the bearing support and keyhole placements were established. SolidWorks was used to accurately model the gears and shafts which allowed the group to create drawings of the gears and shafts as well as a preliminary gearbox layout. Unspecific bearings were used in this step simply to allow the group to create the models. Specific bearings which meet the requirements of the project will be established and used in the final design report.

For the final design report, the final gearbox was formed with all the respective gear, shaft, and bearing calculations. A failure analysis was completed to determine the appropriate materials and face widths that were required to achieve proper safety factors. An extensive MATLAB script was written which too material properties and gear contact specifications as parameters and returned the minimum acceptable face width and the associated safety factors of 1.5 for both bending and surface fatigue. This program assigned a small face width and determined what the associated safety factors would be at that width. If the conditions were not met, the program would increment the face width until adequate safety factors were achieved. With this program, face widths were easily of the critical gear contacts were easily determined with different materials, eventually concluding that 4340 normalized (870°C) steel was the optimal choice of material considering the scope of the project.

This report also includes the finalization of the shaft designs. It was discovered that more space was required to include the housing of the bearings therefore alterations were made to the preliminary shaft designs. Also, the final gear reduction included in the preliminary gearbox design was removed in order to increase the output shaft speed. All of the shafts are shown

through detailed engineering drawings that label critical locations where detailed fatigue analysis was executed. Using a Matlab script developed by the group, critical diameters were found for each shaft, which were the sized up to accommodate appropriate bearings. Fatigue failure analysis was then performed using the stress-life method after having determined all the shaft diameters. Additionally, the shaft used to connect the carriage to the body of the ferris wheel was analyzed to determine the necessary strength for holding up the carriage. Bearings were then selected based on the expected lifetime of the shafts within the gearbox.

The final gearbox housing design was decided upon by the group. This includes the materials used, fasteners, seals, and couplings. The size of the gearbox housing is as follows: 77.2 cm x 58.6 cm x 56.3 cm. The final output speed of the gearbox was changed to 4 rpm. To finish the report, the group reflected on the overall design of the gearbox and commented on what else can be done to the design to improve and optimize it.

References

[1] A. Stewart, “Ain Dubai: How the world’s largest observation wheel was built” 13 September 2021. [Online]. Available: https://www.cnn.com/travel/article/ain-dubai-worlds-largest-observation-wheel/index.html. [Accessed 16 October 2023].

[2] P. Ryan, “First passenger capsule installed on Dubai’s big wheel” 24 August 2020. [Online]. Available : https://www.thenationalnews.com/uae/first-passenger-capsule-installed-on-dubai-s-big-wheel-1.1067692. [Accessed 16 October 2023].

[3] E. Zhan, “140-m tall observation wheel with no center is a thing of beauty” 14 November 2018. [Online]. Available: https://www.guinnessworldrecords.com/news/commercial/2018/11/140-m-tall-observation-wheel-with-no-centre-is-a-thing-of-beauty-542006. [Accessed 16 October 2023].

[4] Z. Linhares, “What goes into building the ferris wheel in Boulevardia? Watch this timelapse video to see” 15 June 2023. [Online] Available: https://www.kansascity.com/news/local/article276452101.html. [Accessed 16 October 2023].

[5] F, Sperling, “Construction measures at Spreepark” 1 August 2021. [Online] Available:https://www.spreepark.berlin/en/planning-construction/construction-measures/. [Accessed 16 October 2023].

[6] R.D. Sussman, “Waagner Biro double and triple tree wheels” [Online] Available: https://amusementparkives.com/amusement-ride-manufacturers/waagner-biro-double-and-triple-tree-wheels/. [Accessed 16 October 2023].

[7] “Sky Whirl” [Online] Available: https://www.pinterest.ca/pin/507921664197544952/. [Accessed 16 October 2023].

[8] “ Disney California Adventure DCA Mickey Mouse fun wheel Pixar Pal-A-Round DCS_8271-4K” [Online] Available: https://www.micechat.com/325069-disneyland-news-heatwave-rolls-in-summer-crowds-thin-out-and-a-musical-tradition-returns/disney-california-adventure-dca-mickey-mouse-fun-wheel-pixar-pal-a-round-dsc_8271-4k/. [Accessed 16 October 2023].

[9] Duchess of Disneyland, “Pixar Pal-A-Round” 16 February 2019. [Online] Available: https://duchessofdisneyland.com/california-adventure/pixar-pal-a-round/. [Accessed 16 October 2023].

[10] O. Bondarenko [Online] Available: https://www.vecteezy.com/photo/2908442-the-electric-motor-with-roller-of-the-ferris-wheel-in-gorky-park-kharkov-ukraine. [Accessed 16 October 2023].

[11] ”Hydraulic drive system for las vegas observation wheel” [Online]. Available: https://www.enerpac.com/en-us/applications/infrastructure/hydraulic-drive-system-for-las-vegas-observation-wheel. [Accessed 16 October 2023].

[12] “Vintage shop built chain drive model double ferris wheel tin hand crank” [Online] Available: https://www.worthpoint.com/worthopedia/vintage-shop-built-chain-drive-model-491880856. [Accessed 16 October 2023].

[13] “Keyway Chart” [Online] Available: https://hallite.com/au/hallite-transeals/transmission-products/keyway-chart/. [Accessed 20 November 2023].

[14] “Tensile-Yield Strength of Steel Chart” [Online] Available: https://amesweb.info/Materials/Steel-Tensile-Yield-Strength-Chart.aspx. [Accessed: 20 November 2023].

[15] “Understanding Yield Strength and Tensile Strength” [Online]. Available: https://www.spex1.com/yield-strength-tensile-strength/. [Accessed 20 November 2023].

[16] Norton, R.L., Machine Design: An Integrated Approach (6th Edition), Pearson – Prentice Hall, 2020

[17] “The Online Materials Information Resource,” MatWeb, https://www.matweb.com/search/DataSheet.aspx?MatGUID=ac54866df849406fa1a8a9d24e7f4d95&ckck=1 (accessed Dec. 4, 2023).

Appendix A

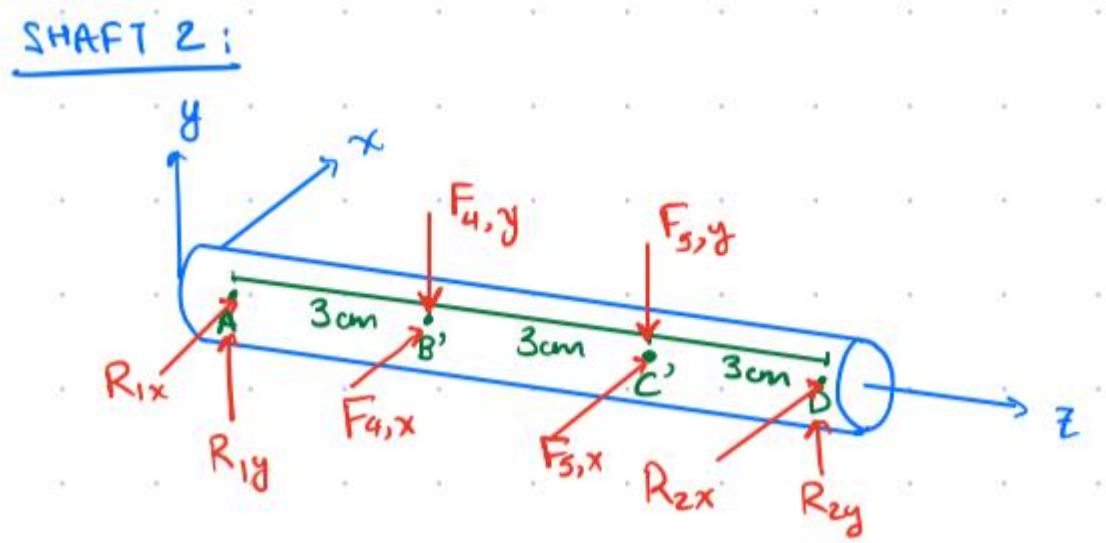

Figure A 1: Shaft 2 FBD

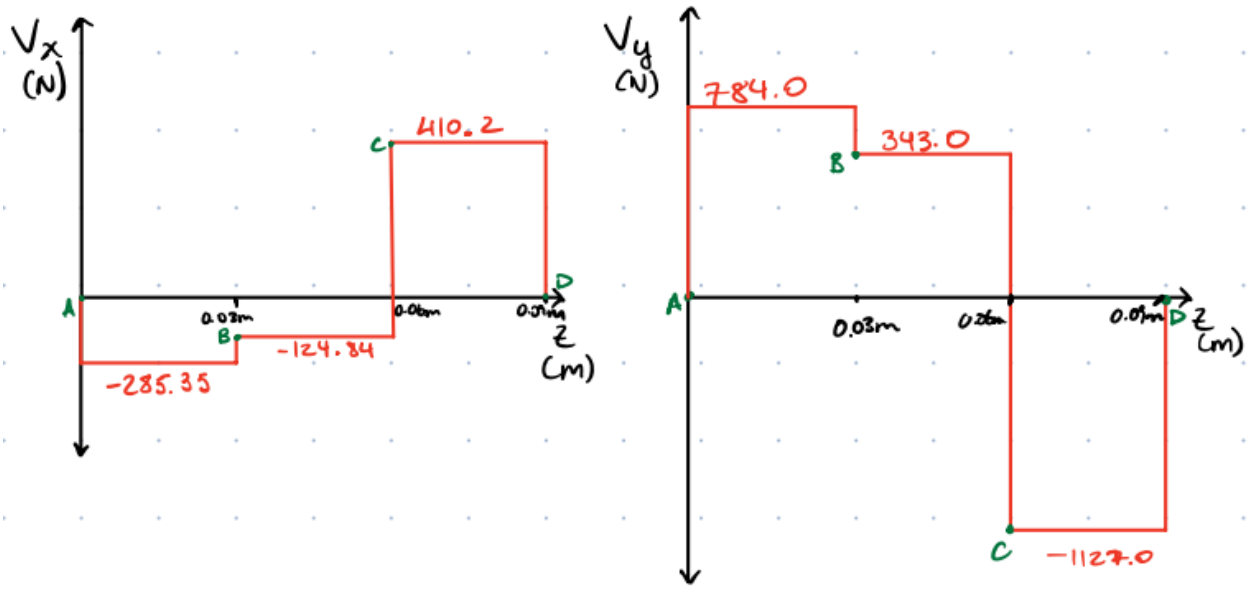

Figure A 2: Shear force diagrams for shaft 2

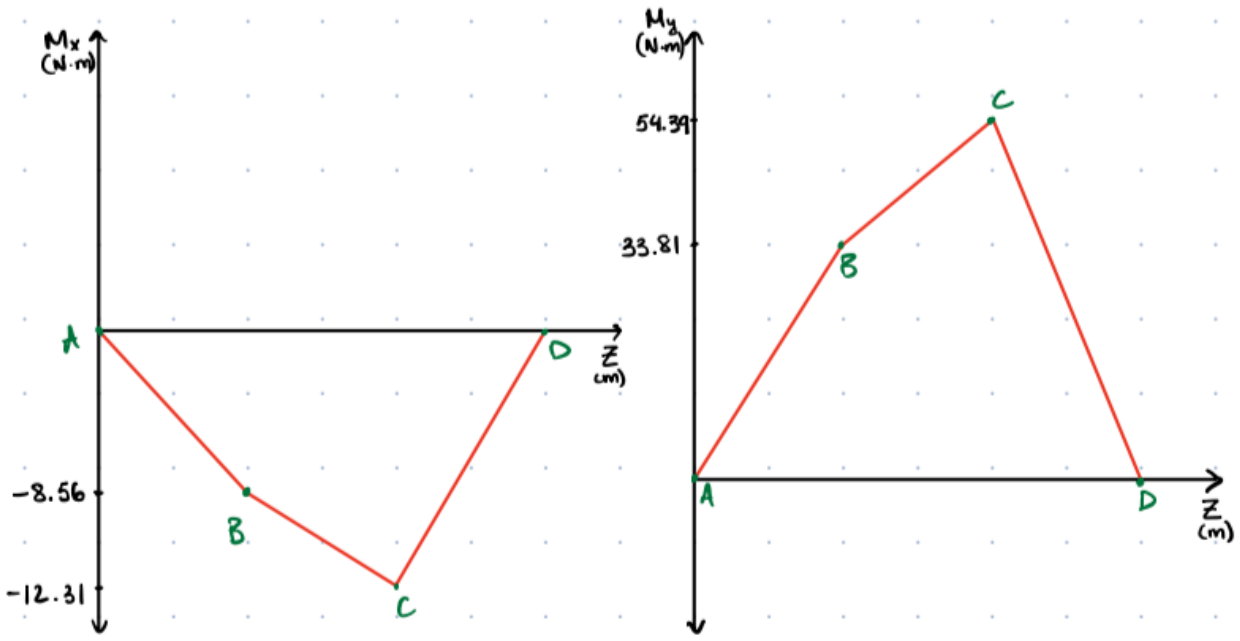

Figure A 3: Bending Moment diagrams for Shaft 2

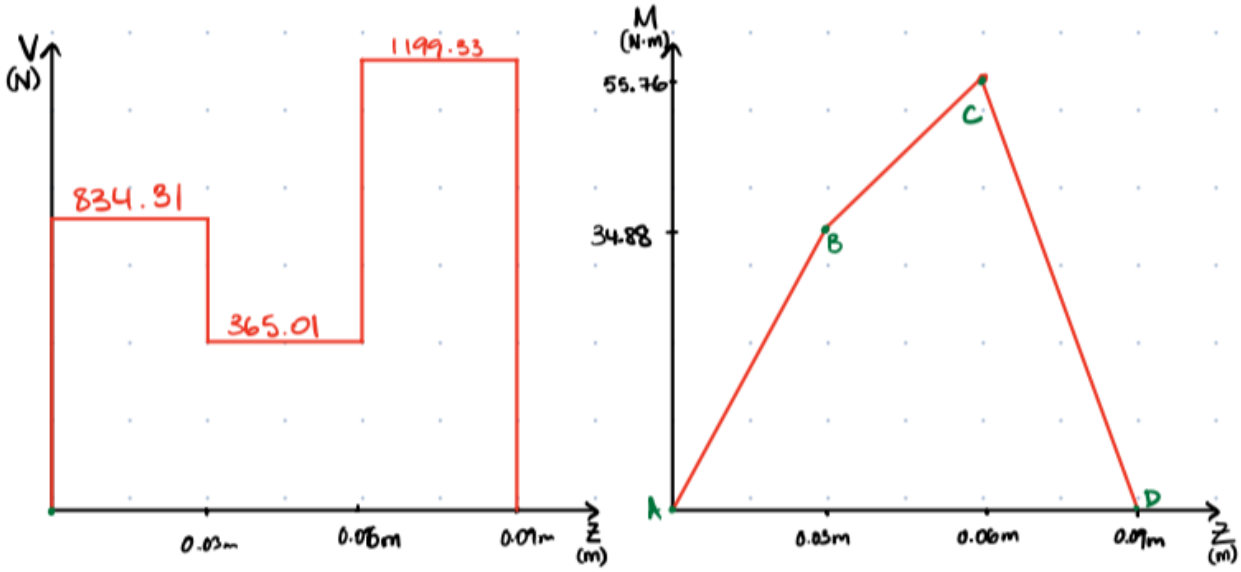

Figure A 4: Combined Shear force and Bending Moment diagrams for Shaft 2

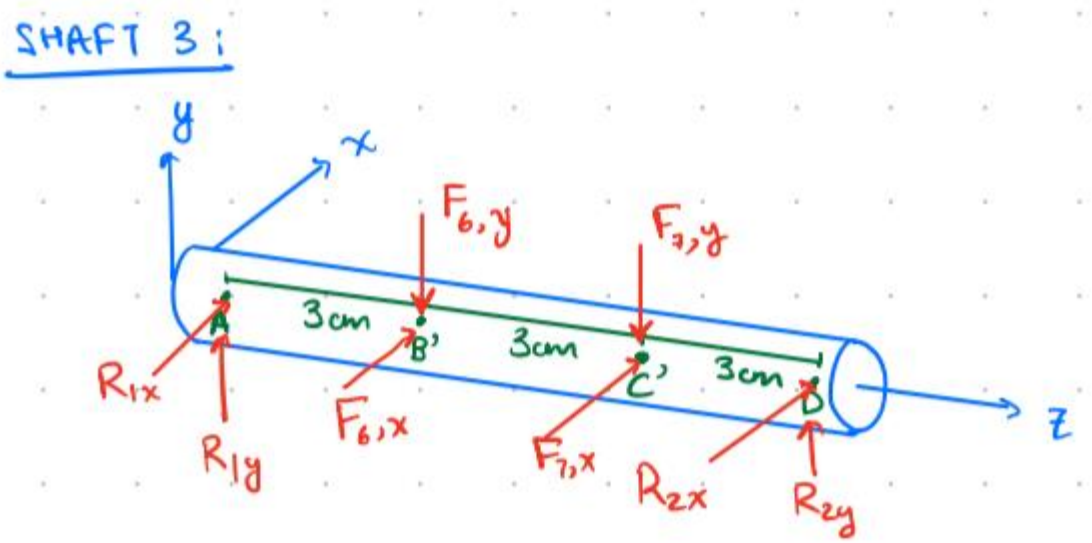

Figure A 5: Shaft 3 FBD

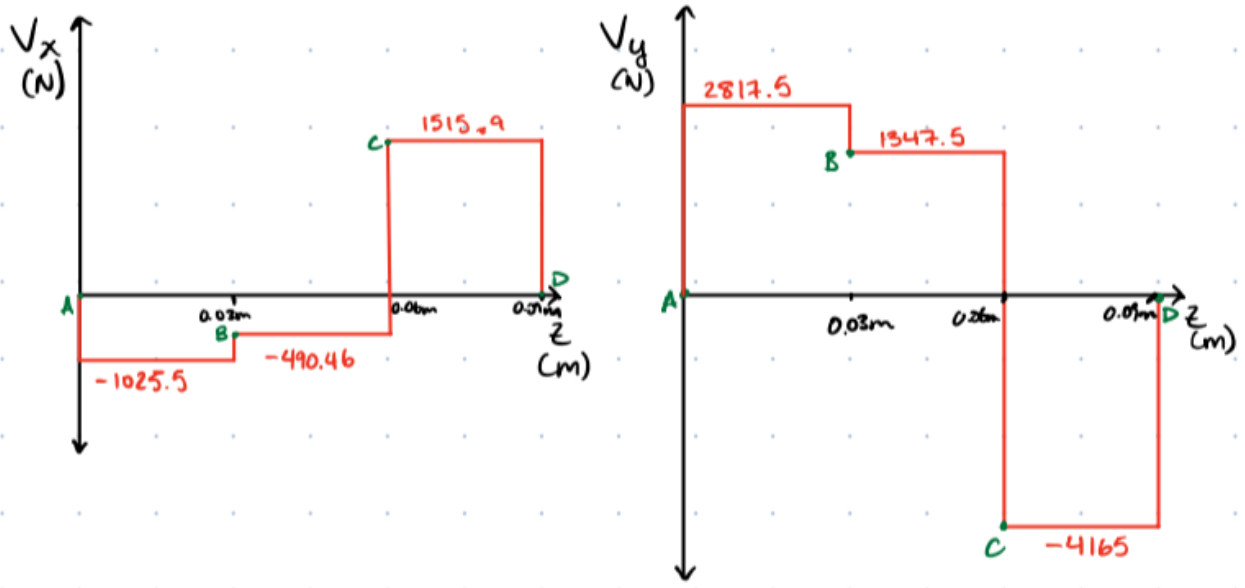

Figure A 6: Shear Force diagrams for Shaft 3

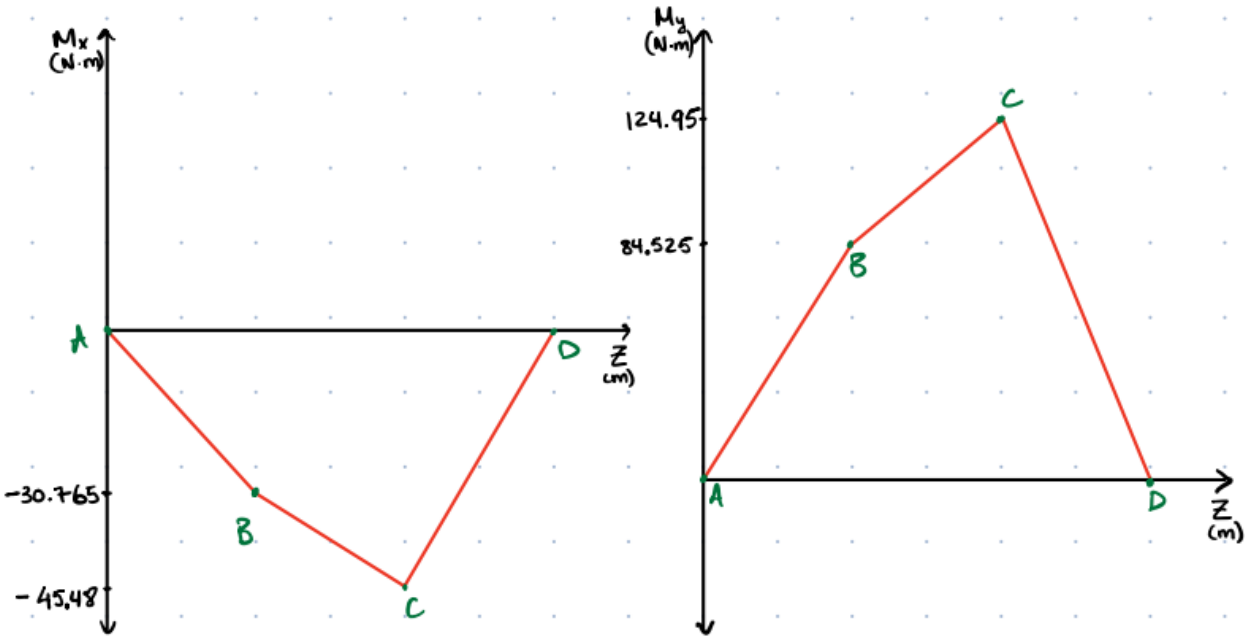

Figure A 7: Bending Moment diagrams for Shaft 3

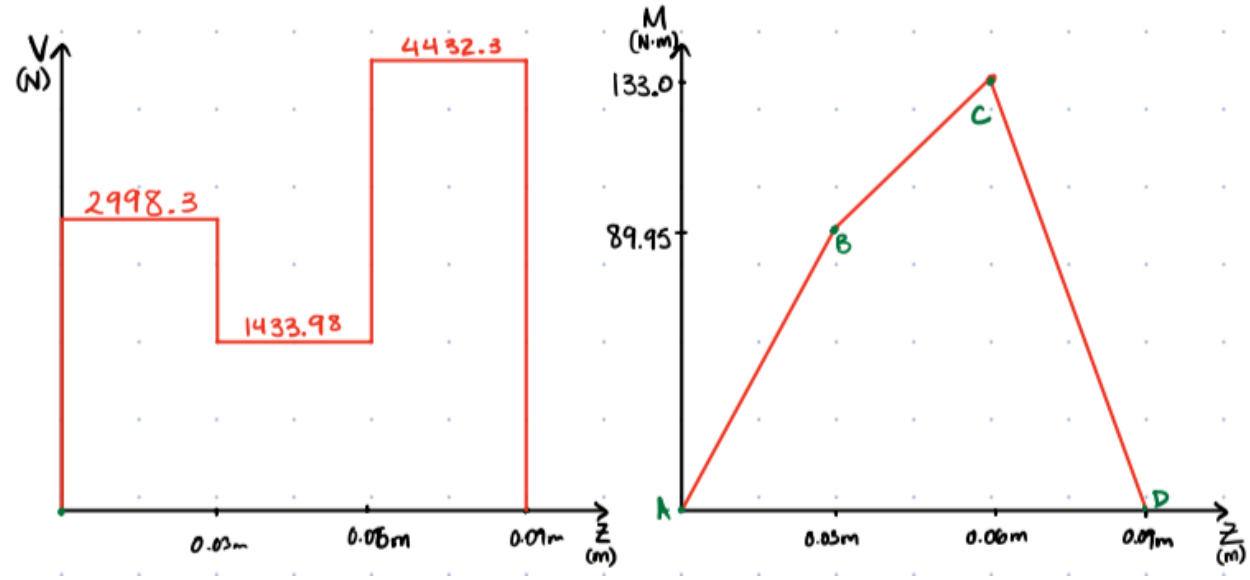

Figure A 8: Combined Shear Force and Bending Moment diagrams for Shaft 3

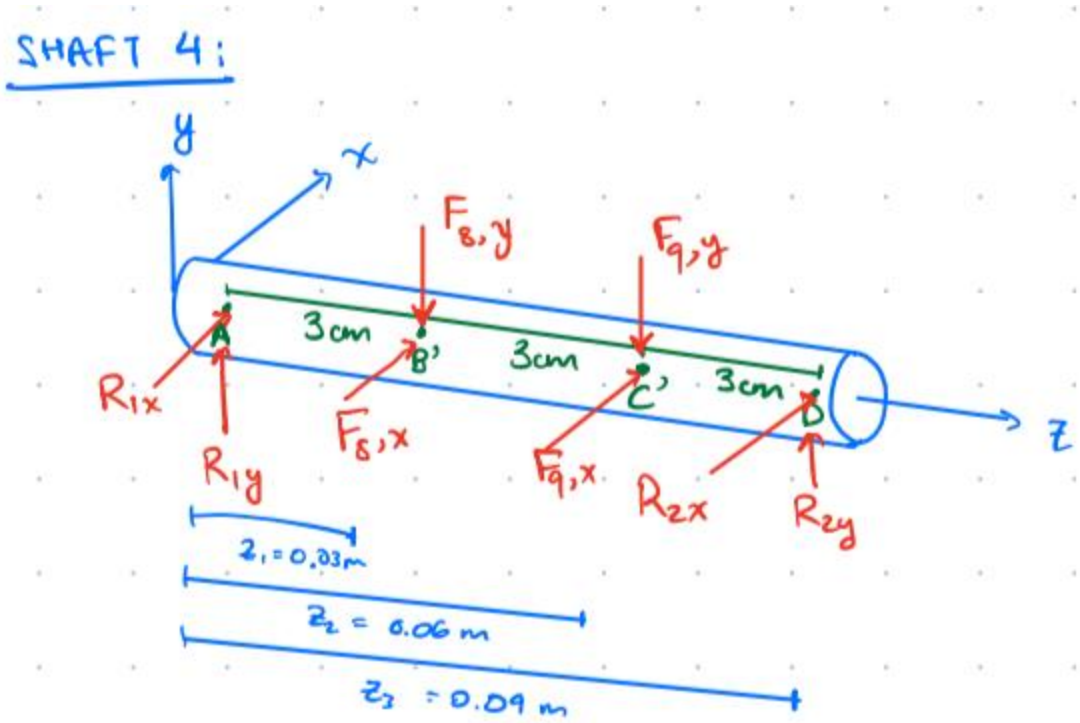

Figure A 9: Shaft 4 FBD

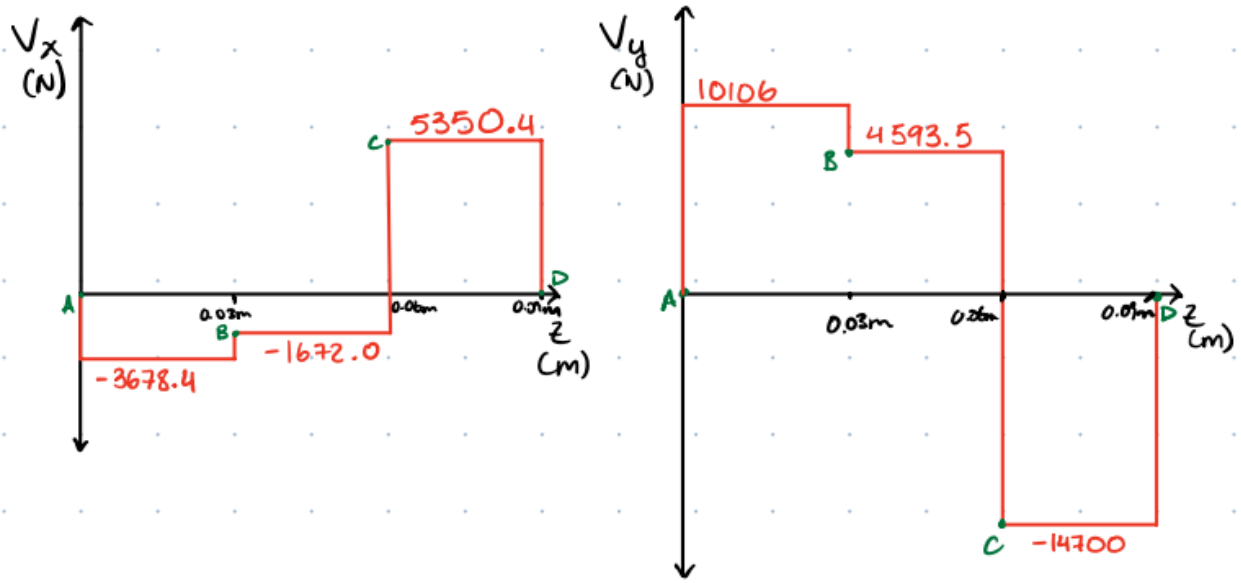

Figure A 10: Shear Force diagrams for Shaft 4

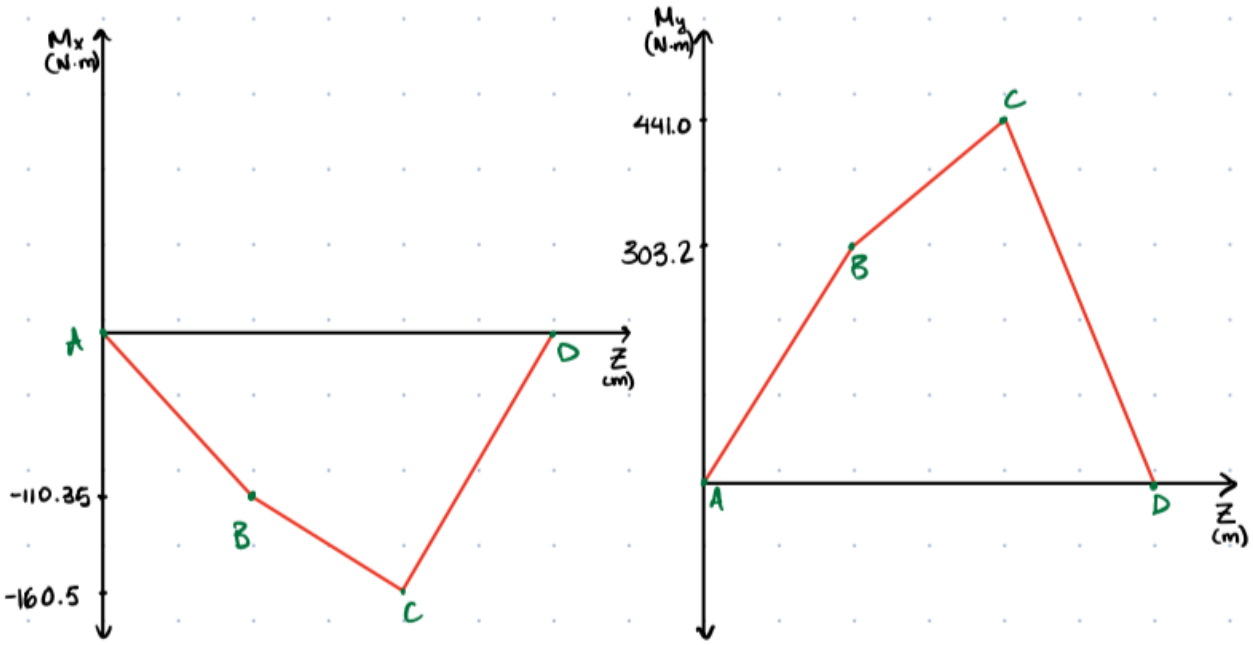

Figure A 11: Bending Moment diagrams for Shaft 4

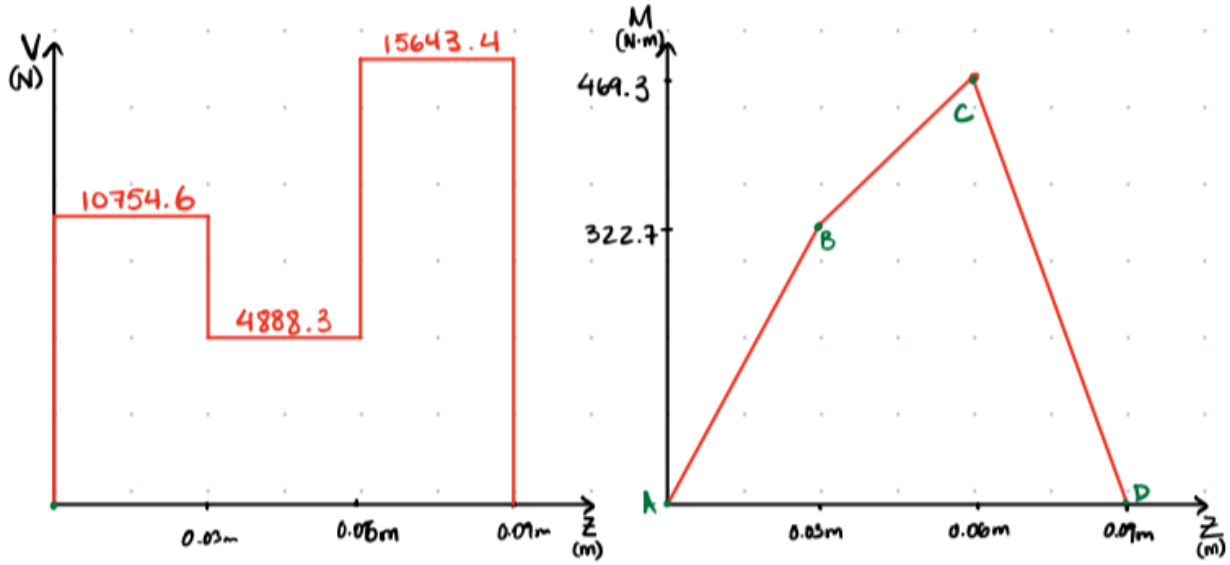

Figure A 12: Combined Shear force and Bending Moment diagrams for Shaft 4

Appendix B

Final completed Shear Force and Bending Moment diagrams for all intermediate shafts within the gearbox.

Shaft 1:

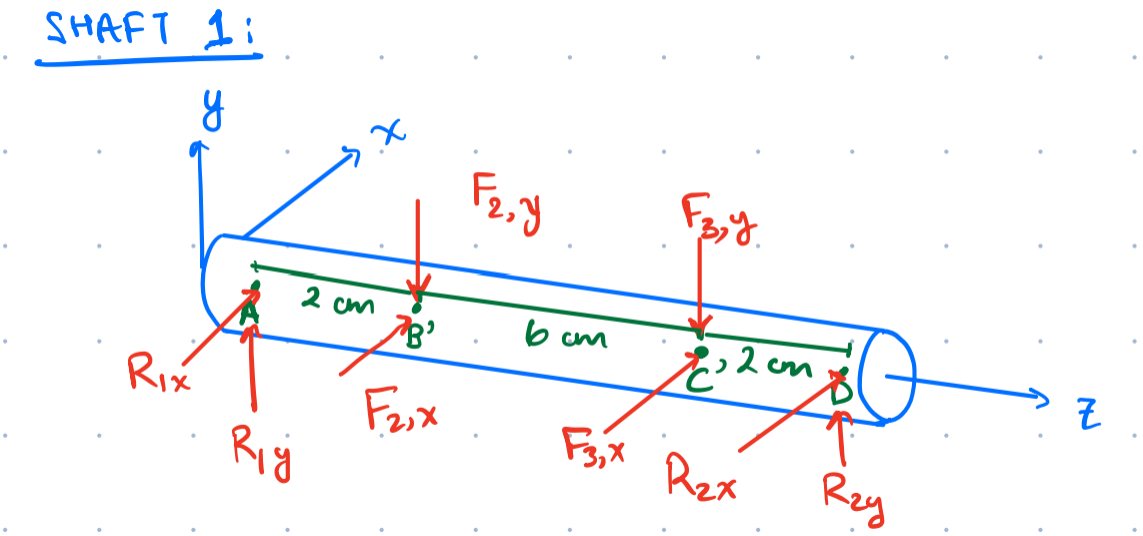

Figure B 1 Shaft 1 FBD

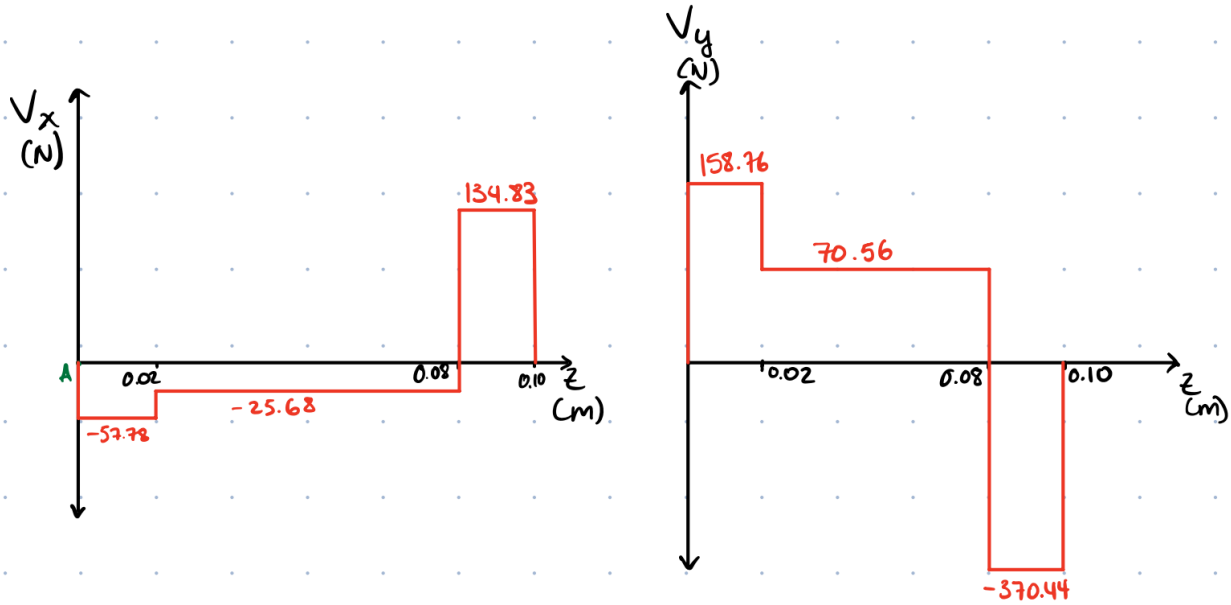

Figure B 2 Shear force diagrams for shaft 1

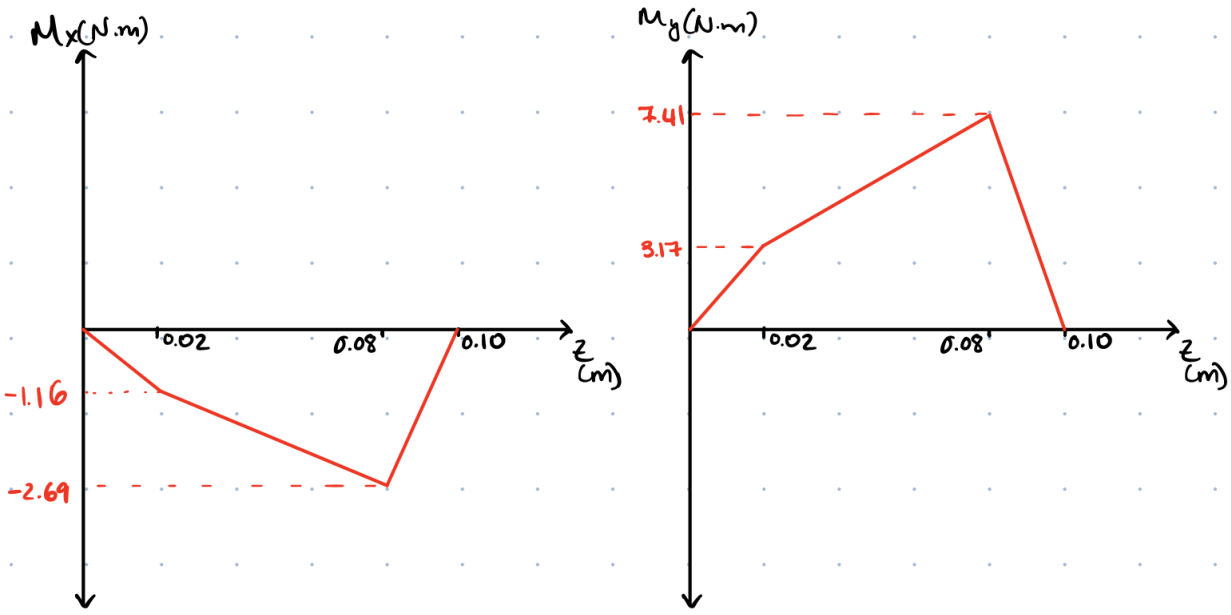

Figure B 3 Bending moment diagrams for shaft 1

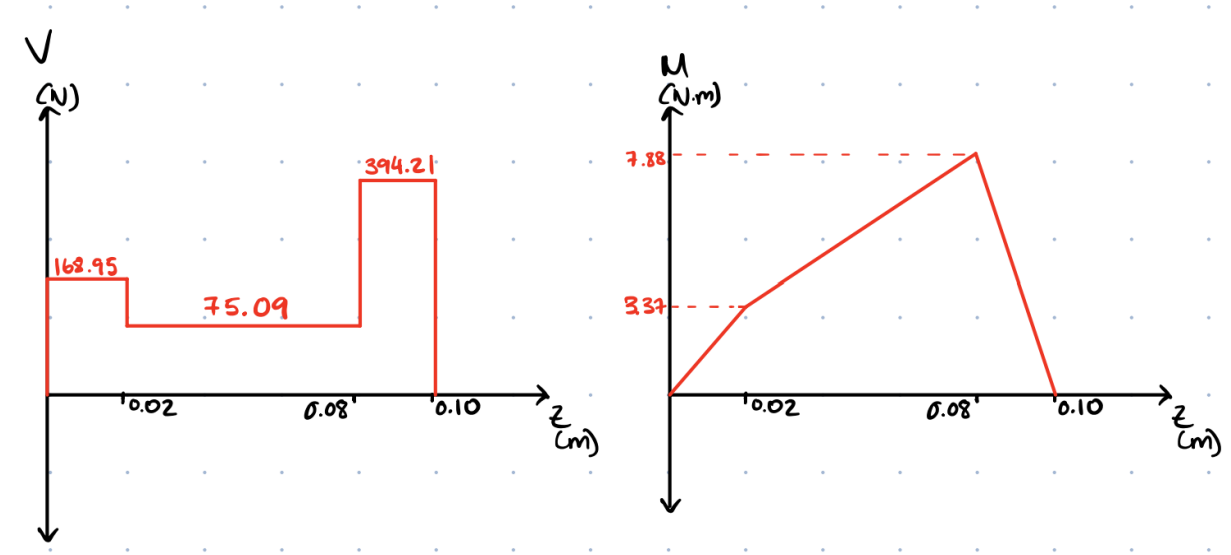

Figure B 4 Combine shear force and bending moment diagrams for shaft 1

Shaft 2:

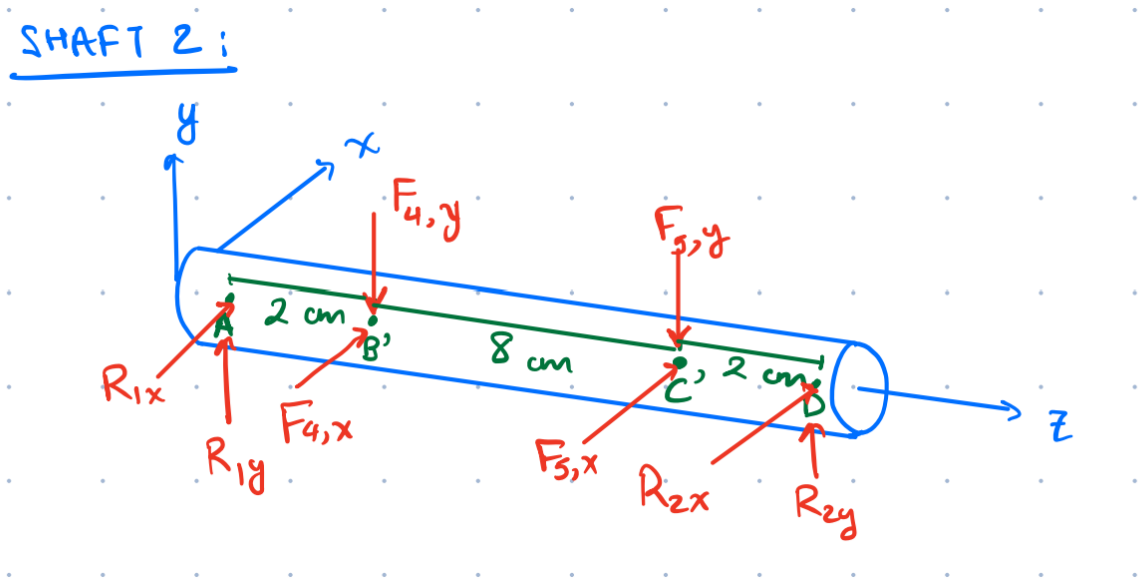

Figure B 5 Shaft 2 FBD

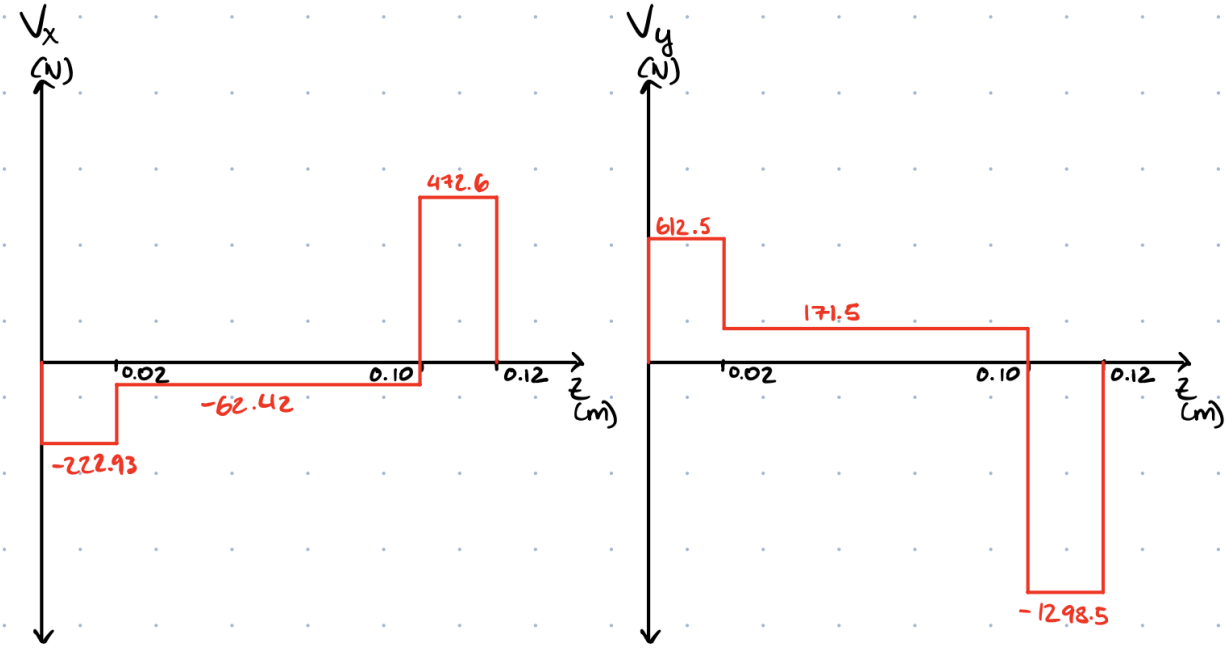

Figure B 6 Shear force diagrams for shaft 2

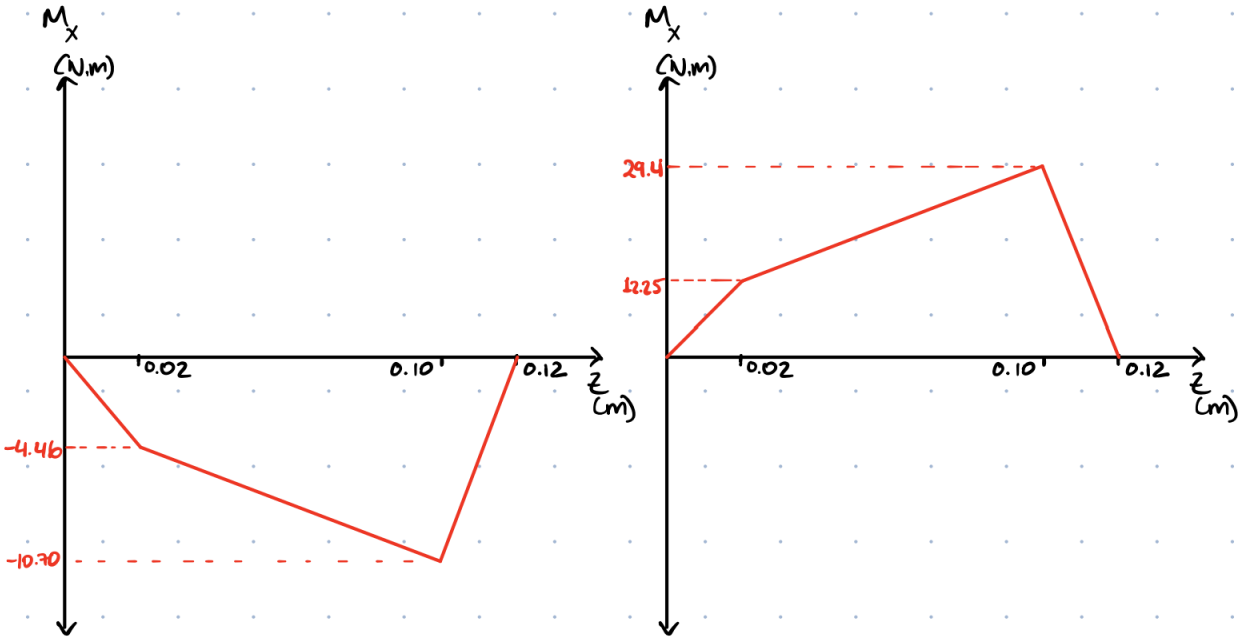

Figure B 7 Bending moment diagrams for shaft 2

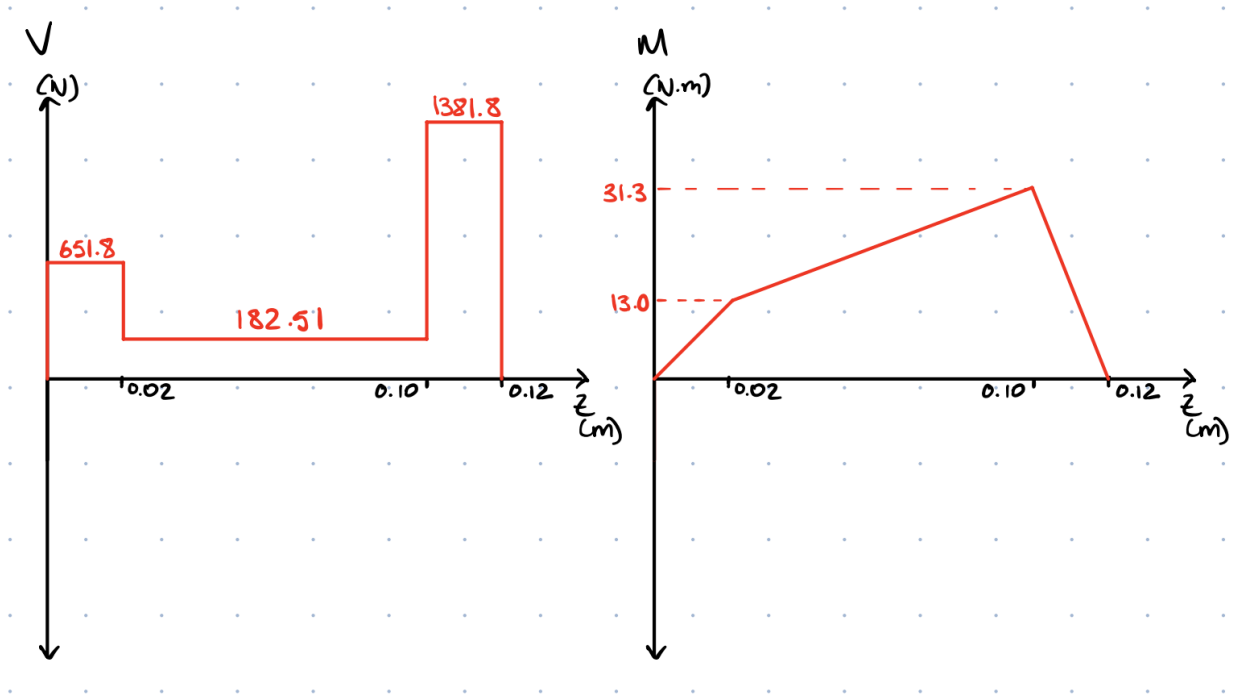

Figure B 8 Combined shear force and bending moment diagrams for shaft 2

Shaft 3:

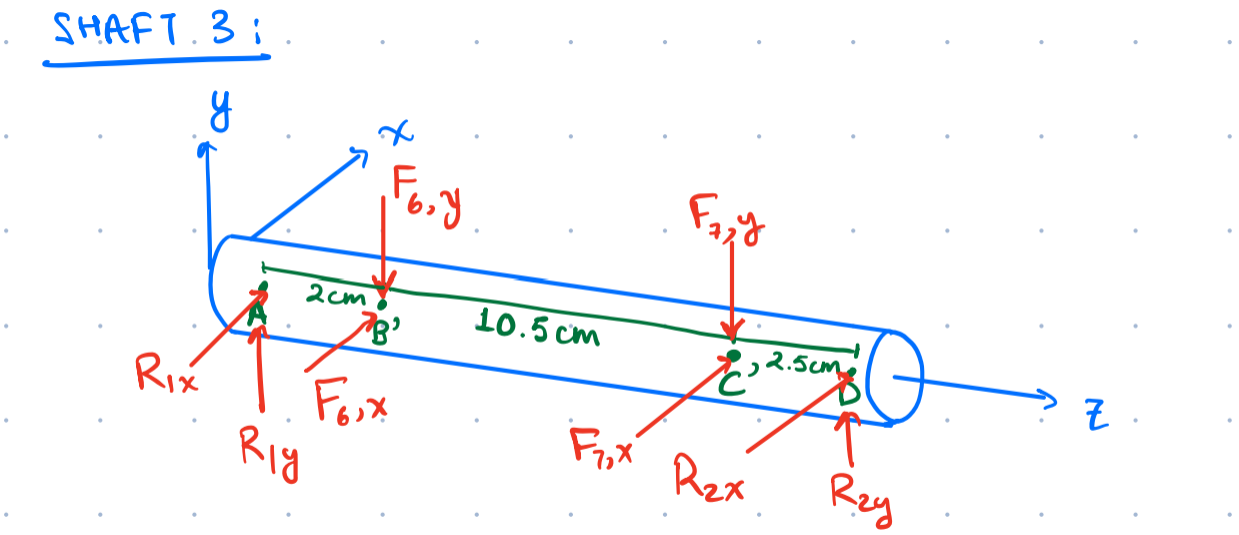

Figure B 9 Shaft 3 FBD

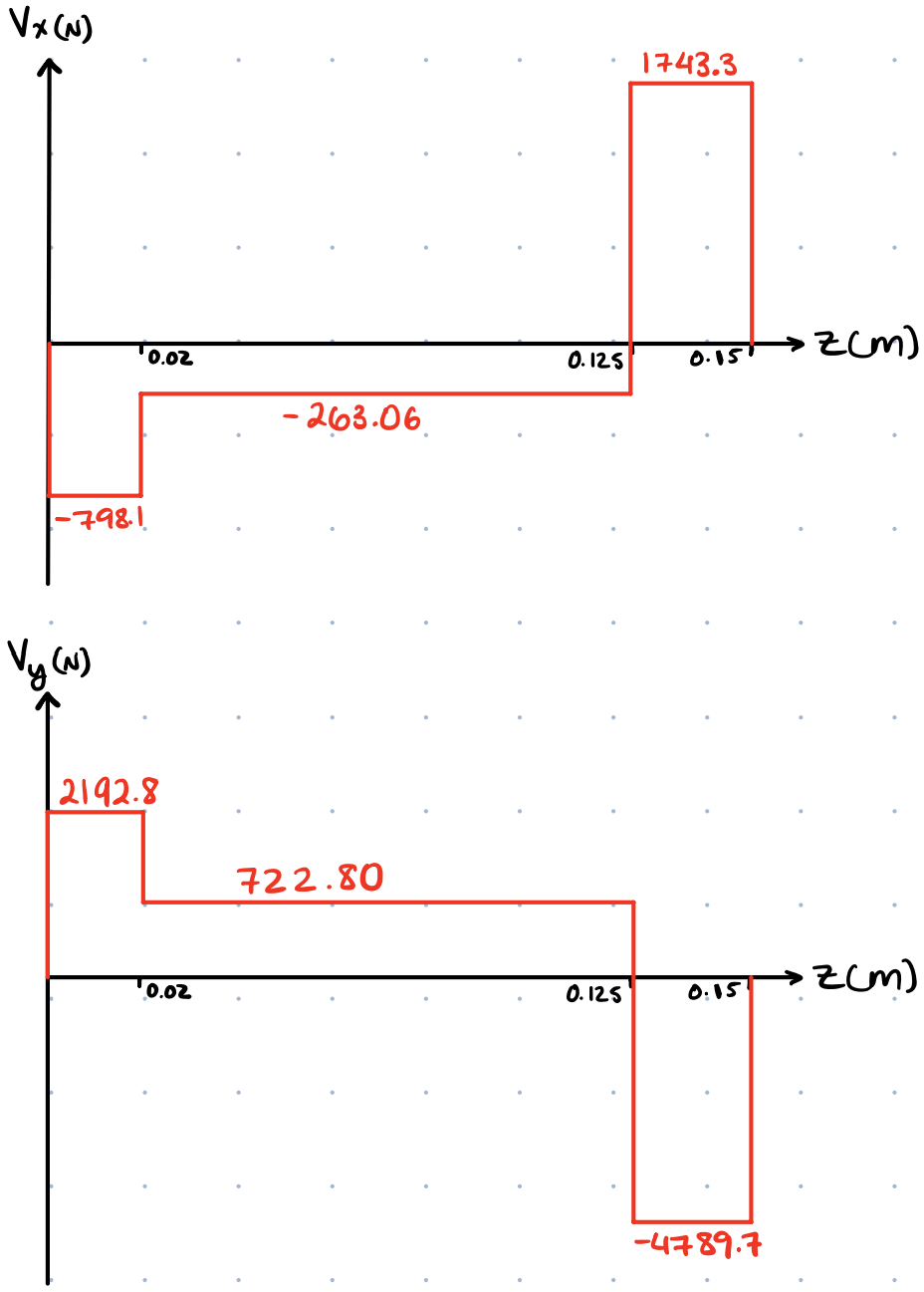

Figure B 10 Shear force diagrams for shaft 3

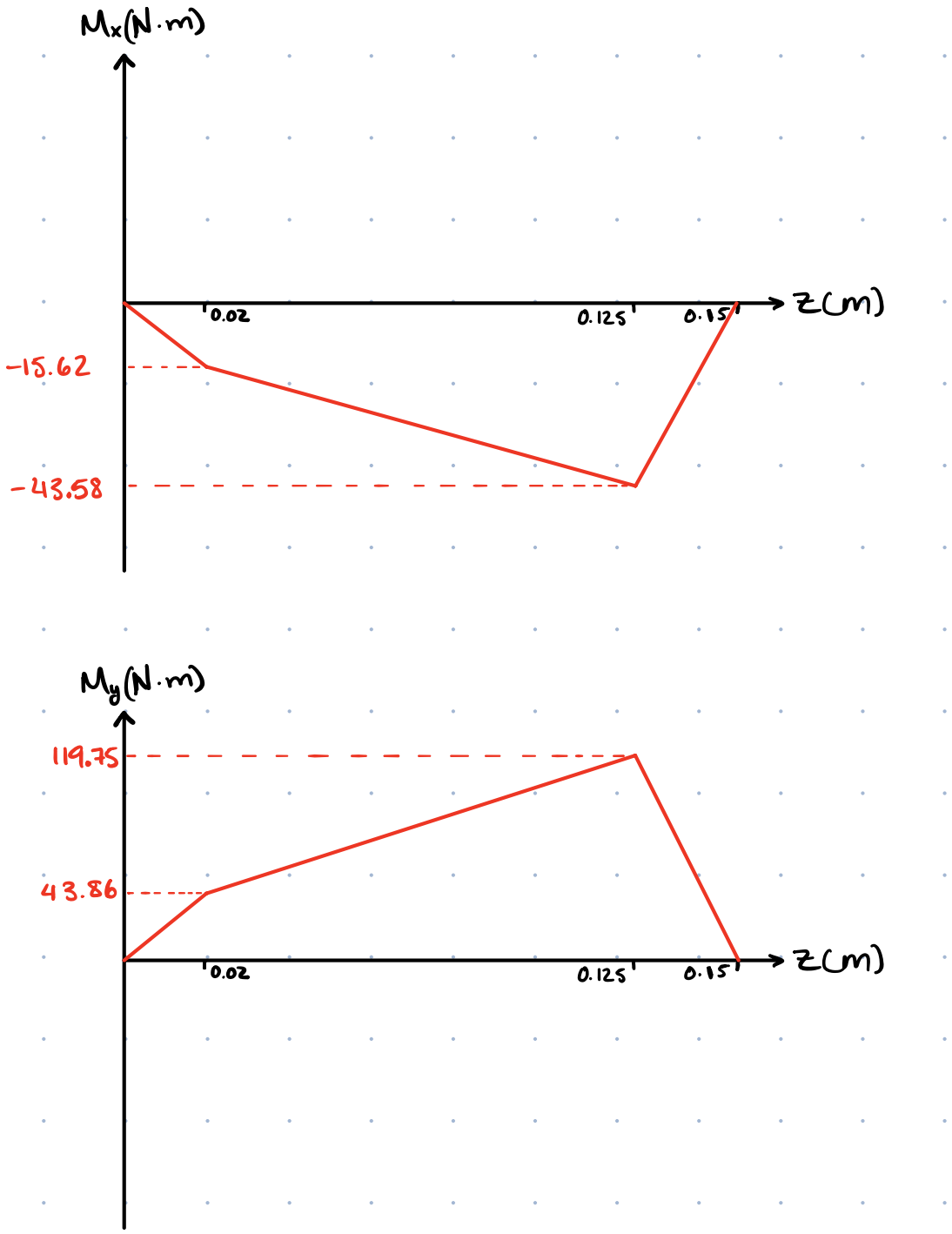

Figure B 11 Bending moment diagram for shaft 3

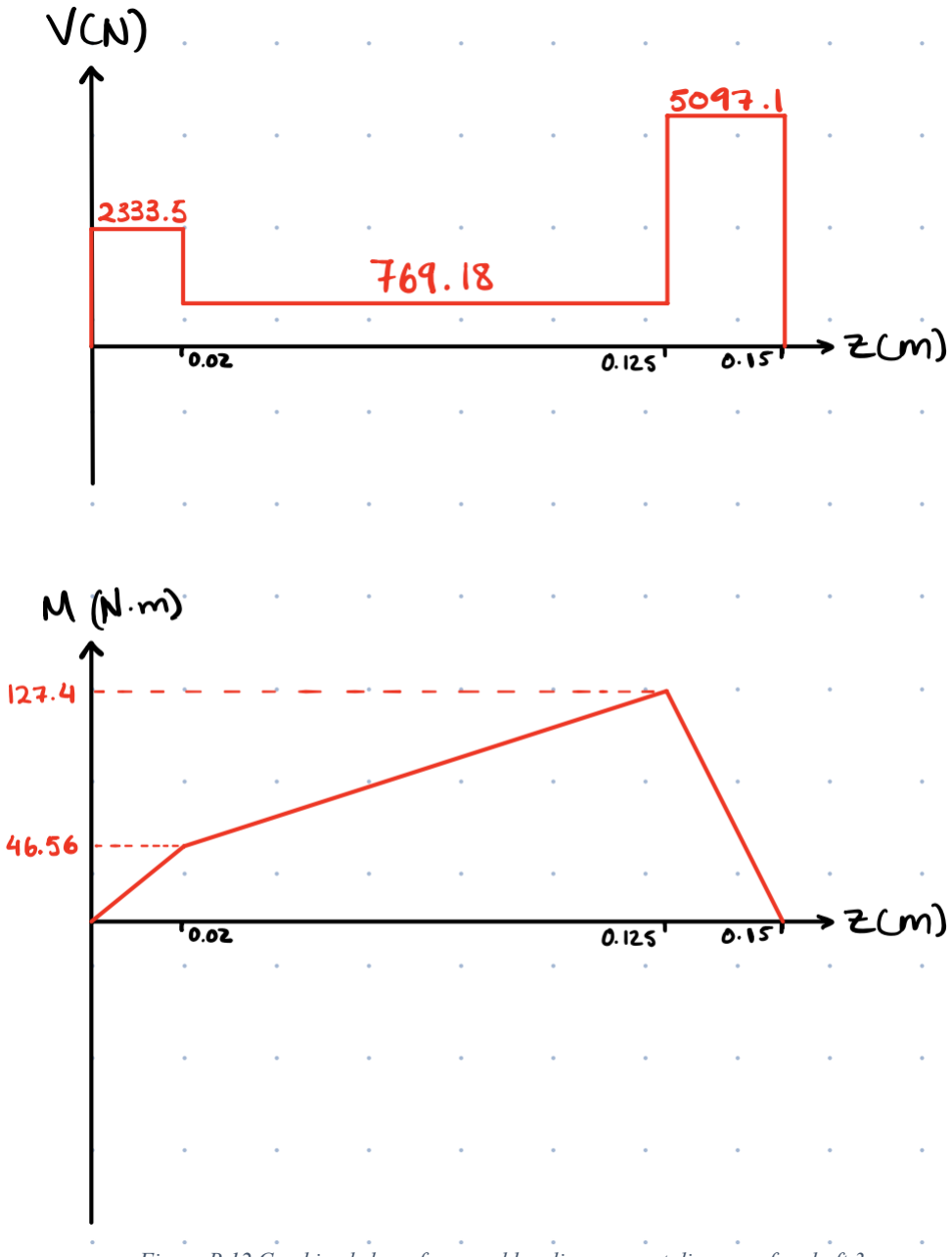

Figure B 12 Combined shear force and bending moment diagrams for shaft 3

Appendix C

Final detailed drawings of all gears

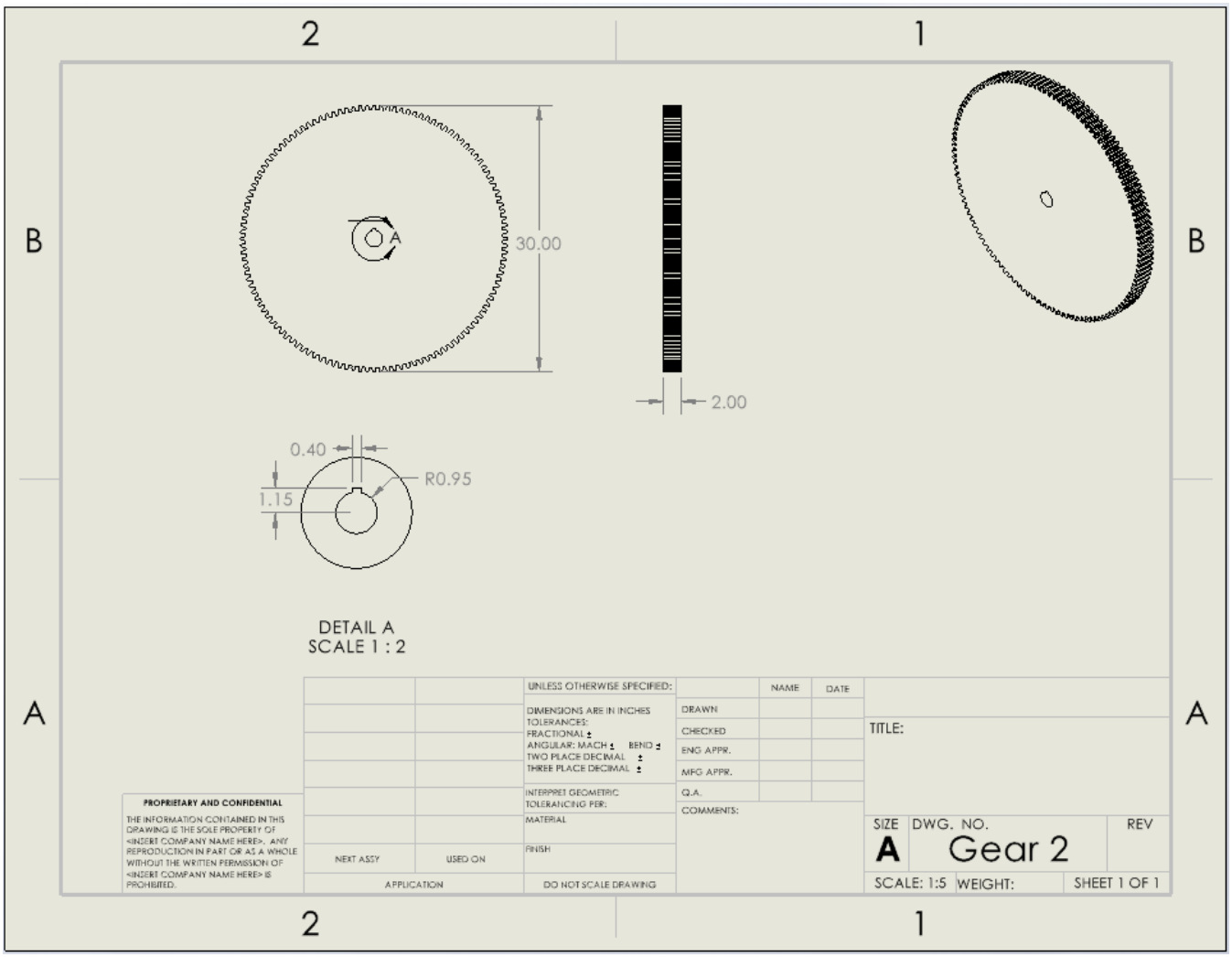

Figure C 1 Detailed Drawing of Gear 2

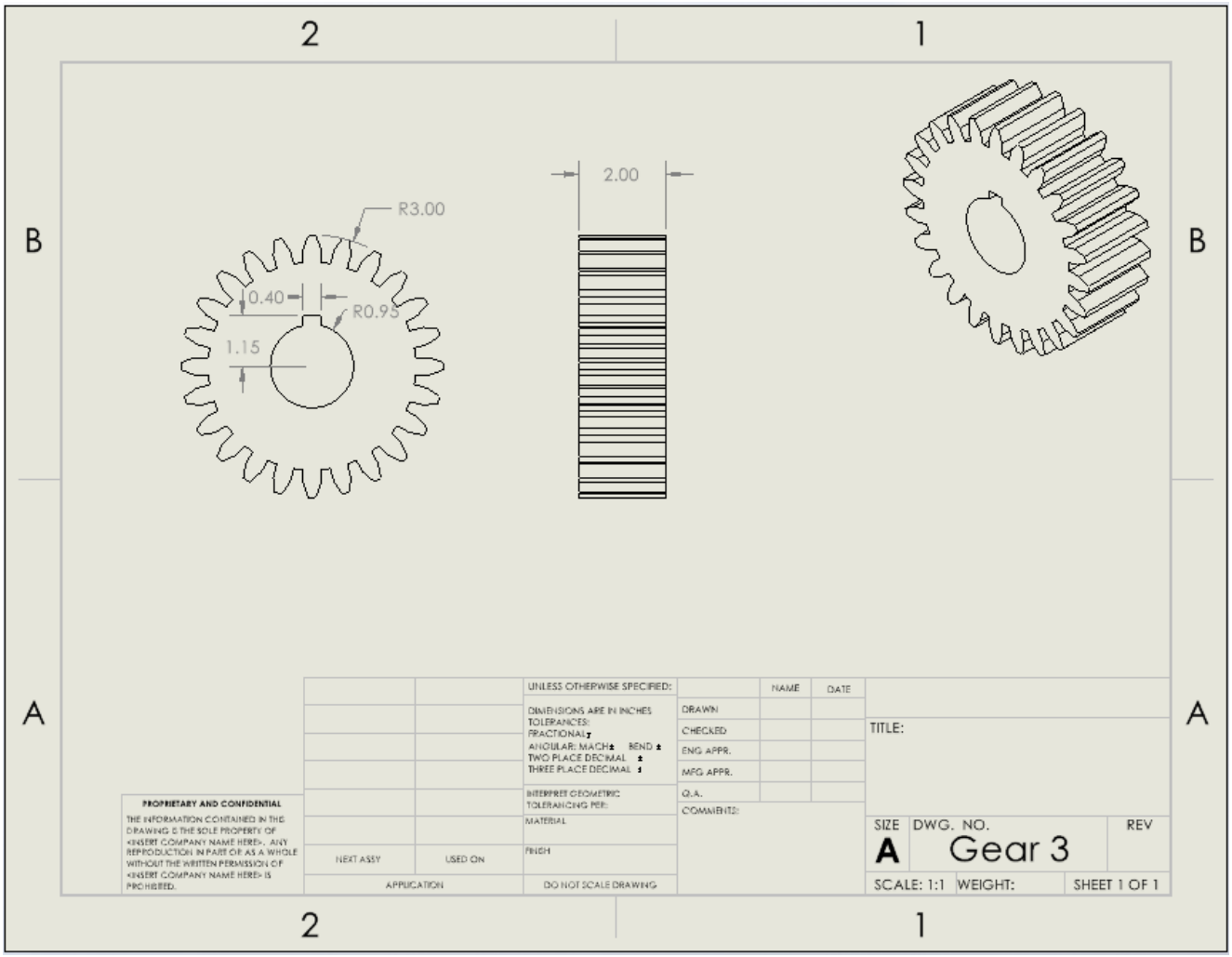

Figure C 2 Gear 3 drawing

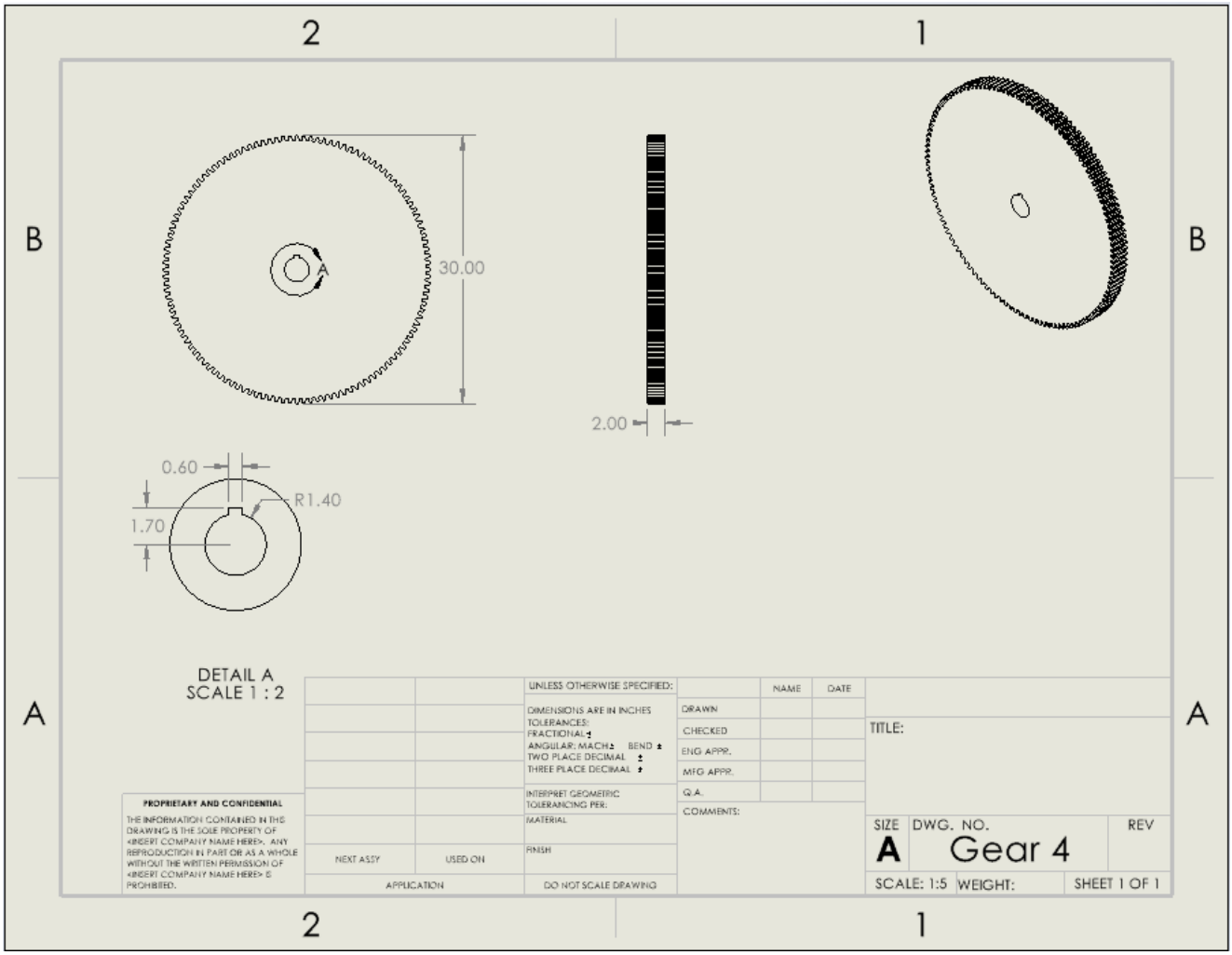

Figure C 3 Detailed Drawing of Gear 4

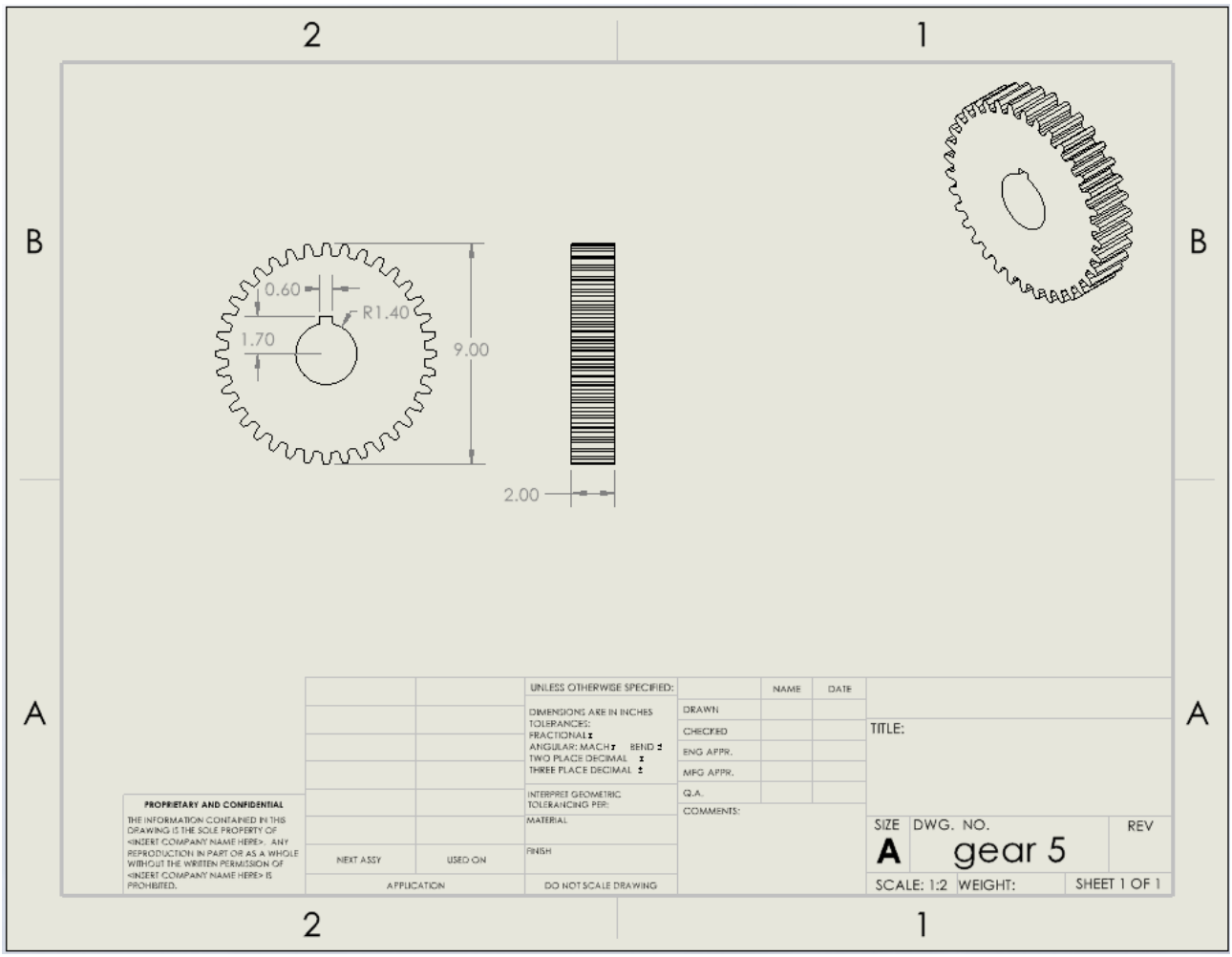

Figure C 4 Detailed Drawing of Gear 5

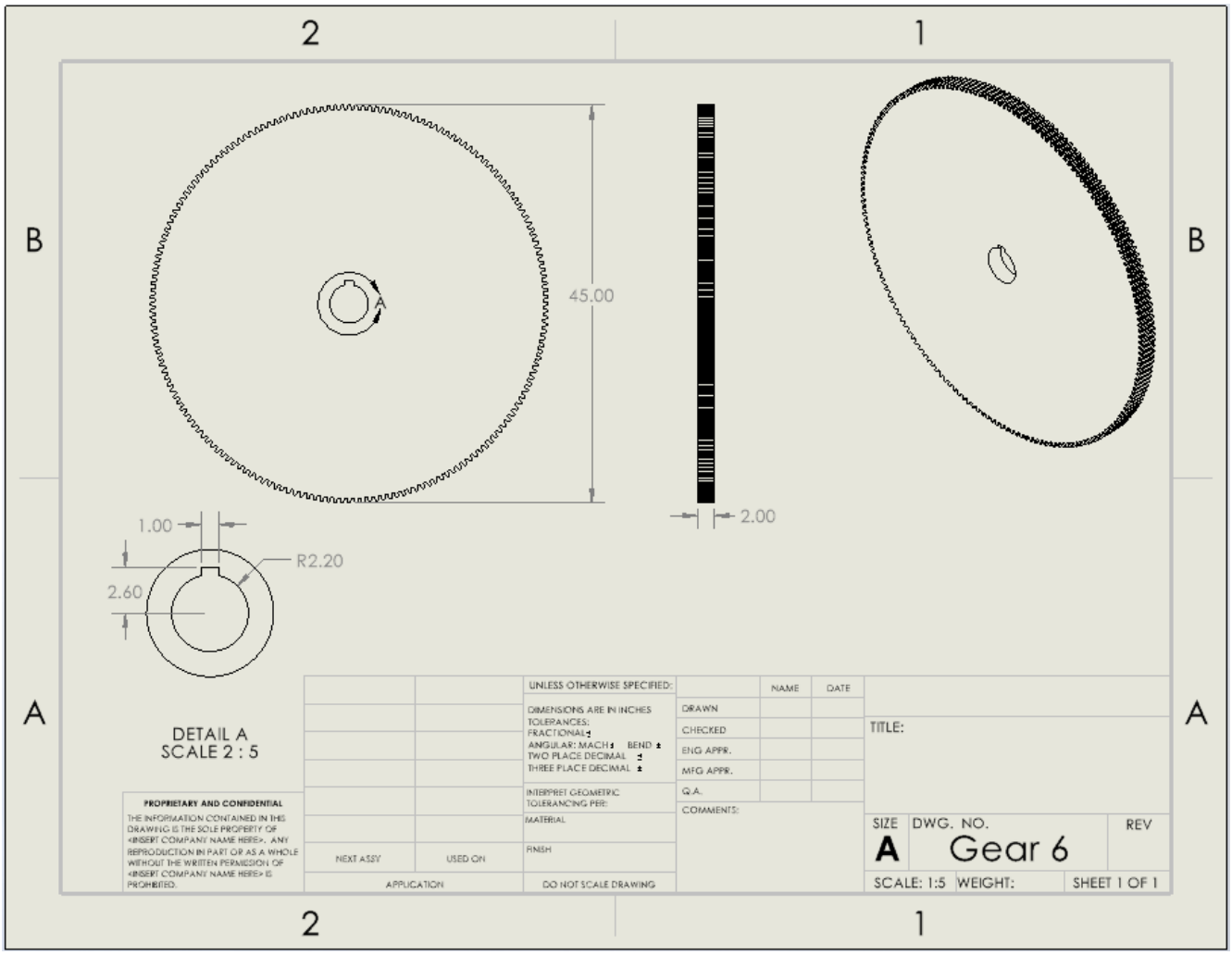

Figure C 5 Detailed Drawing of Gear 6

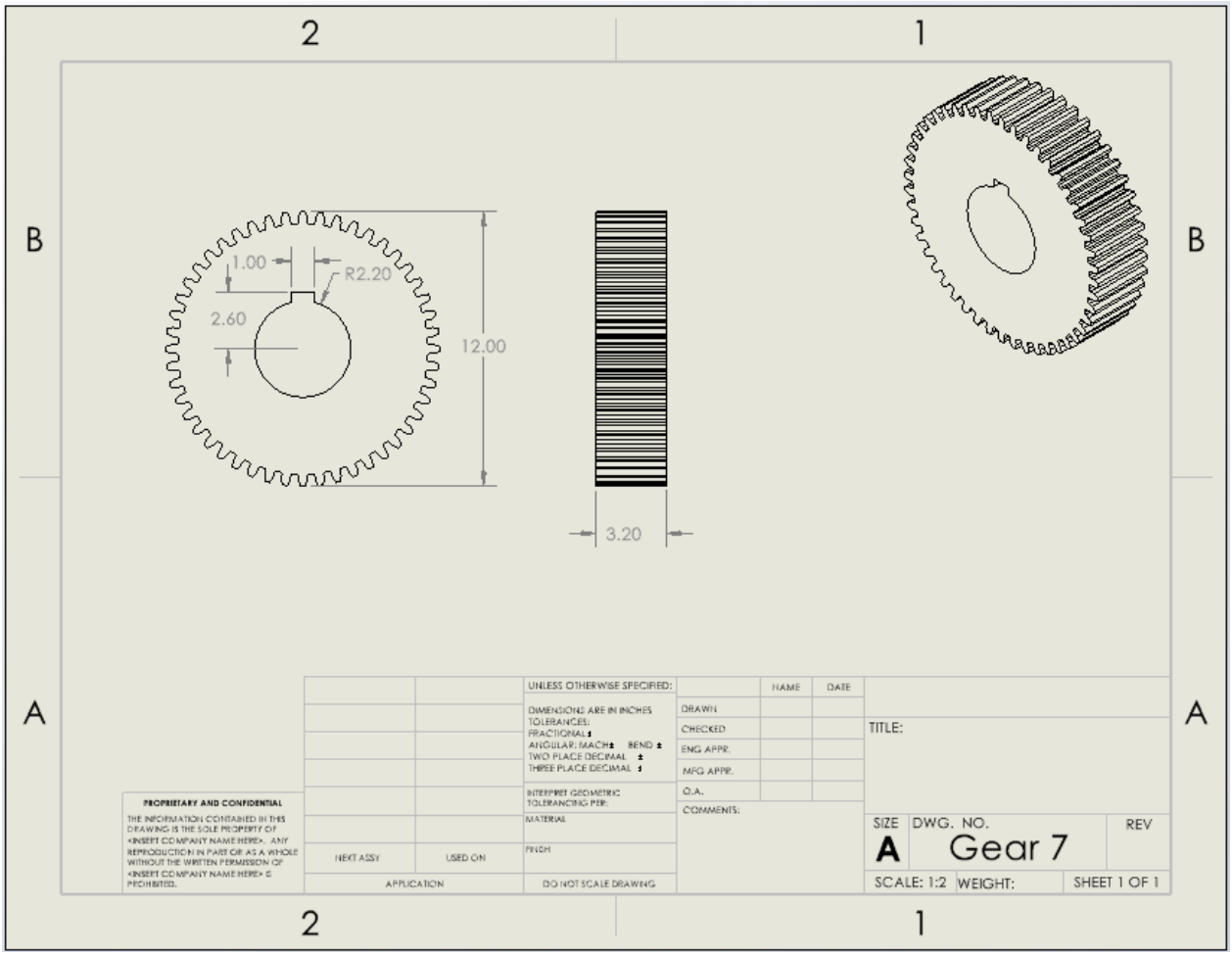

Figure C 6 Detailed Drawing of Gear 7

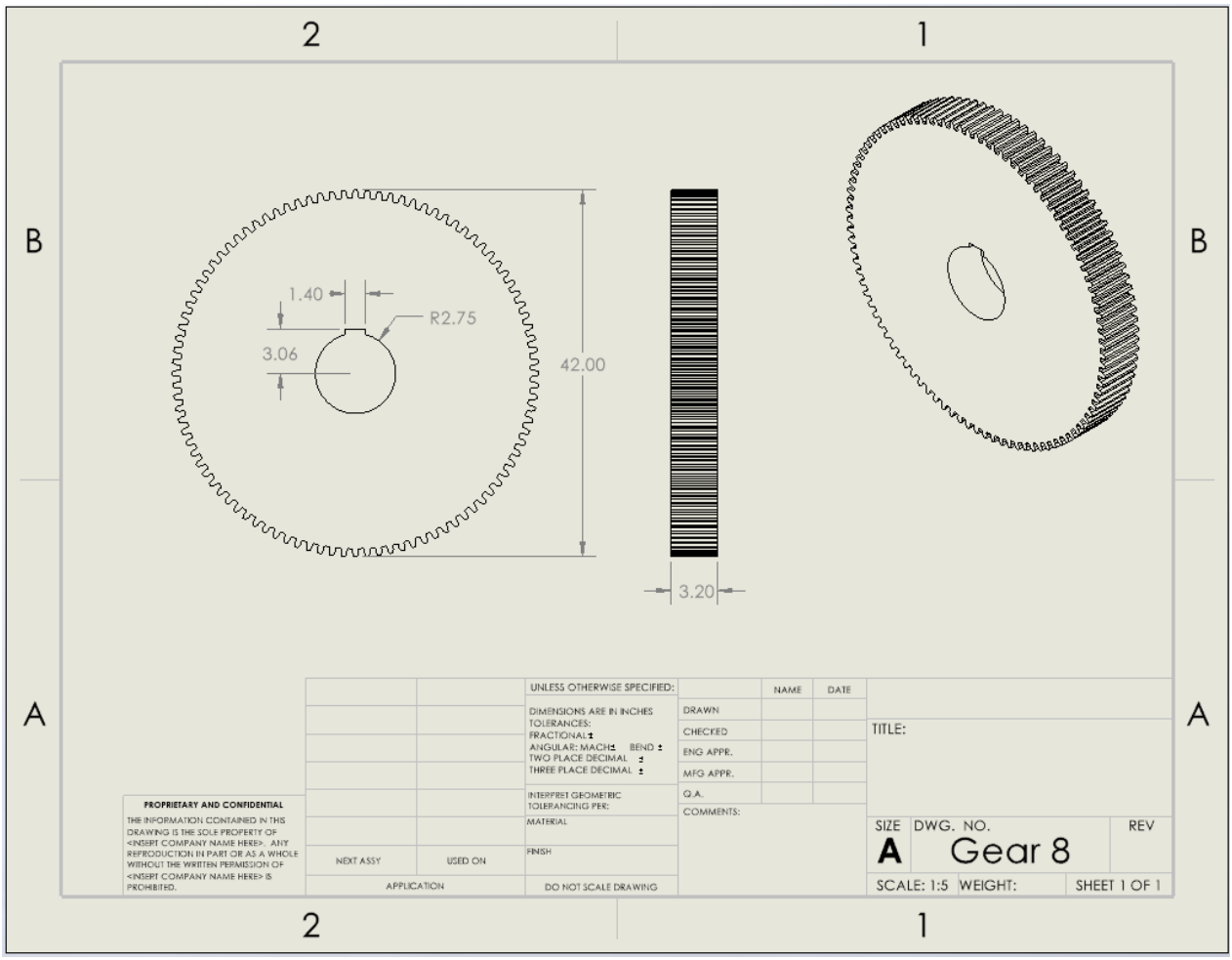

Figure C 7 Detailed Drawing of Gear 8